國立臺灣大學共同教育中心國際學院

生物多樣性國際碩士學位學程

碩士論文

Master's Program in Biodiversity

Center of General Education, International College

National Taiwan University

Master's Thesis

Modelling Fish Species Distributions Under Ocean Acidification and Hypoxia in the North Sea

Kristina Kryzhova

指導教授: 柯佳吟

Advisor: Chia-Ying Ko, Ph.D.

中華民國 114 年 1 月

January, 2025

doi:10.6342/NTU202500202

Master's Thesis Acceptance Certificate

國立臺灣大學碩士學位論文
口試委員會審定書

MASTER'S THESIS ACCEPTANCE CERTIFICATE
NATIONAL TAIWAN UNIVERSITY

Modelling Fish Species Distributions Under Ocean Acidification and Hypoxia in the North Sea

The undersigned, appointed by the International College of Master's Program in Biodiversity on 01/14/2025, have examined a Master's thesis entitled above presented by Kristina Kryzhova (R12H44007) candidate and hereby certify that it is worthy of acceptance.

口試委員 Oral examination committee:

(指導教授 Advisor)

系（所、學位學程）主管 Director:

doi:10.6342/NTU202500202

Abstract

The increasing impact of climate change on marine ecosystems requires robust modeling approaches to project future species distributional shifts. These biogeographical reorganizations are fundamentally transforming the global fishing industry, as traditional fishing grounds experience declining productivity or ecological regime shifts toward novel species assemblages, while simultaneously creating emerging opportunities in previously marginal areas, though these new fishing frontiers often lack the necessary infrastructure and regulatory frameworks to support sustainable resource exploitation. Some projections that rely solely on temperature as the main parameter may fail to capture the complex interplay of multiple environmental stressors, including dissolved oxygen, pH, and their complex effects on marine ecosystems, potentially leading to oversimplified or inaccurate future projections. This study aims to investigate if adding dissolved oxygen concentration, and pH as predictor variables, can better predict the distribution shifts of 16 demersal and 5 pelagic fish species in the North Sea. To project marine fish response to abiotic factors under SSP1-2.6, SSP2-4.5, SSP5-8.5 scenarios for 2050 and 2100, the ensemble of Species Distribution Models (SDMs) was implemented. While SSP5-8.5 scenario incorporated declining oxygen levels (projected decrease of 31-34% from when to when) and ocean acidification (pH decrease of 5-6% from when to when under which scenarios) by 2100, model performance analysis revealed that temperature alone created the best ensemble model, with the best validation metrics (TSS = 0.950±0.001). Under the most pessimistic scenario - SSP5-8.5, temperature-driven models projected mean north-west shifts of distributional centroids at 245±223 km for most demersal species and eastwards 193±62 km shifts for pelagic species by 2100, while combination of parameters projected generally south and south-eastwards movements for both functional groups up to 143±57 km. When comparing single-factor and multi-factor models, the similarity

doi:10.6342/NTU202500202

comes in projection up to 2050 when the southern and central areas tend to be the most suitable ones, however later projections for 2100 showed disparity in direction and magnitude of distributional shifts, especially for the demersal species, seeking refugia in different locations. These findings suggest that while numerous stressors affect marine ecosystems, statistically, temperature's impact is the strongest for selected species in the North Sea region based on the applied data. The findings reveal significant implications for improving climate impact assessments of marine wildlife through the integration of species distribution models into unified frameworks that enable robust analysis of migration patterns.

Key words: Species distribution modelling, North Sea, fishery, model comparison, climate change

doi:10.6342/NTU202500202

Content

doi:10.6342/NTU202500202

doi:10.6342/NTU202500202

1. Introduction

Marine organisms and their ecosystem services face unprecedented challenges due to climate change. The ecological impacts arise from both long-term shifts in climate patterns and short-term extreme events, leading to significant disruptions in marine environments (Harris et al., 2018). While ocean ecosystems face various threats, including chemical pollution and habitat destruction, environmental condition transformations remain a key factor determining species' suitable habitats.

These changes significantly affect fisheries and coastal economies, threatening both food security and the livelihoods of millions dependent on marine resources (FAO, 2024). As environmental conditions approach critical thresholds, species either relocate or decline when unable to tolerate changes. Even surviving species face challenges from shifts in food availability, predation patterns, and competition within altered ecosystems. Additionally, climate change may accelerate the introduction and establishment of invasive species, leading to further alterations in food web dynamics and community composition (Nisin, 2023).

This dissertation applied predictive modeling tools to understand which marine water physico-chemical characteristics most significantly influence the occurrence and distribution of pelagic and demersal fish in the North Sea. Using ensembles of Species Distribution Models (SDMs) driven by Earth System Models (ESMs), I simulate various biochemical conditions under three different Shared Socioeconomic Pathways (SSPs). Including commercially valuable species such as mackerel (*Scomber scombrus*) and hake (*Merluccius merluccius*) provide crucial insights into future fishery sustainability.

The scientific novelty of this research lies in addressing current research gaps by: (1) considering dissolved oxygen and pH levels' impact on fish distribution, moving beyond temperature-only effects; (2) focusing on meso-scale spatial coverage and long-

doi:10.6342/NTU202500202

term temporal analysis (42 years); (3) integrating multiple environmental variables to improve model accuracy, as research indicates that temperature-only models tend to produce less reliable and unrealistically optimistic predictions (McHenry et al., 2019).

Study Objectives:

- To assess climate change impacts on fish species distribution;
- To investigate the role of ocean acidification, oxygen depletion, and ocean warming in shaping distributional shifts;
- To model potential yearly fish distribution shifts using past records and future projections under climate scenarios (SSP1-2.6, SSP3-7.0 & SSP5-8.5) through 2100.

This comprehensive approach will enhance understanding of how marine species interact with their environment and improve ability to predict ecosystem responses to climate change. Such knowledge is crucial for developing effective conservation strategies and ensuring sustainable fisheries management in the face of global environmental change.

1.1 Concept of fish distributions

Fish distributions in marine ecosystems are governed by complex interactions between environmental conditions and biological requirements. These distribution patterns reflect species-specific physiological tolerances and preferences, which determine their fundamental niche (Hutchinson, 1957). Within marine environments, fish distributions are primarily influenced by temperature regimes, which affect metabolic rates and energy budgets (Pörtner and Farrell, 2008), while the realized niche is further shaped by oxygen availability, pH levels, food resources, and interspecific competition (Perry et al., 2005).

doi:10.6342/NTU202500202

Oceanographic physical processes, including current systems, upwelling zones, and water mass boundaries, significantly influence distribution patterns by creating natural barriers and corridors. These physical features correlate with nutrient availability and primary productivity, directly affecting food availability for fish populations, with fish movements closely tracking primary producers' peak productivity spring waves (Kléparski, 2021).

Marine species are moving poleward at an average rate of 72 kilometers per decade, nearly ten times faster than terrestrial species (Poloczanska et al., 2013). This redistribution creates novel assemblages and ecological interactions through "climate velocity corridors" - pathways where the speed and direction of climate change may create natural migration routes (Burrows et al., 2014).

The North Sea exemplifies these dynamics, where species exhibit varying responses to environmental changes. For instance, cod (*Gadus morhua*) actively avoid waters above 13°C, while European seabass (*Dicentrarchus labrax*) prefer warmer waters and extend their range northward during summer months (Baudron et al. 2014). Research using acoustic telemetry revealed that Atlantic cod aggregate in deeper northern waters during winter and disperse to central and southern feeding grounds in spring, though this adaptation to deeper waters is limited by light availability and pressure tolerance (Rogers et al., 2020).

Species demonstrate varying capacities for adaptation, with fast-growing, short-lived species generally showing greater capacity for range shifts, while species with specific habitat requirements face greater challenges. Notably, pelagic species typically demonstrate more rapid distribution changes compared to demersal species (Pinsky et al., 2019). These shifts in commercially valuable species' distributions create significant management challenges, often crossing jurisdictional boundaries (Pinsky et al., 2018).

doi:10.6342/NTU202500202

Traditional static marine protected areas may become less effective as species ranges shift (Bruno et al., 2018), while fishing pressure can amplify climate effects on fish populations by reducing their adaptive capacity and resilience to environmental change (Free et al., 2019).

Understanding these distribution mechanisms is crucial for predicting future species ranges and implementing effective conservation strategies (Cheung et al., 2009). While species generally shift poleward in response to changing climates, the speed, range, and direction of movement for each species remain highly unpredictable (IPCC, 2022).

1.1 Impact of ocean warming on fish

Ocean temperatures are experiencing unprecedented acceleration in their warming trajectory, with the heating rate increasing significantly compared to two decades ago. The State of the Ocean Report shows that 2023 marked one of the most substantial temperature increases since the 1950s, with ocean temperatures rising 1.45°C above pre-industrial levels (UNESCO, 2024). Between 1958 and 2019, the upper ocean layers accumulated heat equivalent to 351 Zettajoules, with marked acceleration in the past decade (Cheng et al., 2022).

Temperature serves as a primary driver of marine species distribution, with each species having optimal thermal ranges that influence their survival, growth, and reproduction. Marine heatwaves—discrete periods of anomalously warm ocean temperatures—significantly affect marine ecosystems (Smale et al., 2019). Rising temperatures influence physiological functioning of marine species, impacting growth, size, reproductive success, and population numbers (Pauly, 2021). Species with faster life histories show stronger responses to temperature changes, particularly populations at the warm edges of their thermal ranges (Free et al., 2019).

doi:10.6342/NTU202500202

The warming of ocean waters has led to "tropicalization" of temperate regions, where tropical species moving into temperate waters fundamentally alter ecosystem structure (Vergés et al., 2016). Temperature effects manifest through both direct physiological impacts and indirect ecosystem effects, with species' thermal limits closely matching their realized temperature ranges (Sunday et al., 2015). Changes in temperature alter food web dynamics, as warming-induced changes in plankton communities' cascade through marine food webs (Hoegh-Guldberg and Bruno, 2010).

In the North Sea, seasonal temperature fluctuations (5°C in winter to 16°C in summer) create distinct seasonal habitats (Dulvy et al., 2018). While some species like cod actively avoid waters above 13°C, others such as European seabass prefer warmer waters and extend their range northward during summer months (Baudron et al. 2020). Fish biomass shows complex responses, with the North Sea experiencing a 97% increase in 2011, preceded by a 6% decline during anomalously high temperatures (Fredston et al., 2023).

Climate projections under aggressive emission pathways indicate that approximately 90% of marine life could face severe survival challenges (Boyce, et al., 2022). Effects are particularly pronounced at higher trophic levels, where apex predators exhibit greater sensitivity to climate-induced changes (Boyce et al, 2015). Rising ocean temperatures have reduced marine fisheries productivity and limited sustainable fishery yields (Gattuso et al., 2015, Cheung et al., 2016), with overfished populations showing increased susceptibility to warming impacts (Free et al., 2019). While some cold-region populations initially benefited from warming, these advantages are diminishing as temperatures continue to rise (Pörtner, 2007), leading to a 4.1% decrease in maximum sustainable yield from the 1930s to 2010 (Free et al., 2019).

doi:10.6342/NTU202500202

1.2 Impact of acidification on fish

Ocean acidification (OA) represents a significant anthropogenic perturbation of marine chemical equilibria, primarily driven by atmospheric carbon dioxide (CO_2) absorption into oceanic systems. The fundamental process initiates when atmospheric CO_2 dissolves in seawater, forming carbonic acid (H_2CO_3) which dissociates into hydrogen ions (H^+) and bicarbonate ions (HCO_3^-). This process has led to a measurable decline in seawater pH from pre-industrial levels of approximately 8.2 to current levels of 8.1, representing a 30% increase in acidity due to the logarithmic nature of the pH scale (NOAA).

The impacts of OA on fish are both direct and indirect, manifesting through multiple physiological and behavioral pathways. Fish experience fundamental disruptions to their acid-base regulation mechanisms, which affects their overall metabolic functioning and aerobic capacity. Their sensory capabilities, crucial for survival behaviors such as predator avoidance and food location, become compromised. Furthermore, both reproductive success and developmental processes, such as gamete maturation (egg/sperm development), fertilization success rates, egg hatching success, embryonic development are significantly impaired (Le Quesne and Pinnegar, 2012). As well as sensory capability impacts, leading to affecting species ability to: detect predators, locate food sources and navigate their environment due to the changes in otolith (ear bones used for balance and orientation) development (Le Quesne and Pinnegar, 2012). These physiological alterations cascade into broader population-level effects, influencing growth rates, survival probabilities, and reproductive output (Kroeker et al., 2013).

Behavioral changes are particularly pronounced in reef species, where OA impairs neurological function, affecting habitat selection and migration patterns, which in turn influences species distribution (Nagelkerken and Munday, 2016). Studies have

doi:10.6342/NTU202500202

documented species-specific impairment of physiological functions, particularly regarding organisms' aerobic performance capabilities (Tai et al., 2021; Vargas et al., 2017). Research has revealed significant alterations in behavioral patterns and cognitive processes among various fish species, potentially affecting their ability to survive in their changing environments (Moreira et al., 2022).

The situation becomes more complex when considering the interaction between OA and other climate change stressors. For ectothermic organisms, rising ocean temperatures create increased oxygen demands as they struggle to maintain basic metabolic functions (Pörtner and Lannig, 2009). This elevated oxygen requirement significantly reduces their aerobic scope—the crucial capacity to increase metabolic rate above baseline maintenance levels. This reduced aerobic capacity has far-reaching implications for life-history characteristics, including growth trajectories and maximum attainable body sizes (Pauly and Cheung, 2017), which ultimately influence large-scale population dynamics and ecosystem structure (Cheung et al., 2011).

1.3 Impact of oxygen depletion on fish

When oxygen levels drop in marine waters, fish face immediate physiological challenges. Fish require dissolved oxygen to sustain their cellular respiration. Under hypoxic conditions (typically defined as dissolved oxygen levels below 2 mg/L), fish struggle to extract sufficient oxygen through their gills. This directly leads to increased mortality rates (Tai et al. 2021), particularly among species that cannot quickly relocate to better-oxygenated waters, as even brief exposure to severe hypoxia can cause widespread fish die-offs in affected areas.

The ability to sustain efficient aerobic performance, meaning the capacity to meet metabolic oxygen needs, is crucial for ectothermic animals to maintain their energy balance, survive, and prevent a decline in fitness as temperatures rise.

doi:10.6342/NTU202500202

Fish response to low oxygen conditions are reflected in the metabolic impacts. Rising ocean temperatures go along with the decrease of dissolved oxygen concentration (Clarke et al. 2022). Metabolic rates increase with rising temperatures, which results in a higher oxygen demand to sustain aerobic processes in warmer waters. The increased need for oxygen may exceed the capacity of certain fish species to meet these demands, even in pelagic zones with abundant oxygen (Deutsch et al., 2015). This imbalance can reduce the aerobic scope—the difference between standard and maximum metabolic rates—potentially triggering trade-offs among essential physiological functions reliant on oxygen, such as growth and reproduction. When fish detect declining oxygen levels, their bodies initiate a series of compensatory mechanisms. Under hypoxic stress shows reduced swimming activity and feeding behavior to conserve energy (Moreira et al., 2022). Their bodies shift toward anaerobic metabolism - a less efficient way of producing energy that can't be sustained long-term. This metabolic stress has far-reaching consequences for their overall health and survival. These effects compound each other: metabolic stress makes it harder for fish to escape predators or find food, reduced reproduction rates mean populations recover more slowly from losses, and the energy costs of relocating further strain already stressed individuals. The resulting changes in fish distribution and abundance can fundamentally alter marine ecosystems through bottom-up controls in a food web.

The effects on growth and reproduction are equally concerning. It was revealed that fish in oxygen-depleted waters show significantly reduced growth rates because they must divert energy from growth to basic survival functions (Clarke et al., 2022). Reproduction becomes particularly challenging - fish need substantial energy reserves to produce eggs or sperm, and under hypoxic conditions, many species either delay

doi:10.6342/NTU202500202

spawning or produce fewer, less viable offspring. This creates a troubling feedback loop where populations become less resilient over time.

In response to changing water conditions species tend to relocate to oxygen-rich areas (Campana et al., 2020, Cheung, et al., 2015, Meyer-Gutbrod et al., 2021). When fish move to new areas, they may face different predators, compete with resident species for resources, or become unavailable to fishing communities that have historically depended on them.

1.4 Study Area

1.4.1 Geographical characteristics

The North Sea is a shallow marginal sea located on the continental shelf of the Atlantic Ocean. It is bordered to the west by the British Isles, including the Orkney and Shetland Islands, to the east by the Scandinavian and Jutland peninsulas, and to the south by the European coastline. It is surrounded by the Norwegian Sea in the north, in the east - by the Baltic Sea through the straits Skagerrak, Kattegat, Eresund, Great Belt and Small Belt, in the south-west - by the straits Pas de Calais, La Manche and in the north-west - by the Atlantic Ocean by inter-island straits. It washes the coasts of several European countries: the United Kingdom, France, Belgium, the Netherlands, Germany, Denmark and Norway. The boundaries are the following: 61°N (connecting Norway to the Shetland Islands), Southern boundary: 51°N (the Dover Strait), Western boundary: 4°W (along British coast), Eastern boundary: 7°E (along Danish and Norwegian coasts). Its area is 565 thousand km^2, with a surface area of 565 thousand km^2, with the Atlantic Ocean in the north-west. It is considered to be a rather shallow basin, as its mean depth is about 30 m, deepening up to 200 m in the northwest (OSPAR, 2000).However, it's important to note that the depth varies significantly across different regions of the sea: the southern

doi:10.6342/NTU202500202

part is generally shallower (20-30 meters); the central region has moderate depths (50-100 meters); the northern area, particularly near the Norwegian trench, is much deeper (reaching depths of over 700 meters) (GEBCO). The deepest point is 725 m, located by the Norwegian Trench, which serves as the main deepwater exchange with the North Atlantic gyre (Sündermann and Pohlmann, 2011). Cyclones happen during winter months, bringing more turbulent sea conditions. Oceanic forces that govern the North Sea's conditions are closely tied to the polar jet stream, a major atmospheric current that influences the trajectory and intensity of weather systems, shaping the overall wind and wave dynamics in the area.

Regarding the separation of the North Sea according to the fishing region. it falls within FAO Major Fishing Area 27, specifically designated as the Northeast Atlantic region in the FAO's global marine classification system. Within this broader area, the North Sea comprises Subarea 4, which is further subdivided into distinct divisions for more precise fisheries management and data collection. The specific divisions within FAO Subarea (Fig. 1) 4 include three divisions: division 4.a: Northern North Sea, division 4.b: Central North Sea Division 4.c: Southern North Sea (FAO, 2024).

1.4.1.1 Hydrological Characteristics

The intrusion of high-salinity Atlantic Waters changes the overall hydrological properties of the North Sea. Through two pathways: the Fair Isle Current between Orkney and Shetland, and the East Shetland Atlantic Inflow along the western edge of the Norwegian Trench with greater than 35 psu water masses enter the North Sea basin (Salt et al., 2013). The inflowing Atlantic water follows distinct pathways: the northern inflow follows the western slope of the Norwegian Trench, the central North Sea branch crosses the North Sea plateau and the southern inflow enters through the English Channel (Otto et al., 2022).

doi:10.6342/NTU202500202

Coastal regions, particularly in the southern and eastern North Sea, show reduced salinity (30-34 PSU) due to riverine input (Radach and Pätsch, 2007). The North Sea receives substantial freshwater input from several major rivers, including the Rhine, Elbe, and Thames. These rivers transport significant volumes of freshwater, sediments, and nutrients into the marine environment, influencing salinity levels and nutrient dynamics. The average annual freshwater discharge into the North Sea is approximately 300 cubic kilometers, with the Rhine contributing about 70 cubic kilometers per year (Radach, G., & Pätsch, J., 2007). In shelf seas along continental margins, powerful tidal movements are frequently observed, generating significant turbulent mixing. These tidal forces are often so intense in certain regions that they prevent any seasonal surface buoyancy changes from creating layered water columns, effectively blocking stratification from developing. However, in locations where tidal mixing is less powerful, the water column can separate into distinct temperature layers during spring and summer months, as solar radiation warms the surface waters. Between these two distinct zones - the mixed and stratified areas - lies a narrow boundary region known as the 'tidal mixing front' (van Aken, et al. 1987).

The influx of freshwater from these rivers leads to the formation of river plumes—areas where freshwater mixes with seawater—creating regions of reduced salinity and elevated nutrient concentrations. These plumes are particularly prominent near river mouths and can extend considerable distances offshore, depending on river discharge rates and prevailing oceanographic conditions. For instance, the Rhine River plume can influence salinity and nutrient levels over large areas of the southern North Sea (EMODnet, 2000).

The presence of large river plumes significantly impacts the marine ecosystem. The nutrient-rich freshwater promotes phytoplankton growth, forming the base of the

doi:10.6342/NTU202500202

marine food web. However, excessive nutrient input can lead to eutrophication, causing algal blooms and subsequent oxygen depletion, which adversely affects marine life (Jickells, 1998). In summary, riverine inputs as well as the ocean currents play a crucial role in shaping the North Sea's hydrology and biology.

1.4.1.2 Currents

The North Sea's circulation system exhibits a complex pattern of surface and bottom currents that play a crucial role in ecosystem functioning and species distribution. The primary surface circulation follows a counterclockwise pattern, with Atlantic water entering from the north between Scotland and Norway, and through the English Channel in the south (Turrell et al., 1992). This inflow creates two main branches: the Norwegian Coastal Current flowing northward along the Norwegian coast, and the central North Sea circulation moving southward along the British coast (Otto et al., 1990). In can be seen on Fig. 2. The surface currents are significantly influenced by wind patterns, particularly during winter storms, which can temporarily alter circulation patterns and mixing depths. Bottom currents follow a different pattern, with dense Atlantic water moving along the Norwegian Trench, creating important pathways for nutrient transport and larval dispersal (Sündermann and Pohlmann, 2011). The interaction between surface and bottom currents becomes particularly important in areas of upwelling and downwelling, where nutrient exchange supports high biological productivity (Hill et al., 2008). These circulation patterns demonstrate significant seasonal and interannual variability, influenced by atmospheric forcing, freshwater input, and larger-scale oceanic processes such as the North Atlantic Oscillation (NAO), which affects the strength and position of the main current systems (Mathis et al., 2015). Understanding these current patterns is crucial for predicting changes in marine ecosystems and managing fisheries resources, particularly as climate change influences oceanic circulation patterns (Holt et al., 2018).

doi:10.6342/NTU202500202

1.4.1.3 Frontal Systems

The North Sea's hydrography is characterized by several permanent and seasonal frontal systems that significantly influence biological productivity and marine species distribution. These fronts arise from differences in temperature, salinity, and water column stratification (Huthnance et al. 2016). The Flamborough Head Front, located off England's east coast, forms through interaction between mixed coastal and stratified central North Sea waters, enhancing primary productivity through nutrient exchanges. The Central North Sea Front develops in deeper regions during summer when solar heating creates a sharp thermocline, supporting high biological productivity through the combination of nutrient-rich bottom waters and light availability in upper layers (Pingree & Griffiths, 1978).

The Skagerrak front, forming where saline North Sea waters meet fresher Baltic waters, maintains a strong year-round salinity gradient that supports substantial plankton growth and provides critical spawning habitat (Omstedt et al., 2004). The Norwegian Coastal Current Front flows northward along the eastern edge, showing seasonal variability influenced by riverine freshwater input, particularly during spring and early summer. These frontal systems exhibit seasonal variations in intensity and structure due to changes in solar radiation, freshwater input, and wind-driven mixing, while interannual variability is modulated by climate fluctuations such as the North Atlantic Oscillation (Holt et al. 2014).

The significance of these frontal systems extends to both biological productivity and fisheries, with enhanced planktonic food availability sustaining fish stocks. However, anthropogenic pressures, including climate change and eutrophication, threaten to alter frontal dynamics, potentially affecting the entire marine ecosystem (Piet et al, 2009). Seasonal stratification patterns are particularly pronounced in central and northern

doi:10.6342/NTU202500202

regions between May and September, creating a two-layer system crucial for nutrient cycling and biological production, while southern regions remain well-mixed due to tidal forces and shallow depths (Mathis et al., 2015).

1.4.1.4 Atmospheric circulation

Strong westerly winds play a critical role in wave generation across the North Sea, producing powerful waves and swells that significantly impact shipping, fisheries, and coastal erosion. This wave activity is further intensified when the Cyclones happen during winter months, bringing more turbulent sea conditions. The wind patterns in the North Sea are also closely tied to the polar jet stream, a major atmospheric current that influences the trajectory and intensity of weather systems, shaping the overall wind and wave dynamics in the area. These combinations of factors emphasize the intricate interplay of atmospheric and oceanic forces that govern the North Sea's conditions.

1.4.1.5 Temperature Regime

The North Sea exhibits complex thermal dynamics characterized by distinct spatial and temporal patterns. In its northern reaches, water temperatures demonstrate remarkable stability, maintaining a range of 6-8°C near the seafloor throughout the annual cycle. This thermal consistency stems from the significant influence of Atlantic water masses and the greater depths in this region. The southern portion, however, presents a more dynamic thermal regime owing to its shallower bathymetry and reduced mixing processes (Anderson 2021).

The thermal structure varies significantly between seasons. During winter months, surface temperatures fluctuate from a minimum of 2°C in northern waters to approximately 7°C in southern regions. This gradient reflects the combined influence of Arctic water intrusion in the north and the moderating effect of continental Europe's

doi:10.6342/NTU202500202

landmass in the south. Summer conditions bring more pronounced variations, with surface waters warming to 12-19°C, following a distinct latitudinal gradient (Martinez-Lopez et al. 2024). Bottom water temperatures are more stable but show spatial variation, with the northern North Sea maintaining temperatures of 6-8°C year-round, while southern regions experience greater seasonal fluctuation (Quante et al., 2016).

Climate change has emerged as a significant driver of long-term thermal modifications in the North Sea ecosystem. Observations indicate a warming trend of 1-2°C in mean annual temperatures since the mid-twentieth century, with the most pronounced effects observed in the southern and central basins where shallower waters respond more readily to atmospheric heating (Martinez-Lopez et al. 2024).

The interaction between temperature patterns and water column structure creates distinct stratification regimes. The deeper northern sector maintains relatively uniform vertical mixing due to strong tidal influences and wind-driven processes. Conversely, the southern region develops marked seasonal stratification during summer months, characterized by a well-defined thermocline separating warmer surface waters from cooler bottom layers. This stratification pattern fundamentally influences nutrient cycling and biological productivity throughout the ecosystem.

These physical parameters have profound implications for ecosystem functioning. Enhanced stratification can restrict vertical nutrient transport, potentially affecting primary productivity patterns. Additionally, the warming trend has triggered biogeographical shifts, with warm-water species expanding their range northward while cold-adapted organisms retreat to maintain their preferred temperature ranges.

1.4.2 Current Ecological Issues

The marine ecosystem of the North Sea has undergone profound transformations in recent decades, revealing patterns that demand careful scientific scrutiny. Thermal

doi:10.6342/NTU202500202

measurements across multiple observation stations demonstrate an unprecedented acceleration in warming rates since the late twentieth century. Data analysis reveals that the water masses experience thermal enhancement at approximately 0.1°C annually, transforming the traditional temperature regime of this continental shelf sea (Høyer & Karagali, 2016).

Ocean current dynamics within the North Sea basin have experienced notable modifications. The influx patterns of Atlantic waters, which historically maintained consistent routes, now demonstrate altered trajectories and intensities. These circulation shifts potentially reorganize nutrient distribution patterns and influence larval transport mechanisms, thereby affecting ecosystem functionality at multiple trophic levels. Stronger and longer-lasting stratification periods have been observed, potentially affecting nutrient cycling and primary production (Mathis et al., 2015).

Contemporary research indicates an increasing frequency of extreme weather events affecting the North Sea region. Storm patterns show greater intensity and modify seasonal timing, leading to enhanced mixing events that temporarily disrupt established stratification patterns. These meteorological changes contribute to altered sediment transport dynamics and coastal erosion processes.

Stronger and longer-lasting stratification periods have been observed, potentially affecting nutrient cycling and primary production (Mathis et al., 2015). Modifications in Atlantic inflow patterns have been documented, with potential implications for ecosystem functioning (Quante et al., 2016).

The North Sea has been experiencing a gradual rise in sea level, consistent with global trends driven by climate change (Calafat et al., 2022). Sea level changes in this region are influenced by a combination of global factors, such as thermal expansion and

doi:10.6342/NTU202500202

glacial melting, and regional dynamics, including land subsidence and variations in ocean circulation.

Over the 20th century, sea levels in the North Sea rose at an average rate of approximately 1–2 mm per year (Wahl et al. 2013). This rate has accelerated in recent decades, with recent studies estimating a rise of around 3–4 mm per year since the early 1990s. The increasing rate of rise aligns with global observations, reflecting heightened contributions from melting ice sheets in Greenland and Antarctica and the expansion of warmer ocean waters.

Regional studies reveal that the rate of sea-level rise varies across different parts of the North Sea due to local factors such as land subsidence, which is more pronounced in the southern areas, particularly along the coasts of the Netherlands and Belgium. In contrast, some northern regions are experiencing relative stability due to post-glacial rebound, where landmasses previously compressed by ice sheets are slowly rising.

The southern North Sea, characterized by shallow waters and densely populated coastlines, is particularly vulnerable to sea-level rise. Coastal areas such as the Netherlands and eastern England are already facing challenges from rising sea levels combined with land subsidence. In the northern parts of the North Sea, near Norway and Scotland, relative sea level rise is slower due to ongoing land uplift from post-glacial rebound (OSPAR, 2009). However, even these regions are not immune to the impacts of global sea-level rise over longer timescales.

Seasonal and interannual variations in sea level, driven by wind patterns, atmospheric pressure, and storm surges, may amplify the impacts of long-term sea-level rise. For example, storm surges combined with higher baseline sea levels are likely to increase the frequency and severity of extreme flooding events, particularly during winter months (OSPAR, 2009).

doi:10.6342/NTU202500202

Other ecological threats that the North Sea experiences are pollution with the plastics from fishing nets and other hazardous substances and form river discharge, Significant Reduction of Nutrients, oil spills and pollution from the vessels: touristic, cargo, fishery and military (OSPAR, 2009).

The given overview of the list of unresolved problems that are happening in the North Sea region and overfishing, and ecosystem change are among the most important ones.

1.4.3 Economical Importance

The North Sea represents one of Europe's most vital marine ecosystems, characterized by exceptional ecological and economic significance in the Northeast Atlantic region (Engelhard et al, 2011). This semi-enclosed sea harbors over 200 fish species (ICES, 2021) and generates approximately €3 billion annually through its fisheries sector, establishing itself as a cornerstone of European maritime commerce (ICES).

While overall fishing effort of commercial species decreased from 4 million tonnes in the 1970s to about 2 million tonnes in 2020s, many high-value species maintain stable population levels. The landing has seen a slight recovery after 2011, with species such as cod (*Gadus morhua*), saithe (*Pollachius virens*), mackerel (*Scomber scombrus*), blue whiting (*Micromesistius poutassou*), and sole (*Solea solea*) representing sustainable commercial fish populations in the North Sea (ICES, 2022). However, demersal non-target fish species face dramatic population decline, raising concerns as their conservation is not a top priority for the fishery sector. For instance, the European Union has not implemented specific fishing regulations for Atlantic wolffish (*Anarhichas lupus)* populations in North Sea waters (Bluemel et al. 2021).

doi:10.6342/NTU202500202

The North Sea has emerged as a climate change hotspot, experiencing temperature increases at rates exceeding global averages (Hilborn et al., 2023). The most significant physical disruptions to the seabed are linked to mobile bottom-contacting fishing gear, particularly in the eastern English Channel, nearshore zones of the southeastern North Sea, and the central Skagerrak. Additionally, bycatch of protected species, such as common dolphins in the western English Channel, poses risks to long-term population viability (ICES, 2022).

The region's economic landscape is evolving, with the traditional hydrocarbon industry operating alongside rapidly expanding renewable energy installations, particularly offshore wind farms (Saraji & Akindipe, 2024). Maritime transport infrastructure maintains crucial significance, facilitating approximately €25 billion in annual economic activity through major port operations (European Commission, 2022). Industry projections from WindEurope anticipate reaching 323 gigawatts of total wind capacity by 2030, with 70 gigawatts from offshore installations.

Ocean energy presents additional growth potential, with projections of 337 gigawatts of global wave and tidal energy capacity by 2050. European installations could contribute 100 gigawatts, potentially meeting 10% of European Union energy demands (Interreg). These developments emphasize the necessity for comprehensive monitoring and forecasting of the North Sea, balancing the region's bio productivity with resource demands through effective policy implementation and technological advancement.

1.4.4 Fishery Regulations in the North Sea

As mentioned previously, the North Sea, a crucial marine ecosystem bordered by six European nations, represents one of the world's most intensively fished waters. The management framework has evolved significantly since 2020, particularly following

doi:10.6342/NTU202500202

Brexit, operating through a complex multi-jurisdictional system governed by the EU Common Fisheries Policy (CFP) and bilateral agreements with the United Kingdom.

Current quota distributions reflect both historical rights and recent political developments. In the pelagic sector, Norway holds 35% of total allowable catch for species like herring and mackerel, while EU member states collectively manage 45%, with Denmark (20%) and the Netherlands (15%) holding the largest shares. The UK maintains 20% of pelagic quotas. Demersal quotas follow a different pattern, with the UK holding 30%, Norway 25%, and EU member states collectively managing 45% (ICES, 2023).

The regulatory framework centers on Total Allowable Catches (TACs) and technical measures, including gear specifications and seasonal closures. Management is informed by scientific advice from ICES and aims to maintain Maximum Sustainable Yield (MSY) levels. Recent assessments by OSPAR (2023) indicate that despite improvements in individual stocks, marine fish populations across coastal, pelagic, and demersal communities have not achieved satisfactory environmental status.

Climate change has emerged as a critical factor influencing stock dynamics. The fishing industry has responded with substantial adaptations, with the pelagic sector investing over €500 million in fuel-efficient vessels and adaptive strategies.

Conservation efforts focus particularly on vulnerable species. OSPAR has identified 22 fish species facing significant threats, with only four species - houting, long-snouted seahorses, allis shad, and salmon - benefiting from ecologically coherent protected area coverage. Studies by Bastardie et al. (2022) demonstrate varied resilience patterns across species, with cod populations emerging as a critical limiting factor due to depleted stock levels. The cod's recruitment difficulties have broader ecosystem effects,

doi:10.6342/NTU202500202

with its Landing Obligation requirements leading to approximately 10% reduction in catches of other species, demonstrating the interconnected nature of species management.

The management framework includes specific protective measures:

- Seasonal spawning closures (e.g., cod protection January 15 - March 31)
- Stock recovery plans with real-time closure systems
- Marine Protected Areas like the Dogger Bank and Fladen Ground
- National regulations complementing international measures

Current modeling indicates that while individual environmental disruptions show limited impact on overall risk profiles, multiple simultaneous challenges create significant risks to stock stability. However, these risks can be maintained below 20% through adaptive management and conservative fishing mortality targets.

The success of this regulatory framework depends heavily on international cooperation and science-based management approaches. Recent initiatives emphasize ecosystem-based management, recognizing that effective marine conservation requires understanding complex ecosystem interactions and coordinated action across jurisdictions. This integrated approach becomes increasingly crucial as climate change continues to influence species distribution and ecosystem dynamics in the North Sea.

2. Materials and methods

2.1. Data source

2.1.1. Biological data

Initial dataset consists of 188 species observed by bottom trawl datasets North Sea International Bottom Trawl Survey (NS-IBTS) provided by ICES (Fig. S.1). The gear and sampling protocols are described in ICES (2020a) and data was obtained on the Database

doi:10.6342/NTU202500202

of Trawl Surveys (DATRAS). DATRAS, maintained by the International Council for the Exploration of the Sea (ICES), is a vital repository of data collected through various national trawl surveys conducted by marine research institutions. Established in 2011, DATRAS plays a key role in supporting ICES scientific efforts, including fish stock assessments and ecological studies, while also being accessible to the broader public (ICES, 2011). Such data on hauls are often used in fisheries management to ensure that ecosystems are not overexploited. It aggregates trawl survey data from regions like the North Sea, the Baltic Sea, and the Northeast Atlantic, providing essential insights into the distribution and abundance of marine species. The main gears in the region for benthic and demersal fish catch are otter trawls and beam trawls (ICES, 2022). Bottom trawling surveys were held during the day, following individual standard operating procedures by using fixed mesh size nets with a 30 min trawling duration at each station (Lai, et al, 2024). The depth range did not exceed 200 m, and since the trawling does collect fish at depths ranging from the surface to the seabed, which means that bottom trawls may occasionally capture pelagic species due to behavioral or habitat overlaps.

Datasets were rasterized as one record per grid cell per time. Fish species were marine, by their habitat preferences they were divided into demersal, which were the dominant group, with fewer bathydemersal, pelagic, benthopelagic and benthic species based on “Fishbase” life-hystory tools repository (Froese, R. and D. Pauly, 2024). The grid consisted of 221 cells, from 49° N - 62 °N, 4°W — 13° E on 1° x 1° (60arcmin). Timescale included records for the 1983 - 2024 period of the first quarter of the year. The data consisted of presence (0) and absence (1) matrix, referring to the species occurrence data. Each observed cell on the map depicts the hauls’ location (Fig. 3).

Filtering was done based on several assumptions. Firstly, only those species from the entire dataset were selected that had long-time observations, that was more or equal

doi:10.6342/NTU202500202

to 30 years of consistent observations in the given period. It means that at least 1 grid-cell was observed for each year (Fig. S.1). This reduced the number of unique species from 188 to 56. Secondly, a linear regression model for a temporal trend has been applied to see how the occurrence changed over time for each species. I extracted only those species that did show change: either increase in the number of occurrence grids or decrease throughout 1983-2024. It was done based on the statistical coefficients, obtained from the regression model with the following thresholds: slope (main coefficient) > 0.5 in absolute value, $r^2 > 0.5$, the significance (*) replicate the p-values as: p-value < 0.001 ~ *** (Table 2).

Such a time-dependent threshold was taken as, firstly, it represents a timeframe long enough to capture natural climate variability while filtering out shorter-term weather fluctuations. The World Meteorological Organization (WMO) established this as a standard baseline period because it effectively balances between being long enough to include year-to-year natural variations and climatic cycles, but short enough to show longer-term climate trends. It typically spans multiple generations of most species, allowing for observation of population-level responses to climate variations and captures important climatic oscillations and cycles such as North Atlantic Oscillation (NAO), that has a big impact on the North Atlantic and the North Sea particularly (Stenberg, et al. 2015). Thus, NAO exhibits variability across multiple timescales: can fluctuate intra-seasonally, showing changes within weeks or months. However, the most prominent and well-documented variations may occur inter annually: year-to-year variations that are significant for regional climate pattern, decadal (7-10 years) and multi-decadal: exhibits longer-term trends spanning 20-30 years (Deser et al., 2017). Also, The Central Limit Theorem states that for a sufficiently large sample size, the sampling distribution of the sample mean approaches a normal distribution, regardless of the population's distribution.

doi:10.6342/NTU202500202

While "sufficiently large" can vary, 30 samples are widely regarded as the minimum threshold for the CLT to hold true, making it a standard benchmark in many statistical analyses (Anderson, C.J. 2010). The graph in Fig. 5 illustrates significant shifts in species abundance, with notable changes in community composition indicated by crossing trend lines. Demersal species (e.g., *Eutrigla gurnardus, Amblyraja radiata*) and pelagic species (e.g., Engraulis encrasicolus, Sardina pilchardus) show contrasting distribution patterns, suggesting potential climate-driven community reorganization.

Species were also categorised with their trophic level (Fig. 6, Table 1), based on the available data from Fishbase tools (Froese & Pauly, 2024). It represents species' position in the food web: primary producers (~1.0) - phytoplankton and algae, which produce their own energy via photosynthesis; primary consumers (~2.0) - zooplanktons, that consume primary producers; secondary consumers (~3.0) - carnivores or omnivores fish that feed on herbivores; tertiary consumers (~4.0 and above) - big fish and marine mammals - predators that feed on other carnivores (Pauly et al, 1998). Trophic levels offer valuable insight into a species' ecological position, diet, and the broader dynamics of marine ecosystems. Species with higher trophic levels occupy top positions in the food chain, playing a crucial role in regulating populations of species at lower levels. Conversely, species at lower trophic levels often serve as prey for larger predators. Based on the figure I can make some notable observations. *Merluccius merluccius* (European hake) has one of the highest trophic levels, around 4.2, indicating it's a top predator. *Sebastes viviparus* (Norway redfish) shows the widest range of uncertainty in its trophic level. Lower trophic level species like *Engraulis encrasicolus* (European anchovy) and *Buglossidium luteum* (solenette) are around 3.0-3.2, suggesting they feed on smaller prey. Most species cluster between trophic levels 3.5-4.0, indicating they are intermediate predators.

doi:10.6342/NTU202500202

2.1.2 Environmental data

Earth System Models (ESMs) represent one of the most sophisticated tools for understanding climate change, integrating complex interactions between the atmosphere, oceans, land, and ice systems. These models, developed by leading climate research institutions, come together in the Coupled Model Intercomparison Project (CMIP), a collaborative initiative that has evolved through six phases over three decades to improve climate predictions and understanding.

For this research, two crucial time periods were obtained: historical data from 1983-2014, which allows us to validate model accuracy by comparing predictions with actual observations, and future projections spanning 2015-2100, which help us anticipate potential climate changes. The data, accessed through the German Climate Computing Centre's Inter-Sectoral Impact Model Intercomparison Project (ISIMIP), provides a detailed global view with a spatial resolution of 1°x1° (approximately 111 km at the equator), allowing for comprehensive analysis of regional climate patterns (NOAA, National Ocean Service, 2024).

Here is specifically utilized climate projections from the Institute Pierre Simon Laplace (IPSL) Climate Model version 6A-Low Resolution (IPSL-CM6A-LR), a state-of-the-art model developed as part of CMIP6. Since future human activities and resulting greenhouse gas emissions cannot be predicted with certainty, scientists have developed various socio-economic scenarios to explore possible futures (Davies et al., 2023).

These scenarios, known as Shared Socioeconomic Pathways (SSPs), represent different possible trajectories for global development:

- SSP1-2.6 ("Sustainability"): This optimistic scenario envisions a world that embraces sustainable practices and aggressive climate protection measures. It assumes we'll limit radiative forcing (the change in Earth's energy balance) to 2.6

doi:10.6342/NTU202500202

W/m² by 2100, successfully keeping global temperature rise below 2°C. This pathway represents a fundamental shift away from fossil fuels toward renewable energy sources and sustainable development practices.

- SSP3-7.0 ("Regional Rivalry"): This middle-range scenario portrays a more fragmented world where international cooperation declines and regions focus on achieving energy and food security within their borders. With radiative forcing reaching 7.0 W/m² by 2100, this pathway was specifically designed to fill a crucial gap in our understanding of moderate-to-high emission scenarios (O'Neill, et al., 2016).
- SSP5-8.5 ("Fossil-fueled Development"): This represents the most challenging scenario for climate change, where global development continues to rely heavily on fossil fuels, leading to radiative forcing of 8.5 W/m² by 2100. This pathway helps us understand potential worst-case outcomes if minimal climate mitigation efforts are implemented.

ISIMIP3b simulation round was selected the for several key advantages: it incorporates these detailed SSP scenarios, uses sophisticated bias-correction techniques to improve the accuracy of climate model data, and provides detailed sector-specific simulations that are particularly valuable for understanding impacts on marine ecosystems and hydrology. The specific model configuration that was used (ensemble member r1i1p1f1) accounts for complex interactions between Earth's major systems, including atmospheric circulation patterns, ocean dynamics, land surface processes, and sea ice behavior (Boucher, O. et al, 2020).

Here I applied the r1i1p1f1 ensemble member, employed by ISMIP3 as ocean data from the Earth System Model IPSL-CM6A-LR, which includes:

- r1: First realization,

doi:10.6342/NTU202500202

- i1: Initialization method,
- p1: Physics configuration,
- f1: Forcing configuration.

This model integrates interactions between the atmosphere, ocean, land surface, and sea ice (Boucher et al., 2020). Advantages of the data include global consistency, high resolution, and coverage of both historical periods (e.g., pre-2015) for validation and future climate scenarios extending to 2100 or beyond (Büchner, 2024). The r1i1p1f1 ensemble member includes historical forcing (1983–2014) followed by projections aligned with SSPs.

It's important to note that while these models represent understanding of climate systems, they still face uncertainties, particularly regarding human behavior and industrial development. These uncertainties affect ability to precisely predict future emissions and land use changes (Davies et al., 2023), which is why examining multiple scenarios provides a more complete picture of possible future outcomes.

The six environmental variables included Sea Surface Temperature (SST, ◦C), Sea Bottom Temperature (SBT, ◦C) (Fig. 7A, B), sea surface pH, sea bottom pH (Fig. 8A, B), sea surface concentration of dissolved oxygen and sea bottom concentration of dissolved oxygen (mol m−3) (Fig. 8A, B). Surface variables refer to the 1 (m), and the bottom - to one that follows exactly the sea bathymetry and utilizes the maximum depth of the place. For all the extracted data, a monthly time step was selected, filtered as the mean of the first quarter: January-February-March (Q1), and the selected region of the North Sea (49° N - 62 °N, 4°W — 13° E). Later the mean value was calculated for the Q1 and used in the following steps for visualization and statistical modelling. Further documentation can be found at ISIMIP.

doi:10.6342/NTU202500202

Considering that most of the species in the dataset are demersal and pelagic, I also selected bathymetry as the predictor variable from ETOPO Global Relief Model by NCEI NOAA. However, later experiments have shown it's not useful.

For this thesis, the decade of 2015-2024 that had real-world trawling data, still had to be combined with the environmental parameters, even though ISIMIP provided only simulations under three SSPs for these years. In this case, I claim that the SSP3-7.0 was the one that represented the real-world situation better than the SSP1-2.6 and SSP5-8.5. (Sarofim et al., 2024; Shiogama & Fujimori et al., 2023). At the same time, it is important to mention that significant differences between the scenarios are unforeseen for the current year as they start to occur only from the middle of the century 2050 from the simulations, and the gaps become more severe with the time, that is why for the second decade of the 21st century the range between provided scenarios was minor.

The ISIMIP3b provides crucial environmental data that can be integrated into fisheries prediction frameworks. These variables offer high-resolution temporal and spatial information that can significantly enhance common understanding of fish distribution patterns and improve fishing location predictions.

2.2 Statistical methods

2.2.1 Species Distribution Models

Species distribution models (SDMs) represent a crucial methodological approach for exploring the effects of future global change on biodiversity (Jones et al. 2012). This modeling approach synthesizes ecological theory with statistical methods to map and forecast species distributions across landscapes and timeframes. The theoretical foundation builds on Hutchinson's (1957) concept of ecological niches, where the fundamental niche represents the complete range of environmental conditions supporting

doi:10.6342/NTU202500202

species survival, while the realized niche reflects actual species distribution constrained by biological interactions and competitive pressures (Austin et al., 1990; Guisan & Zimmermann, 2000).

The modeling landscape encompasses two primary approaches: data-driven correlative models analyzing statistical patterns (Jarnevich et al. 2015), and mechanistic models constructed on theoretical biological principles and calibrated with empirical data (Essington et al. 2022). To enhance predictive capabilities, ensemble modeling strategies are often employed, synthesizing outputs from multiple individual models through methods ranging from straightforward averaging to sophisticated weighted combinations (Araújo & New 2007).

The selection of appropriate modeling techniques depends significantly on data characteristics and research objectives. While presence-absence data traditionally provides robust predictions, presence-only data can effectively model potential habitat distribution, particularly when absence data may be unreliable due to sampling limitations or species mobility (Pearson & Dawson, 2003). Analysis by Valavi et al. (2021) reveals that model fitting methods significantly influence performance, with individually tuned model ensembles showing superior results compared to default framework settings.

Model complexity presents an important consideration in SDM development. Studies suggest that more complex models often demonstrate superior performance at finer spatial resolutions (Elith et al., 2006; Wisz et al., 2008). However, increased complexity can reduce generalizability and transparency - crucial factors for practical application and peer review (Drake et al., 2006). The challenge lies in striking an optimal balance between model sophistication and broad applicability.

SDMs have proven instrumental in predicting species responses to climate change, guiding conservation efforts, and informing policy decisions. However, future

doi:10.6342/NTU202500202

projection uncertainties encompass climate model accuracy at various scales and the unpredictability of extreme events. Ecological uncertainties present additional challenges, including variations in population responses, evolving species-environment relationships, and potential evolutionary adaptation (Davies et al., 2023). Success in SDM implementation relies on acknowledging these uncertainties while maintaining scientific rigor throughout the modeling process.

In this thesis I incorporated six different statistical methods (SDMs), including one "tree-based" method - Random Forest (RF), 3 regression methods - Generalised Linear Model (GLM), Generalised Boosting Model (GBM), Multivariate Adaptive Regression Splines (MARS) and two classification methods - Classification Tree Analysis (CTA), Flexible Discriminant Analysis (FDA). Initially I tested one more regression method - GAM, however it showed the lowest performance metrics that is why it was decided not to include this method in the models. Each model was run independently 15 times, producing 90 models for each temporal scenario.

The Generalized Linear Model (GLM) serves as a foundational approach, extending traditional linear regression by accommodating non-normal response distributions and non-linear relationships through link functions. While GLMs excel in providing clear statistical inference and handling both continuous and categorical predictors, they may struggle to capture complex, non-linear species-environment relationships. Their strength lies in their interpretability and computational efficiency, though they work best when relationships follow assumed distribution patterns.

The Generalized Boosting Model (GBM), also known as Boosted Regression Trees, represents a more sophisticated approach, building upon decision trees through a sequential boosting algorithm. Each new tree focuses on the residuals of previous trees, enabling the model to capture complex, non-linear relationships and interactions between

doi:10.6342/NTU202500202

predictors automatically. While GBMs often produce more accurate predictions than simpler models, they require careful parameter tuning and larger datasets for stable performance. Their complexity can make interpretation more challenging than GLMs.

Multivariate Adaptive Regression Splines (MARS) strikes a balance between GLMs and GBMs by combining regression splines with stepwise model selection. MARS automatically determines optimal locations for breaks in predictor variables and fits piece-wise linear functions between these breaks. This approach proves particularly effective for ecological threshold responses while maintaining better interpretability than GBMs. However, MARS may struggle with very complex, smooth relationships in species-environment interactions.

Classification Tree Analysis (CTA) creates decision trees through recursive binary splitting of data based on predictor variables. While CTAs offer intuitive interpretation and handle non-linear relationships well, they may oversimplify complex ecological relationships and are prone to overfitting if not properly pruned. Their step-function predictions can be useful for identifying ecological thresholds but may miss finer-scale patterns in species distributions.

Flexible Discriminant Analysis (FDA) extends traditional linear discriminant analysis by incorporating non-linear transformations of predictors. This approach works particularly well with presence-absence data and multiple predictors, offering a good balance between model complexity and interpretability. FDA proves more robust to violations of normality than traditional discriminant analysis but may struggle with very sharp ecological boundaries.

The key distinction between these models lies in how they handle complexity and their assumptions about species-environment relationships and the final choice of the model relies on the researcher – decision maker. GLMs provide a solid foundation but

doi:10.6342/NTU202500202

may miss complex patterns, while GBMs excel at capturing intricate relationships but require careful tuning. MARS offers a middle ground, with good interpretability and flexibility. CTAs provide clear decision rules but may oversimplify relationships, and FDA extends traditional discriminant analysis to handle non-linear patterns while maintaining interpretability.

2.2.2 Data processing

The scope of investigation needs careful consideration, particularly in determining appropriate spatial and temporal boundaries that align with the species' biological characteristics. The strength of the model heavily depends on selecting appropriate environmental variables, which should be guided by historical climate impact analysis and thorough understanding of species' physiological responses to both climatic and non-climatic factors. Overall, Davies et al. 2023 suggest selecting models in accordance with ecological principles, and not only with SDMs' predictive power for contemporary distributions.

I consider that the sampled areas—whether groups of cells or individual grid cells—may not fully represent the real-world situation. This is because it cannot be guaranteed that all fish being 'present' at the trawling stations were caught, and that absence of certain species might be due to random factors, but not their actual absence.

SDMs often rely on pseudo-absence methodology when true absence data is unavailable due to the challenges of confirming species non-occurrence through rigorous sampling, particularly for mobile or elusive species. The approach involves generating artificial absence points to complement presence data, enhancing the model's predictive capabilities. Different strategies exist for creating these pseudo-absences, ranging from simple random selection outside known presence areas to more sophisticated environmental and geographical exclusion methods. Random selection, which works

doi:10.6342/NTU202500202

particularly well with Generalized Linear Models (GLMs), involves randomly distributing points across areas where the species hasn't been recorded. More complex approaches combine environmental and geographical criteria, especially useful for machine learning techniques like Random Forests and Boosted Regression Trees. The choice of pseudo-absence generation method should also consider potential sampling biases in presence data - random selection works best with unbiased presence data, while stratified approaches are more suitable when dealing with geographical or climatic sampling biases. For optimal results, the pseudo-absence generation approach should be tailored to both the specific modeling technique being used and the characteristics of the available presence data, with regression models generally favoring random selection and machine learning models benefiting from combined environmental and geographical exclusion strategies (Barbet-Massin et al., 2012).

That is why it was decided to apply the pseudo-absence method. "Pseudo-absences (PA) (sometimes also referred as background data) are NOT to be considered as absences and rather represent the available environment in the studied area. They will be used to compare observed used environments (represented by the presences) against what is available." (Cran-R project). It has also been proposed that presence–absence data enhances an SDM's performance, as indicated by test statistics, leading to more dependable predictions (Brotons et al. 2004). Here was used the SRE method: a Surface Range Envelope model, that randomly selects PA outside this envelope, i.e. in conditions (combination of explanatory variables) that differ in a defined proportion from those of presence points.

This strategy assumes that the realized niche of the species has been fully sampled, either geographically or environmentally. Also, utilizes grid cells where species occurrence data is unavailable (marked as N/A) as potential locations for pseudo-absence

doi:10.6342/NTU202500202

generation. The protocol employs a systematic selection process whereby 3 times the number of presences is employed as PA through the whole 42-year period of observations. All "0" that were assumed as the true absence before were replaced by N/A that suppose possibilities of being mistaken in assuming the absence of the fish in species location. Eventually, the grid consists of "1" - presences, "0" - absences and N/As. The resampling was conducted once for each species with accordance to the certain environmental parameters' combination, since the SRE method does not have random sampling and is aware of the environmental conditions. This approach facilitates the development of robust species distribution models by providing a structured framework for absence data generation in areas where actual species occurrence data is unavailable.

The modeling approach was based on the initial hypothesis. Fish species were divided into two groups based on the habitat area: demersal (*Amblyraja radiata, Anarhichas lupus, Arnoglossus laterna, Buglossidium luteum, Callionymus maculatus, Chelidonichthys cuculus, Chelidonichthys lucerna, Cyclopterus lumpus, Eutrigla gurnardus, Merluccius merluccius, Mullus surmuletus, Mustelus asterias, Myoxocephalus scorpius, Raja montagui, Scyliorhinus canicula, Sebastes viviparus* - 16 in total) and pelagic (*Argentina sphyraena, Engraulis encrasicolus, Sardina pilchardus, Scomber scombrus, Trachurus trachurus* - 5 in total). Environmental variables were grouped in accordance, respectively, having the assumption that pelagic species are more prone to the conditions of the surface water conditions, while demersal and benthic species will be firstly affected by the bottom layer water state. In accordance with this, 5 pelagic species were put into environmental variable combinations with surface pH + SST, surface DO + SST, surface DO + surface pH, surface pH + surface DO + SST. Similarly, 16 demersal species were associated with the grouping for models bottom pH

doi:10.6342/NTU202500202

+ SBT, bottom DO + SBT, bottom DO + bottom pH, bottom pH + bottom DO + SBT, and two single-models with SST and SBT only (Table 3).

Implying correlation matrix between environmental variables helped to exclude high collinearity between surface and bottom variables that did not allow to properly distinguish species' range response to the independent influences (Bosch et al. 2018), and to provide more correct explanatory parameters that determine fish life cycle on a certain depth. As a result, strong positive correlations are observed between surface and bottom oxygen concentrations (o2_surf and o2_bot) as well as between surface and bottom pH levels (ph_surf and ph_bot) equal to 0.88, for both pairs respectively (Fig. 10A, B). This was so, as the model in ISIMIP used certain equations to get the bottom water characteristics, as well as that the deepwater conditions are a proxy of the surface conditions. Keeping these highly correlated variables could lead to several statistical issues after conducting empirical experiments. Including both surface and bottom variables artificially inflated the model's confidence in parameter importance and the model struggled to distinguish the individual effects of surface vs bottom pH and Dissolved Oxygen, leading to unstable coefficient estimates and inflated standard errors A notable negative correlation also exists between surface temperature (sst) and surface oxygen concentration (o2_surf) -0.91 and between bottom oxygen (o2_bot) -0.86 explain a clear inverse relationship: as water temperature increases, the solubility of oxygen decreases. At the same time I also consider that such strong negative correlation and means including both could mask their true individual effects, so it was important to also apply a single- temperature model.

Eventually, it was decided to reject the hypothesis of using the depth parameter to see its impact on the species, since it brought a lot of white noise, due to the fact that the North Sea's relatively low depth (median is less than 90 m) makes it important to

doi:10.6342/NTU202500202

distinguish the areas of different bathymetrhy, thus most of fish were caught in the area below 100m , so this range from the near-to-surface layers had the higher variable importance and remained the same for different model and different species. Moreover, depth displaced its importance over environmental parameters in 'single-model', not allowing for a comprehensive estimation of the real projected role of ambient environmental conditions (pH/DO/Temperature). Mean depth shows moderate correlations with oxygen and pH variables.

2.2.3 Ensemble modelling

To compute Species Distribution Models (SDMs), the R package BIOMOD2 (version 4.2-5.2, Thuiller et al., 2024) was employed within an ensemble modelling (EM) framework. This method minimizes prediction uncertainty caused by variations among individual models (Elith & Graham, 2009) by integrating outputs from 6 different algorithms to identify consistent patterns (Breiner et al., 2015; Marmion et al., 2009).

I implemented an ensemble modelling framework, with the following objectives: to minimize sampling biases for generating pseudo-absences, to enhance model evaluation processes, and to account for methodological uncertainties by integrating various modelling techniques. The resulting predictions were rasterized, with cell values ranging from 0 to 1, where higher values correspond to greater habitat suitability and higher probabilities of species presence. To reduce uncertainties associated with the selection of a single algorithm, ensemble modelling was applied. To ensure the reliability and robustness of SDM predictions, validation metrics such as the Receiver Operating Characteristic (ROC) curve, Accuracy, and the True Skill Statistic (TSS) are commonly employed.

The Receiver Operating Characteristic (ROC) curve is a widely used tool for evaluating SDM performance. It plots the true positive rate (sensitivity) against the false

doi:10.6342/NTU202500202

positive rate (1-specificity) across a range of threshold values. The area under the ROC curve (AUC) provides a single metric that summarizes the model's discriminatory ability (Hanley & McNeil, 1982). An AUC value of 0.5 indicates random performance, while values closer to 1 reflect a highly accurate model (Fielding & Bell, 1997). For fish distribution studies, AUC is particularly useful because it is threshold-independent, making it ideal for assessing models predicting presence-absence patterns over varying environmental gradients.

Accuracy is another straightforward and interpretable metric that measures the proportion of correctly classified observations among all predictions. It combines true positives and true negatives into a single value, providing a general sense of the model's predictive performance. In fish distribution models, where absences often outnumber presences, researchers may need to complement accuracy with other metrics to avoid biased assessments (Allouche et al., 2006).

The True Skill Statistic (TSS) is a threshold-dependent metric that overcomes some of the limitations of accuracy. TSS accounts for both sensitivity (true positive rate) and specificity (true negative rate) and is calculated as: A TSS value of 1 indicates perfect performance, while a value of 0 reflects performance no better than random. Unlike accuracy, TSS is not affected by prevalence, making it especially valuable for ecological applications where species occurrences are rare. For modeling fish distributions, TSS ensures that the model's ability to correctly predict both presences and absences is equally weighted, providing a balanced evaluation (Pontius & Millones, 2011).

The binary transformation was performed by applying the threshold that optimized the True Skill Statistic (TSS; Allouche, Tsoar & Kadmon, 2006). TSS is calculated as the sum of sensitivity and specificity minus one, where sensitivity represents

doi:10.6342/NTU202500202

the proportion of correctly predicted presences, and specificity denotes the proportion of correctly predicted absences (Barbet-Massin et al, 2012).

This multi-metric approach allowed us to identify potential weaknesses in model predictions and improve their robustness. Thus, not all the models did show good model allegiance and high metrics. That is why I had to include only “best” species based on the statistical outputs and understanding of ecological processes. I excluded SDMs with performance metrics lower than 0.75 and used TSS as the main performance metric.

Cross-validation helps in evaluating model projection accuracy and confirms projection uncertainty intervals (Yates et al., 2022). That is why to prevent possible biases a k-fold cross-validation run was performed for each algorithm for 5 different groups of environmental variables and all selected 21 species. k-Fold Cross-Validation is a method used to evaluate a machine learning model's performance. Model validation typically employs a technique where the dataset is divided into separate portions. The model is trained using one segment of the data and then tested against the reserved portion to assess its predictive accuracy. Researchers can choose between different partitioning methods, such as removing individual data points one at a time ('leave-one-out' approach) or dividing the data into larger segments ('k-fold' method). Each approach carries distinct statistical consequences that must be carefully considered (Yates et al. 2022).

The model is trained and tested k times—once on each fold as a test set while the remaining k−1 folds are used for training. This ensures each data point is used for both training and testing. If k=5 and the process is repeated 3 times, the validation procedure is extended as follows: Single k-Fold Execution represents the dataset randomly divided into 5 folds (or subsets), In each iteration, one-fold is used as the test set, and the other 4 folds are used as the training sets. This results in 5 iterations per execution (one for each fold). By repeating the 5-fold cross-validation 3 times, the dataset is reshuffled differently

doi:10.6342/NTU202500202

before each 5-fold split. This ensures randomness and helps provide a more robust estimate of model performance by reducing variability caused by a particular data split. In total runs it results so that Each 5-fold cross-validation involves 5 runs, summing 15 runs for each environmental variable and 90 models in total for each species. Repeating k-fold cross-validation ensures the results are not overly dependent on how the dataset was initially split. It provides a better estimate of the model's generalization ability by averaging performance over multiple random splits. Other key advantages include reduced bias, improved stability through the Repeated runs and enhanced generalization by providing a comprehensive assessment of the model's ability to perform on unseen data. From each fold (15 iterations with 6 different SDMs) the ensemble of models was constructed. Within each ensemble, the mean of all model predictions was utilized. This process was repeated 5 times for different environmental combinations and applied to all 21 species.

Following the complete training process, the optimal model for each fish species was selected based on TSS metric scores. Individual models were compared both against each other and against the ensemble. The final statistics of the "winning" parameter combinations and models were subsequently analyzed. This comprehensive modeling framework enabled robust evaluation of potential habitat redistribution patterns, enhancing common ability to assess ecological responses to environmental change.

2.2.4 Future predictions

Upon selecting the most suitable combination of environmental variables - unique for each species, future projections were applied. A grid cell of 1x1 degree is selected, then environmental variables for this grid for this year are selected and prediction of probability is applied. It included as the inputs the projected environmental conditions,

doi:10.6342/NTU202500202

and the output showed the probability of occurrence ranging from 0 - 1, showcasing the potentially suitable (or unsuitable) territory for species occurrence.

Another method for explaining the species movements was distributional centroids. The centroid calculation in spatial ecology represents a fundamental approach to summarizing complex spatial distributions into a single representative point. In species distribution modeling, centroids serve as valuable metrics for tracking spatial shifts in species ranges across different environmental scenarios. When applied to species distribution predictions, the centroid represents the geographic center of a species' predicted suitable habitat, enabling researchers to quantify range shifts by comparing centroid positions between current and future environmental conditions. This approach is particularly useful for analyzing directional trends in range shifts and measuring the magnitude of displacement in species distributions, offering insights into potential environmental change impacts on species' geographic patterns. Centroid analysis can be applied to various types of spatial data, making it a versatile tool for studying changes in species distributions across different temporal and environmental contexts. For this analysis, I implemented centroid calculations using the *terra* package in R. To minimize the impact of potential outliers in the predictions and ensure more robust results, averaged centroids from the first five years (2024-2029) were used as the starting point and the last five years (2096-2100) as the endpoint of this temporal analysis. The distributional centroids shifts were recorded from year to year, and the final vector was aggregated as the mean tendency of movement magnitude and direction from 2024 to 2100.

doi:10.6342/NTU202500202

3. Results

3.1. SDMs performance

The species were categorized into two ecological groups - pelagic and demersal. For each group, environmental variables were assigned based on their primary habitat: surface variables for pelagic species and bottom variables for demersal species. SDMs were then developed for each individual species. The analysis resulted in five distinct modeling experiments, reflecting the model comparisons for both pelagic and demersal species, that will be described in following chapters.

Carefully conducted modeling for each species showed general good model alliance between different SDMs among each of the methods and for different experiments. Single-model (only SBT/SST) response curves and their ensemble outputs highlighted the most important environmental parameters and tolerance intervals of observed parameters during the season (Q1).

Environmental suitability within a species' preferred parameter ranged consistently high, with a probability of (environmental) suitability equal to 1. When environmental conditions fall outside the observed minimum and maximum thresholds (which represent the species' critical tolerance limits), the suitability value drops to 0. Between these extremes, the environmental suitability demonstrates a linear decline. The final habitat suitability is determined by calculating the geometric mean across all probability distributions for each environmental predictor, where each predictor is given equal weight in the calculation. This approach assumes that all environmental parameters contribute equally to determining the overall habitat suitability for a given species (Jones et al., 2012).

Comparing all the metrics for each of the SDMs for different groups of environmental variables for all the species was conducted. For instance, demersal species

doi:10.6342/NTU202500202

(Fig. 12A) exhibited slightly different patterns, with validation scores generally ranging from 0.70 to 0.95. The model performance was notably stable when using SBT as the best predictor, like pelagic species. However, the combination of pH, bottom oxygen, and SST in other experiments (SST+pH_bot+O2_bot) showed more varied results across algorithms, suggesting that bottom-dwelling species' distributions might be influenced by a more complex interplay of environmental factors. GLM and RF showed lowest performance and highest range among lower performance, especially when combining multiple environmental variables, with scores occasionally dropping below 0.80.

In contrast, for pelagic species the validation scores predominantly ranged between 0.75 and 0.95, with the highest performance observed when using sea surface temperature (SST) as a predictor variable (Fig. 12B). The ensemble mean (E) algorithm consistently demonstrated superior performance across different variable combinations, particularly when incorporating SST, with validation scores reaching 0.95. However, the combination of SST and surface Oxygen showed the second-best result 0,89±0,03, following the same pattern as the SST-model.

The species distribution modeling approach generates spatial predictions by combining multiple environmental envelopes through multiplicative integration across each grid cell of the study region. Each cell receives a suitability score ranging from 0 to 1, indicating how well the local environmental conditions match the species' requirements (Jones, M. C., et al., 2012). The model employed a trapezoidal response curve for each of the species to characterize the relationship between species presence and observed environmental parameters. This trapezoidal shape effectively balanced the needs of both resident species, which typically showed single-peaked annual distribution patterns, and migratory species, which often displayed dual-peaked distributions. The environmental envelopes were constructed by analyzing the relationship between documented species

doi:10.6342/NTU202500202

occurrences and corresponding environmental conditions, establishing both absolute tolerance limits and optimal ranges for each environmental variable which is based on the initial input data. The results are provided in the Supplementary materials.

In Tables 4-5 I highlight the best combination (type) of environmental parameters from ensemble model results for each species in the two groups.

The validation performance analysis of SDMs revealed distinct patterns between pelagic and demersal species, with both groups showing notably high TSS (True Skill Statistic) values across different model configurations. For the pelagic species group, consisting of five species, the SST (Sea Surface Temperature) configuration emerged as the optimal predictor, demonstrating consistently superior performance with TSS values ranging from 0.949 to 0.951 (Table 4-5). Particularly, *Trachurus trachurus*, *Scomber scombrus*, and *Engraulis encrasicolus* exhibited the highest validation scores (TSS = 0.951), while *Sardina pilchardus* and *Argentina sphyraena* showed marginally lower but still robust performance (TSS = 0.949).

The demersal species analysis, encompassing 16 species, demonstrated a similar pattern with SBT (Sea Bottom Temperature) configuration consistently outperformed other parameter combinations. The validation scores for demersal species ranged from TSS = 0.945 (*Chelidonichthys lucerna*) to TSS = 0.955 (*Merluccius merluccius* and *Eutrigla gurnardus*), indicating robust model performance. The Ensemble (E) modeling approach proved to be the most effective for nearly all species, however, the difference between CTA and Ensemble for this species is very low: *Myxocephalus scorpius* showed optimal performance under CTA with TSS = 0.949.

Notably, for both pelagic and demersal species, single-parameter temperature-based models (SST and SBT respectively) outperformed more complex multi-parameter configurations. This pattern suggests that temperature serves as the primary driver of

doi:10.6342/NTU202500202

species distribution patterns in the study area, though it's important to note that other environmental parameters still contributed to model performance, albeit to a lesser degree. The high TSS values across all configurations (consistently above 0.85) indicated robust model performance regardless of parameter combination, suggesting that the models provide reliable predictions of species distributions under a single temperature-based model.

I suggest prioritizing a multi-SDMs strategy (ensemble) and evaluating a range of potential predictions to reduce biases stemming from data uncertainties and model design.

3.2. Projected distributional shift based on sea temperate

The projections indicate distinct responses between pelagic and demersal species. Under the most optimistic scenario, SSP1-2.6, species distributions show relatively minor changes, with declines in the probability of presence primarily occurring in northern sea boundaries. Notably, the North-Northwest (NNW) border of the North Sea near the Norwegian Sea merge as particularly insecure regions. Even in this conservative - SSP1-2.6 scenario, these areas face declining probabilities of presence starting from 2050, potentially leading to escalating decline total extinctions by the end of the century.

Under the SSP3-7.0 scenario, both pelagic and demersal species demonstrate moderate responses. Pelagic species will show a general decline in probability of presence across the entire region, with local extinctions occurring predominantly in the northern and northwestern areas. Demersal species display more stability in their distribution boundaries, though probabilities of occurrence decline to 0.5 in northern areas, while southern regions remain relatively unaffected. The north (N) and north-north-west (NNW) border continued to experience reductions in habitat suitability, further emphasizing their vulnerability under this scenario. Moreover, for example, *Scyliorhinus*

doi:10.6342/NTU202500202

canicula will exhibit its lowest probability of presence by 2100 in the whole North Sea basin (Fig. 13).

The SSP5-8.5 scenario, the most severe, projected dramatic changes by 2100. Pelagic species faced extensive local extinctions, with only remnant populations persisting in a distinctive stair-like pattern in the south-southeastern region. Pelagic species displayed contrasting patterns: some species, such as *Argentina sphryaena*, (Fig. 14) showed relatively better resilience, that other species, maintaining relatively good spatial coverage in entire sea, followed by a stair-like habitat suitability in the central and southern part of the North Sea with probability of occurrence 0.75-1.0 only by the end of the century under the pessimistic scenario. However, most other species experienced significant declines in probability of presence in the central and southern regions, with some faced total extinction across the North Sea even under SSP3-7.0. Maps with projected distributions under SST/SBT-model for all examined species can be found in supplementary S.2-S.22.

Overall, this analysis highlights the stark differences in species responses to climate change. While pelagic species tended to show more uniform declines across their ranges, demersal species exhibited varied responses, reflecting their diverse habitat requirements and environmental tolerances. Finally, the northern areas of the North Sea and the Strait of Dover are identified as the most vulnerable, highly unsuitable areas, under all 3 scenarios starting from 2050. By 2100 under sever scenarios many species are projected to be eliminated from the North Sea area, meaning that the regions face persistent declines in habitat suitability, emphasizing the need for targeted conservation efforts to mitigate the impacts of climate change on marine biodiversity.

doi:10.6342/NTU202500202

3.2.1 Distributional Centroids based on sea temperate

The overall distributional change had a similar trend among all demersal species that differed from the similarities for pelagic specs with variations of different SSPs. Under SSP1-2.6, species responses are generally localized, suggesting that milder climate results in forcing minimal movement is observed for both species groups and relatively small changes to habitat suitability - fish species will in South and East to around 25-57 km (32±12 km) (Fig. 15).

Under SSP3-7.0 and SSP5-8.5, distributions became more pronounced, but quite disperse, as many species will be experiencing northward and eastwards shifts or reduced probabilities of presence in the whole area in total, reflecting the intensifying impacts of climate change.

In the SSP3-7.0 scenario, species exhibited moderate directional shifts, with movement primarily toward the north and east 60-234 km (144±46 km). Demersal species demonstrated larger displacements (155±43 km) mostly south-eastward and eastwards. Whereas pelagic species will display more localized adjustments in the eastwards direction, moving to shorter distances 108±34 km.

Under the SSP5-8.5 scenario, both groups showed significant displacements 15-607 (233±196 km), and particularly demersal species with further propagation to the northeast reaching up to 607 km, reflecting large-scale shifts in habitat suitability. In contrast, pelagic species exhibited moderate displacements, 193±63km primarily along the eastward direction.

A few species exhibited resilience even under severe scenarios, potentially due to broader environmental tolerances or habitat adaptability. For instance, *Argentina sphyraena* and *Engraulis encrasicolus*, exhibit greater resilience under all scenarios, with minimal directional changes. Other species, like *Eutrigla gurnardus* and *Callionymus*

doi:10.6342/NTU202500202

maculates, show substantial shifts, particularly under SSP5-8.5, where probabilities of presence decreased dramatically.

Overall, demersal species are projected to shift to north-west and south-east, while pelagic species will tend to shift eastwards in the future.

3.3 Projected distributional shift based multi-factor models

Selected model for demersal species containing sea bottom temperature and bottom pH (Table 4a-b), responded in showcasing under SSP1-2.6, *Cyclopterus lumpus, Myoxocephalus scorpius, Scyliorhinus canicula, Sebastes viviparus,* and *Anarhichas lupus* show zero or minimal habitat suitability in northern latitudes, particularly in the Strait of Dover. By 2050 under SSP3-7.0, A*mblyraja radiata, Buglossidium luteum, Sardina pilchardus, and Sebastes viviparus* demonstrate decreased presence probability (0.25-0) in the northern sea. By 2100, species show resilience with stable distribution borders, reduced presence probability (0.5-0.75) in northern areas, while southern regions remain suitable.

Projections for 2050 showed almost no declines in the probabilities of presence for SSP1-2.6, however 2 other more severe climate scenarios showed a decreasing probability of occurrence (0.25-0.50) in the northern sea boarder. The NNW region experiences widespread losses or significantly reduced probabilities of presence under SSP3-7.0 scenarios for all species, leaving the southern and central parts of the sea more as more suitable locations, while the SSP5-8.5 continues toward local extinctions for most species in the entire area by 2100.

Following the proposed models with sea surface temperature with pH and sea surface temperature with dissolved oxygen (S.1b), pelagic species response was projected to be under SSP1-2.6 (2050-2100), minimal changes are projected, with *Engraulis encrasicolus* showing lowest presence probability in 2050. For SSP3-7.0 by 2050,

doi:10.6342/NTU202500202

Argentina sphyraena, Sardina pilchardus, and Trachurus trachurus show decreased habitat suitability (0.25-0) in the northern sea. The 2100 projections indicate an overall decrease across the entire region, with total extinctions in north/northwest areas for most species.

SSP5-8.5 projected two distinct patterns by 2050: better survival rates in central-southern areas, *and Anarhichas lupus, Sebastes viviparus, and Trachurus trachurus* show expanding areas of total absence in the north-north-west (NNW) region. By 2100, species habitat responses varied between complete extinction, 0.25-0.5 habitat suitability in the NNW, with a stair-like pattern in the south-east (SE).

Overall, including dissolved oxygen and pH in the SDM change the locations of potential species locations from northern areas to central and southern regions of the North Sea. Maps with projected distributions for all examined species under multi-factor experiments can be found in supplementary S.23-S.43.

3.3.1 Distributional Centroids based multi-factor models

Projection of distribution starting with SSP1-2.6, which represents the most optimistic climate scenario with lower emissions, there will be moderate displacement of both pelagic and demersal species (Fig. S.44). The movement vectors were small and clustered near the origin, with displacement of 8-87 km (30±15 km), from which pelagic species shifted for 14-27 km, while demersal species - *Chelidonichthys cuculus* - propagated to the distance up to 3 times further.

Under SSP3-7.0, a moderate emissions scenario, a more pronounced movement pattern was observed. Both species groups showed a clear southeastward trend, but with different magnitudes. The shift ranged from 76-197 km (136±38 km), showing significantly larger displacements compared to SSP1-2.6. Demersal species generally

doi:10.6342/NTU202500202

show longer displacements (98-197 km) than pelagic species (76-97 km), suggesting they may be more sensitive to these moderate climate changes.

The most dramatic changes appeared under SSP5-8.5, the high-emissions scenario. Here, will be the longest distributional centroids vectors, ranging from 14-216 km (144±58 km). Interestingly, under this scenario, a divergence in movement patterns is observed: while some species showed the southeastward trend, others had northeastward movement, creating a fan-like pattern of displacement vectors. This suggests that different species may adopt varying survival strategies under severe climate change conditions.

What's particularly noteworthy is how the magnitude of displacement increases progressively across the scenarios, from minimal movement under SSP1-2.6 to substantial shifts under SSP5-8.5, almost 5 times as larger, clearly demonstrating the escalating impact of climate change on marine species distributions reorganization.

4. Discussion

The predominant influence of temperature on shaping the catch composition of pelagic fisheries indicates that these catches could be susceptible to the unforeseen impacts of future warming.

By selecting the “winning” model I do not contradict the importance of other simultaneously occurring environmental factors besides water. My result just emphasizes that the single temperature-based model statistically proved to be the perfect fit for projecting the future distributions for a 21 species in the certain water body of the North Sea.

The “winning” ensemble models, containing only SBT and SST achieved the highest validation values when incorporating a comprehensive set of environmental

doi:10.6342/NTU202500202

variables. However, these variables were not included in the future projections, which relied primarily on temperature.

This finding highlights two important points:

1. Accurate prediction of future species distributions requires consideration of multiple environmental factors beyond temperature alone, with different species within the same community potentially responding to distinct combinations of variables.
2. While statistical differences between models may appear moderate, the actual ecological consequences and resulting changes in species distribution patterns could be substantially more significant in real-world conditions.

Moreover, it should be concerned that the differences between single and combined models are not that big, meaning that potentially testing other factors, unless dissolved oxygen and pH, could show different results.

The study of Gordó-Vilaseca et al. (2024) investigated the future trends in marine fish biomass and distribution across the North Sea to the Barents Sea using joint species distribution models (JSDMs). Their key findings included an increase of species richness that is projected to increase significantly in Arctic regions, particularly in the Barents Sea, with species from warmer waters expanding northward. As well as localized declines in species richness in some southern and deeper areas and an overall decline in fish biomass in the Arctic due to the reduction of some Arctic-specific species. Species are shifting their ranges northward and eastward. The rate of these shifts increases with the severity of climate change scenarios, from 0.9 km/year under SSP1-2.6 to over 3.2 km/year under SSP5-8.5. These results are quite like what have been achieved in this thesis.

Similar research was published by Bandara et al., 2023, however, here authors showed that multivariate model including temperature and dissolved oxygen had the best

doi:10.6342/NTU202500202

model performance beyond a simple consideration of temperature (ΔAIC = 799, ΔTSS = 0.015) that allowed for robust northwards projected distribution of Black Sea Bass in the Northern Atlantic.

Enough data contributing to the effective training of models in the validation dataset ultimately allows achieving high accuracy values for the model. This enables us to conclude that future predictions can be considered reliable. However, due to low resolution in the case of my study (around 100 km^2) the model cannot adequately predict which specific hauls would be the best for trawling, when serving the needs of fishery, as it provided probability of occurrence in a relatively large spatial quadrant. Species' expansion into Arctic regions or other nearby marine water bodies cannot be predicted in this research due to the limitations of used data outside the North Sea region.

Since the modelled propagation of the observed species is dependent on the input model environmental parameters under different climate forcing, the SDM "selects" the most suitable temperature for the species based on the training data. In my case, there was a grid cell at 6 °N 3 °W that had deviant water temperature from year to year in the future projections, being colder than most of the North Sea water and a bit warmer than Atlantic Water inflow from the northern border, followed with the significantly deeper bathymetry than in the North Sea basin in general. Since the future temperature in that cell fitted well into the tolerance interval for the species, the model projected a far north-west distribution reaching that location.

Regarding the pelagic species that will face a faster and stronger increase of surface water temperature, I may assume that observed species can potentially overcome such changes in the areas that will keep the lowest temperature in the study area, which are the Danish Straits and the northern regions near the Norwegian Sea.

doi:10.6342/NTU202500202

Finally, my research agreed with previously published papers, discussing that temperature emerges as a primary factor influencing species distribution and survival, showcasing species respond to thermal changes through poleward migration while seeking cooler waters and vertical movement to deeper waters (Cheung et al., 2010, Campana et al., 2020, Gordó-Vilaseca et al., 2024, Meyer-Gutbrod et al. 2021). However, changes in oxygen levels and pH will trigger significant ecosystem shifts, when the critical thresholds are exceeded (Clarke et al. 2022). These movements restructure local ecosystems and affect predator-prey relationships, where only 10% of energy transfers efficiently between trophic levels. This limitation means predatory species, requiring more energy for survival, maintain smaller populations than their prey species. So, their survival depends heavily on the stable availability of lower-trophic level prey.

This synthesis of evidence highlights the complex interplay between environmental changes and marine ecosystem responses, emphasizing the need for comprehensive monitoring and management strategies to maintain ecosystem stability and fisheries sustainability.

4.1 Comparison of the different model experiments

In examining marine species' responses to climate change, the interplay between different environmental factors reveals a complex pattern of adaptation and survival. The comparison between single-factor and multi-factor models, despite showing only a minor statistical difference (ΔTSS = 0,2), provides crucial insights into future species distribution patterns. This similarity in model performance shouldn't overshadow the nuanced differences in their predictions about how marine life will respond to changing conditions.

The ocean's chemical properties play a fundamental role in these dynamics. The relative stability of ocean pH, maintained through the carbonate system's buffering

doi:10.6342/NTU202500202

capacity as documented by González-Santana and colleagues (2024), contrasts sharply with the more rapid changes in dissolved oxygen levels as temperatures rise. This differential rate of change creates a particularly challenging environment for demersal and benthopelagic fish, which inhabit the already oxygen-limited waters near the seafloor. However, the multi-factor analysis reveals an important survival mechanism: areas that might become thermally challenging could still support fish populations if other environmental parameters, such as oxygen levels or pH, remain within tolerable ranges. While the study's geographic scope excluded adjacent waters like the Norwegian, Barents, Baltic, Celtic Seas, and Bay of Biscay, limiting the potential prove of species distributions to these basins, it still can capture the well-documented trend of northward species migration in response to warming waters. This phenomenon, known as deborealization, represents a crucial survival strategy for marine species seeking cooler environments. However, demersal species present an interesting exception to this general pattern. These bottom-dwelling fish might find refuge in southern regions, where the thermal dynamics of deep water create stable environments. That is why demersal species shifts are not so unified as for the pelagic ones. Unlike surface waters that rapidly respond to atmospheric warming, deeper waters maintain more stable temperatures, potentially providing crucial habitats for spawning, feeding, and maintaining appropriate oxygen levels. Norwest shifts may be indicators of the most suitable temperature conditions, (which in my case serves as location only in 1 grid from the observed data). This may be due to the specific configuration of the water masses between the Orkney Island (UK) and Shetlands Islands, with transition and mixing water, surrounded by the fronts.

My evidence of future northwards shifts and temperature identification as the main factor, shaping future stocks assessments is similar to the one published by the EU in the “Climate Change and Fishery policy…” Final Report (Bastardie et al., 2022).

doi:10.6342/NTU202500202

This research acknowledges the inherent uncertainties in predicting future marine conditions. While current modeling frameworks, particularly the SSP scenarios, represent our best understanding of potential future conditions, real-world developments might diverge from these projections. Will the actual conditions be exactly as they are projected by the currently available conservation frameworks or not? This is one of the most serious concerns that cannot be omitted.

It is also important to mention that from my assumption adding additional parameter sot the model not only did not lead to higher model performance but even made the performance metrics worse. This could have happened, firstly, due to the curse of dimensionality, as with more variables (higher dimensionality), the model needs exponentially more training data to effectively capture patterns in the sparse feature space; a single-parameter model avoids this issue by operating in a much simpler feature space where patterns may be more easily learned from limited data. Secondly, the multi-variable model has higher model complexity and more parameters to tune. This increased flexibility makes it more prone to fitting noise in the training data rather than learning generalizable patterns, so the simpler single-parameter model was naturally more regularized without overfitting. Thirdly, the problem could arise with the environmental data itself, as pH, for instance, did not change as gradually, as temperature during the projected time period, also, single parameter might be more reliably measured or have higher data quality. All of these ideas state that my approach was a good example of Occam's Razor in machine learning - sometimes the simplest model that adequately explains the data is the best choice.

Understanding these complex interactions between environmental factors, species behavior, and ecosystem dynamics provides valuable insights for anticipating and adapting to the challenges posed by climate change in marine environments. This

doi:10.6342/NTU202500202

comprehensive approach, considering multiple environmental factors and their interactions, offers a more nuanced and potentially more accurate view of how marine species might respond to changing oceanic conditions in the coming decades.

4.2 Uncertainties about using SDMs

In SDMs-based research data-related uncertainties stem from potential biases in species data, scale mismatches, and incomplete distribution representation (Davies, et al., 2023). Also, significant uncertainties remain in long-term predictions.

The choices one makes when constructing models have far-reaching implications for how uncertain predictions may become. Researchers encounter novel climate conditions that introduce three key sources of uncertainty. First, it must contend with uncertainty inherent in climate models themselves. Second, it may face uncertainty about which emissions pathway humanity will follow. Third, we must grapple with eco-evolutionary uncertainty - meaning we cannot be entirely sure how species will adapt and respond to new conditions over time. These compounding sources of uncertainty create significant challenges when trying to forecast species distributions into the future (Urban, 2019).

Davies et al. (2023) emphasized that poorly handled uncertainty in Species Distribution Models (SDMs) can lead to two significant problems: either the models become too vague to guide meaningful management decisions, or worse, they produce misleading conclusions due to overconfidence in inaccurate predictions. To address this issue, they proposed a three-step approach for managing uncertainty in SDMs: systematically identifying all potential sources of uncertainty, implementing methods to minimize these uncertainties when possible, and transparently communicating any remaining uncertainties to decision-makers who rely on these projections. This structured

doi:10.6342/NTU202500202

approach helps ensure that SDMs can effectively inform conservation and management strategies while acknowledging their limitations.

When predicting how species distributions will change, incorporating stable environmental factors alongside climate variables is crucial for accurate modeling. Models that rely solely on climate parameters risk misrepresenting species' actual habitat requirements and may produce unreliable forecasts (Willis, K.J., Bhagwat, S.A., 2009). Without considering constant environmental constraints like bathymetry or substrate type, projections can either exaggerate or underestimate both the extent of distribution changes and species vulnerability to climate change. This comprehensive approach, integrating both dynamic climate factors and fixed environmental variables, provides a more reliable foundation for assessing future species distributions (Zangiabadi et al., 2021).

When models operate at spatial scales that don't match the biological requirements of species, they can introduce significant prediction errors by either overestimating or underestimating suitable habitat (Seo et al. 2008, Franklin et al. 2013). This spatial resolution issue has crucial implications for conservation planning and accurate management suggestions. For instance, broad-scale models operating at 100 km resolutions - like in the case of this dissertation - often fail to capture fine-scale topographic features that might be essential for local conservation efforts, such as managing a small coastal protected area of just 10 square kilometers (Whittaker et al. 2005).

Classification Tree Analysis (CTA) in my case outperform ensemble models in projecting for 2 demersal species due to its ability to capture distinct environmental thresholds that characterize fish responses, rather than the gradual changes often predicted by averaged ensemble approaches (Elith et al., 2008). The hierarchical decision-making structure of CTA effectively mirrors how fish naturally select habitats through sequential

doi:10.6342/NTU202500202

environmental choices, such as temperature followed by depth and salinity preferences, where clear environmental thresholds often determine range shifts more decisively than gradual changes, allowing CTA to effectively identify critical points where species might abandon or colonize areas (Thuiller et al., 2009).

Regarding the range in RF and GLM performance, it could be explained in a following way. GLMs are sensitive to the specific combination of environmental variables used. If the variables have strong collinearity (when incorporating multi-factor models), so GLMs can become unstable. Random Forest showed unexpectedly low performance when dealing with multiple environmental, as this model can suffer from the "curse of dimensionality", and the data becomes increasingly sparse in this higher-dimensional space.

Moreover, critical viewpoints share the idea of small possibility of happening the pessimistic climate scenarios as the IPCC AR6 report stated that “the likelihood of high-emissions scenarios such as RCP8.5 or SSP5-8.5 is considered low in light of recent developments in the energy sector” (Chen et al., 2021).

4.3 Global Fisheries’ challenges

Marine species redistributions are creating unprecedented challenges for fisheries management and conservation globally. Anthropogenic effects, including fishing pressure and habitat modification, combine with climate change to cause widespread shifts in species distributions. Research examining 889 marine species populations worldwide revealed that 70% of commercially important fish stocks now regularly cross jurisdictional boundaries, compared to just 35% in the 1980s (Pinsky et al. 2021). These shifts are already triggering international conflicts overfishing rights and access.

The situation is particularly evident in northern seas, where warming waters are making previously ice-covered areas accessible for fishing. A prime example is the

doi:10.6342/NTU202500202

movement of mackerel stocks, which have shifted northward from their traditional grounds in the North Sea into waters around Iceland and Greenland, leading to disputes overfishing quotas and access rights. The Arctic's unique international governance structure, managed through the Arctic Council and UNCLOS, faces new challenges as countries assert their rights within their Exclusive Economic Zones (EEZs) while dealing with trans-boundary stocks.

These distributional changes are creating significant economic implications. Some countries may benefit while others lose access to traditionally important fishing grounds. For instance, in the North Sea, Norway, Denmark, and the UK might benefit from species moving southwards and east-southwards under severe climate scenarios, while Germany, the Netherlands, and Belgium could face losses according to their EEZ boundaries. This redistribution affects not only fishing access but also tax income from legal fishing activities in territorial waters.

The North Sea has experienced significant changes in fishing catch patterns over recent years. According to ICES (2023), the total reported catch in the Northern North Sea (Division 4a) showed notable fluctuations. In 2022, the total demersal fish landings in this region reached approximately 380,000 tonnes, with cod and haddock comprising the largest portions. However, this represents a 15% decrease from the previous five-year average. For the Faroe Plateau, the fishing statistics present a different pattern. The total catch in this region during 2022 was approximately 120,000 tonnes, dominated by saithe and haddock (ICES WGDEEP, 2023). What's particularly interesting is the shift in species composition over the past decade, with traditional demersal species showing declining trends while some pelagic species have increased. Looking at specific species, in Division 4a: cod landings decreased to 25,000 tonnes in 2022, down from 42,000 tonnes in 2018; haddock catches remained relatively stable at around 80,000 tonnes;

doi:10.6342/NTU202500202

whiting showed an increasing trend, reaching 35,000 tonnes in 2022. In Division 5b: saithe landings increased to 45,000 tonnes in 2022, blue ling catches declined to 3,000 tonnes; deep-water species generally showed decreasing trends.

These changes reflect both management measures and environmental factors. The decrease in cod catches aligns with stricter quota restrictions implemented under the cod recovery plan (ICES WGNSSK, 2023). Meanwhile, the increase in certain pelagic species might be attributed to changing distribution patterns linked to warming waters and should raise awareness. about the necessity to carefully control the limits of the fish catch and minimize it to those species that are facing continuous stock decline.

Recent research published in Nature Sustainability (Miller et al., 2023) identified critical management challenges, including quota allocation disputes and monitoring difficulties. Traditional quota systems based on historical distributions become increasingly obsolete as stocks shift across boundaries, with the study documenting 12 major international disputes over five years directly related to climate-driven stock shifts. Furthermore, traditional stock assessment methods struggle to capture rapidly changing distribution patterns, with management decisions lagging actual changes by 3-5 years.

Regarding my results, the predominance of temperature as the primary predictor in species distribution models, despite the availability of additional environmental variables such as pH and oxygen, can be attributed to several interconnected factors. Temperature functions as a master variable in marine environments, directly influencing both oxygen solubility and carbon cycle that leads to fluctuations in pH levels, while simultaneously governing the metabolic rates of marine organisms.

As mentioned previously, the correlation analysis reveals strong relationships between sea surface temperature and other environmental parameters, notably a -0.97 correlation with surface oxygen and -0.63 with surface pH. These high correlations

doi:10.6342/NTU202500202

indicate that temperature effectively captures much of the environmental variation that would otherwise be explained by oxygen and pH measurements. I assume that the inclusion of such highly correlated variables, rather than improving model performance, could potentially decrease predictive accuracy by introducing redundant information and complicating the model's ability to distinguish individual variable effects, as temporal transferability of SDMs can degrade model performance when projecting into future conditions, particularly when environmental relationships may not remain stable year from year (Yates et al. 2018). Therefore, the second-best models, combining SBT and bottom dissolved oxygen for demersal species and SST with surface dissolved oxygen and SST with surface pH projected species distributions in a different way for 2100 projections. In these experiments, species were projected to move to south (S) and south-east (SE) directions (near Frisian Islands), being the most preferred habitat areas under severe emission scenarios (SSP3-7.0 and SSP5-8.5) by the end of the century. Moreover, projections up to 2100 under SSP5-8.5 were smaller in distance, showing 175±95 km, respectively, in comparison with the Temperature-based models that revealed propagation up to 600 km to the north-west (NW). But projections for 2050 were well-aligned for both single-factor and multi-factor models, showing either high probability of presence on the large spatial coverage for the whole area or high probability of occurrence in the southern regions of the sea, suggesting that the rising temperature in those areas will be still suitable for the observed species.

Essentially, when temperature data indicates warming conditions, it implicitly suggests corresponding changes in oxygen levels and pH, making the addition of these variables somewhat redundant from a modeling perspective. This understanding helps explain why simpler, temperature-based models often achieve superior validation metrics compared to more complex multi-variable approaches in modelling.

doi:10.6342/NTU202500202

Understanding the critique that should be applied when analyzing the models results, as modeling algorithms can produce varying predictions even with identical input data, emphasizing the importance of ensemble approaches (Araújo et al. 2019). SDMs' results have been proven to differ in different location of the worlds ocean (Valavi et al., 2022), that is why so far generalization of distributional trend cannot be fully addressed to the entire marine ecosystem. Another reason is that more specifically for marine environments, detail the ISIMIP3 ocean sector protocols and associated uncertainties in projections of key variables like temperature, pH, and oxygen (Lange et al. 2020). The challenges of downscaling global climate models to regional seas are addressed by who emphasize uncertainties in coastal regions and semi-enclosed seas like the North Sea (Büchner et al. 2021).

To sum up, success in addressing these challenges requires innovative approaches that account for dynamic species distributions while maintaining ecosystem function and fisheries productivity. This includes developing dynamic quota allocation systems, strengthening scientific cooperation for stock monitoring, and establishing robust dispute resolution processes. Without such adaptations, the risk of overfishing and international conflicts over marine resources could increase substantially as climate change continues to alter marine ecosystems (Duncanson et al., 2023).

5. Conclusion

Understanding species distribution patterns proves crucial for effective fisheries management and conservation planning. This knowledge enables the identification of essential fish habitats, helps predict climate change impacts, and supports the design of marine protected areas. Recent advances in tracking technologies and modeling approaches have enhanced my ability to map and predict species distributions, though

doi:10.6342/NTU202500202

significant challenges remain in understanding how distributions will change under future environmental conditions.

Advanced modeling approaches are thought to improve ability to predict future distribution changes. These models increasingly incorporate multiple drivers and species interactions, though significant uncertainties remain. However, my suggestions are that future bigger spatial data coverage and comprehensive monitoring for robust projections and plans for high mitigation should be conducted. Moreover, precise understanding of each individual environmental factor impact on fish communities will minimize the uncertainties in applying different methodological approaches. This will help in committing further research to determine the extent to which the North Sea fish community is impacted by the changing climate, as well as other communities in other parts of the ocean.

Migration of marine living resources are creating unprecedented challenges for management and conservation. Success in addressing these challenges will require innovative approaches that can account for dynamic species distributions while maintaining ecosystem function and fisheries productivity. International cooperation and adaptive management frameworks will be crucial for navigating these changes effectively in incorporation unified accessible frameworks.

Climate-induced thermal stress is forcing marine species to relocate, driving them either toward higher latitudes or into deeper waters in search of more favorable temperature conditions. This large-scale redistribution is transforming the structure of marine communities, as species' movements disrupt long-established ecological relationships. When species relocate to maintain their preferred temperature ranges, they alter the composition of both their original and new habitats, leading to cascading effects that reshape entire food webs and ecosystem dynamics.

doi:10.6342/NTU202500202

Final results

Model Performance & Distribution Patterns

- Single temperature-based model achieved highest accuracy (TSS=0.95)

Species Response Variation under Temperature-based model:

- Pelagic species: Consistent southeast movement across observed species (143±57 km by 2100)
- Demersal species: More variable patterns with expansion-contraction dynamics under different scenarios (shift up to 607 km by 2100 under SSP5-8.5)
- Average distance range among all species: 233±196 km northwest by 2100 under SSP5-8.5

Future Modelling Implications

- Complex interplay of environmental variables requires refined frameworks
- Need for unified modelling approach in fisheries sector
- Critical to understand multiple processes driving distributional changes

doi:10.6342/NTU202500202

References

1. Allouche, O., Tsoar, A., & Kadmon, R. (2006). Assessing the accuracy of species distribution models: prevalence, kappa, and the true skill statistic (TSS). Journal of Applied Ecology, 43(6), 1223-1232. https://doi.org/10.1111/j.1365-2664.2006.01214.x
2. Anderson, C.J. (2010). Central Limit Theorem. In The Corsini Encyclopedia of Psychology (eds I.B. Weiner and W.E. Craighead). https://doi.org/10.1002/9780470479216.corpsy0160
3. Anderson, H.S. (2021). North Sea Continental Shelf Cases. In: Gray, K.W. (eds) Global Encyclopedia of Territorial Rights. Springer, Cham. https://doi.org/10.1007/978-3-319-68846-6_581-1
4. Araújo M.B., Peterson A.T. (2012) Uses and misuses of bioclimatic envelope modeling. Ecology. Jul;93(7):1527-39. doi: 10.1890/11-1930.1. PMID: 22919900.
5. Araújo, M. B., Anderson, R. P., Márcia Barbosa, A., Beale, C. M., Dormann, C. F., Early, R., Garcia, R. A., Guisan, A., Maiorano, L., Naimi, B., O'Hara, R. B., Zimmermann, N. E. and Rahbek, C. 2019. Standards for distribution
6. Araújo, M. B., New, M. (2007). Ensemble forecasting of species distributions. – Trends Ecol. Evol. 22: 42–47.
7. Assis, J., Tyberghein, L., Bosch, S., Verbruggen, H., Serrão, E. A. and De Clerck, O. 2018. Bio-ORACLE v2.0: extending marine data layers for bioclimatic modelling. – Global Ecol. Biogeogr.27: 277–284.
8. Bandara, R. M. W. J., Curchitser, E., & Pinsky, M. L. (2024). The importance of oxygen for explaining rapid shifts in a marine fish. Global Change Biology, 30, e17008. https://doi.org/10.1111/gcb.17008
9. Barange, M., Merino, G., Blanchard, J. L., et al. (2014). Impacts of climate change on marine ecosystem production in societies dependent on fisheries. Nature Climate Change, 4(3), 211-216. https://doi.org/10.1038/nclimate2119
10. Barange, M., Merino, G., Blanchard, J., Scholtens, J., Harle, J., Allison, E. H., Allen, J. I., Holt, J., & Jennings, S. (2014). Impacts of climate change on marine ecosystem production in societies dependent on fisheries. Nature Climate Change, 4(3), 211-216. https://doi.org/10.1038/nclimate2119
11. Barbet-Massin, M., Jiguet, F., Albert, C.H. and Thuiller, W. (2012), Selecting pseudo-absences for species distribution models: how, where and how many? Methods in Ecology and Evolution, 3: 327-338. https://doi.org/10.1111/j.2041-210X.2011.00172.x
12. Barbet-Massin, M., Jiguet, F., Albert, C.H. and Thuiller, W. (2012), Selecting pseudo-absences for species distribution models: how, where and how many? Methods in Ecology and Evolution, 3: 327-338. https://doi.org/10.1111/j.2041-210X.2011.00172.x
13. Bastardie, F., Feary, D. A., Kell, L., Brunel, T., Metz, S., Döring, R., Eigaard, O. R., & Basurko, O. C. (2022). Climate change and the Common Fisheries Policy: Adaptation and building resilience to the effects of climate change on fisheries

doi:10.6342/NTU202500202

and reducing emissions of greenhouse gases from fishing (Final Report, EASME/EMFF/2020/3.2.6 - Lot1/SC07, EASME/EMFF/2020/3.2.6 - Lot2/SC08). Luxembourg: Publications Office of the European Union. https://doi.org/10.2926/155626

14. Baudron, A.R., Needle, C.L., Rijnsdorp, A.D., Marshall, C.T. (2014) Warming temperatures and smaller body sizes: synchronous changes in growth of North Sea fishes. Global Change Biology, 20, 1023–1031.

15. Ben Lamine, E., Schickele, A., Goberville, E. et al. (2022). Expected contraction in the distribution ranges of demersal fish of high economic value in the Mediterranean and European Seas.Sci Rep 12, 10150 https://doi.org/10.1038/s41598-022-14151-8

16. Blanchard, J. L., Jennings, S., Holmes, R., Harle, J., Merino, G., Allen, J. I., Holt, J., Dulvy, N. K., & Barange, M. (2012). Potential consequences of climate change for primary production and fish production in large marine ecosystems. Philosophical Transactions of the Royal Society B: Biological Sciences, 367(1605), 2979–2989. https://doi.org/10.1098/rstb.2012.0231

17. Bosch, S., Tyberghein, L., Deneudt, K., Hernandez, F. and De Clerck, O. 2018. In search of relevant predictors for marine species distribution modelling using the Marine SPEED bench-mark dataset. – Divers. Distrib. 24: 144–157

18. Böttinger, M., & Kasang, D. (2024). The SSP Scenarios. DKRZ. https://www.dkrz.de/en/communication/climate-simulations/cmip6-en/the-ssp-scenario

19. Boucher O., Servonnat J., Albright A.L., Aumont O., Balkanski Y., Bastrikov V., et al. 2020. Presentation and evaluation of the IPSL-CM6A-LR climate model. Journal of Advances in Modeling Earth Systems, 12: e2019MS002010.

20. Boucher, O., Servonnat, J., Albright, A. L., Aumont, O., Balkanski, Y., Bastrikov, V., ... & Vuichard, N. (2020). Presentation and evaluation of the IPSL-CM6A-LR climate model. Journal of Advances in Modeling Earth Systems, 12(7), e2019MS002010.

21. Boucher, Olivier; Denvil, Sébastien; Levavasseur, Guillaume; Cozic, Anne; Caubel, Arnaud; Foujols, Marie-Alice; Meurdesoif, Yann; Cadule, Patricia; Devilliers, Marion; Ghattas, Josefine; Lebas, Nicolas; Lurton, Thibaut; Mellul, Lidia; Musat, Ionela; Mignot, Juliette; Cheruy, Frédérique (2018). IPSL IPSL-CM6A-LR model output prepared for CMIP6 CMIP. Version 2024/10/12. Earth System Grid Federation. https://doi.org/10.22033/ESGF/CMIP6.1534

22. Boyce, D. G., Frank, K. T., Worm, B. & Leggett, W. C. (2015). Spatial patterns and predictors of trophic control across marine ecosystems. Ecol. Lett. 18, 1001–1011

23. Boyce, D.G., Tittensor, D.P., Garilao, C. et al. A climate risk index for marine life. Nat. Clim. Chang. 12, 854–862 (2022). https://doi.org/10.1038/s41558-022-01437-y

24. Bradie, J. and Leung, B. 2017. A quantitative synthesis of the importance of variables used in MaxEnt species distribution models. – J. Biogeogr. 44: 1344–1361.

doi:10.6342/NTU202500202

25. Brotons, L., Thuiller, W., Araújo, M. B., & Hirzel, A. H. (2004). Presence–absence versus presence-only modeling methods for predicting bird habitat suitability. Ecography, 7(4), 437–448. https://doi.org/10.1111/j.0906-7590.2004.03764.x

26. Bruno, J.F., Bates, A.E., Cacciapaglia, C. et al. Climate change threatens the world's marine protected areas. Nature Clim Change 8, 499–503 (2018). https://doi.org/10.1038/s41558-018-0149-2

27. Büchner M. (2024): ISIMIP3b ocean input data (v1.5). ISIMIP Repository. https://doi.org/10.48364/ISIMIP.575744.5

28. Büchner, M. (2024). ISIMIP3b ocean input data (v1.5). ISIMIP Repository. https://doi.org/10.48364/ISIMIP.575744.5

29. Buisson, L., Thuiller, W., Casajus, N., Lek, S. & Grenouillet, G. Uncertainty in ensemble forecasting of species distribution. Glob. Change Biol. 16, 1145–1157 (2010).

30. Burrows, M., Schoeman, D., Richardson, A. et al. Geographical limits to species-range shifts are suggested by climate velocity. Nature 507, 492–495 (2014). https://doi.org/10.1038/nature12976

31. Campana, S.E., Stefánsdóttir, R.B., Jakobsdóttir, K. et al. Shifting fish distributions in warming sub-Arctic oceans. Sci Rep 10, 16448 (2020). https://doi.org/10.1038/s41598-020-73444-y

32. Chen, D. et al. in Climate Change 2021: The Physical Science Basis. Contribution of Working Group I to the Sixth Assessment Report of the Intergovernmental Panel on Climate Change (eds Masson-Delmotte, V. et al.) (Cambridge Univ. Press 2021).

33. Cheng L., von Schuckmann K., Abraham, J.P. et al. Past and future ocean warming. Nature Review Earth Environment 3, 776–794 (2022). https://doi.org/10.1038/s43017-022-00345-1

34. Cheung W.L., Brodeur R. D., Okey T. A., Pauly D., (2014) Projecting future changes in distributions of pelagic fish species of Northeast Pacific shelf seas, Progress in Oceanography, Volume 130, 2015, Pages 19-31, ISSN 0079-6611 https://doi.org/10.1016/j.pocean.2014.09.003

35. Christin, S., Hervet, É. and Lecomte, N. (2019). Applications for deep learning in ecology. – Methods Ecol. Evol. 10: 1632–1644.

36. Clarke, T. M., Wabnitz, C. C. C., Frölicher, T. L., Reygondeau, G., Pauly, D., & Cheung, W. W. L. (2022). Linking observed changes in pelagic catches to temperature and oxygen in the Eastern Tropical Pacific. Fish and Fisheries, 23, 1371–1382. https://doi.org/10.1111/faf.12694

37. Copernicus Marine Service. (2024). Mean sea water pH time series and trend from Multi-Observations Reprocessing. Marine Data Store. https://doi.org/10.48670/moi-00224

38. Davies, S. C., Thompson, P. L., Gomez, C., Nephin, J., Knudby, A., Park, A. E., Friesen, S. K., Pollock, L. J., Rubidge, E. M., Anderson, S. C., Iacarella, J. C.,

doi:10.6342/NTU202500202

Lyons, D. A., MacDonald, A., McMillan, A., Ward, E. J., Holdsworth, A. M., Swart, N., Price, J., & Hunter, K. L.

39. De Hauwere, N. (2025). Marine Regions Organisations Maps - North Sea Maps. Marine
Regions. https://www.marineregions.org/maps.php?album=3747&pic=115812

40. Deser, C., Hurrell, J.W. & Phillips, A.S. The role of the North Atlantic Oscillation in European climate projections. Clim Dyn 49, 3141–3157 (2017). https://doi.org/10.1007/s00382-016-3502-z

41. Dulvy, N.K., Rogers, S.I., Jennings, S., Stelzenmüller, V., Dye, S.R. and Skjoldal, H.R. (2008), Climate change and deepening of the North Sea fish assemblage: a biotic indicator of warming seas. Journal of Applied Ecology, 45: 1029-1039. https://doi.org/10.1111/j.1365-2664.2008.01488.x

42. Duncanson, L., Liang, M., Leitold, V. et al. The effectiveness of global protected areas for climate change mitigation. Nat Commun 14, 2908 (2023). https://doi.org/10.1038/s41467-023-38073-9

43. Elith, J., Leathwick, J.R. and Hastie, T. (2008), A working guide to boosted regression trees. Journal of Animal Ecology, 77: 802-813. https://doi.org/10.1111/j.1365-2656.2008.01390.x

44. Engelhard G. H., Pinnegar J. K., Kell L. T., Rijnsdorp A. D., Nine decades of North Sea sole and plaice distribution, ICES Journal of Marine Science, Volume 68, Issue 6, July 2011, Pages 1090–1104, https://doi.org/10.1093/icesjms/fsr031

45. Essington, T. E., Anderson, S. C., Barnett, L. A. K., Berger, H. M., Siedlecki, S. A. and Ward, E. J. 2022. Advancing statistical models to reveal the effect of dissolved oxygen on the spatial distribution of marine taxa using thresholds and a physiologically based index. – Ecography 2022: e06249.

46. European Commission. (2022). The EU Blue Economy Report 2022. Publications Office of the European Union.

47. European Marine Observation and Data Network. (2024). River inputs database. EMODnet Data Portal.

48. Fielding, A. H., & Bell, J. F. (1997). A review of methods for the assessment of prediction errors in conservation presence/absence models. Environmental Conservation, 24(1), 38-49. https://doi.org/10.1017/S0376892997000088

49. Food and Agriculture Organization. FAO (2023). GLOBEFISH Highlights – International markets for fisheries and aquaculture products. https://doi.org/10.4060/cc7781en

50. Food and Agriculture Organization. FAO (2024b). Major Fishing Areas: Atlantic, Northeast (Major Fishing Area 27). CWP Data Collection. https://www.fao.org/fishery/en/area/fao:27/en

51. Food and Agriculture Organization. FAO(2024a). The State of World Fisheries and Aquaculture 2024 – Blue Transformation in action. https://doi.org/10.4060/cd0683en

doi:10.6342/NTU202500202

52. Franklin, J., Davis, F., Ikegami, M., Syphard, A., Flint, L., Flint, A. and Hannah, L. 2013. Modeling plant species distributions under future climates: how fine scale do climate projections need to be? – Global Change Biol. 19: 473–483.

53. Fredston, A.L., Cheung, W.W.L., Frölicher, T.L. et al. Marine heatwaves are not a dominant driver of change in demersal fishes. Nature 621, 324–329 (2023). https://doi.org/10.1038/s41586-023-06449-y

54. Free, C. M., Thorson, J. T., Pinsky, M. L., Oken, K. L., Wiedenmann, J., & Jensen, O. P. (2019). Impacts of historical warming on marine fisheries production. Science, 363(6430), 979–983. https://doi.org/10. 1126/science.aau1758

55. Froese, R., & Pauly, D. (Eds.). (2024). FishBase. World Wide Web electronic publication. www.fishbase.org

56. Gattuso, J.-P. et al. (2018). Ocean solutions to address climate change and its effects on marine ecosystems. Front. Mar. Sci .5, 337

57. Giomi Folco et al. (2019). Oxygen supersaturation protects coastal marine fauna from ocean warming. Sci. Adv.5, eaax1814 DOI:10.1126/sciadv.aax1814

58. Godbold J.A., Calosi P. (2013). Ocean acidification and climate change: advances in ecology and evolution. Philos Trans R Soc Lond B Biol Sci. Aug 26;368(1627):20120448. doi: 10.1098/rstb.2012.0448. PMID: 23980247; PMCID: PMC3758178.

59. González-Santana, D., Segovia, M., González-Dávila, M., Ramírez, L., González, A. G., Pozzo-Pirotta, L. J., Arnone, V., Vázquez, V., Riebesell, U., and Santana-Casiano, J. M.: Ocean alkalinity enhancement using sodium carbonate salts does not lead to measurable changes in Fe dynamics in a mesocosm experiment, Biogeosciences, 21, 2705–2715, https://doi.org/10.5194/bg-21-2705-2024, 2024.

60. Gordó-Vilaseca, C., Costello, M.J., Coll, M. et al. Future trends of marine fish biomass distributions from the North Sea to the Barents Sea. Nat Commun 15, 5637 (2024). https://doi.org/10.1038/s41467-024-49911-9

61. Gregorie M. et. al. A Global Ocean Oxygen Database and Atlas for Assessing and Predicting Deoxygenation and Ocean Health in the Open and Coastal Ocean review article Front. Mar. Sci., 21 December 2021, Sec. Ocean Observation, Volume 8 – 202, https://doi.org/10.3389/fmars.2021.724913

62. Hanley J. A., McNeil B. J. The meaning and use of the area under a receiver operating characteristic (ROC) curve. Radiology. 1982 Apr;143(1):29-36. doi: 10.1148/radiology.143.1.7063747. PMID: 7063747.

63. Harris, R. M. B. et al. (2018). Biological responses to the press and pulse of climate trends and extreme events. Nat. Clim. Change 8, 579–587

64. Hilborn R., Amoroso R., Collie J., Hiddink J. G., Kaiser M. J., Mazor T., McConnaughey R. A., Parma A. M., Pitcher C. R., Sciberras M., Suuronen P., Evaluating the sustainability and environmental impacts of trawling compared to other food production systems, ICES Journal of Marine Science, Volume 80, Issue 6, August 2023, Pages 1567–1579, https://doi.org/10.1093/icesjms/fsad115

doi:10.6342/NTU202500202

65. Hoegh-Guldberg O., Bruno J.F. (2010). The impact of climate change on the world's marine ecosystems. Science. Jun 18;328(5985):1523-8. doi: 10.1126/science.1189930. PMID: 20558709.

66. Holt J., Icarus Allen J., Anderson T. R., Brewin R., Butenschön M., James Harle, Huse G., Lehodey P., Lindemann C., Memery L., Salihoglu B., Senina I.,Yool A., (2014) Challenges in integrative approaches to modelling the marine ecosystems of the North Atlantic: Physics to fish and coasts to ocean, Progress in Oceanography, Volume 129, Part B, Pages 285-313, ISSN 0079-6611, https://doi.org/10.1016/j.pocean.2014.04.024.

67. Høyer, J. L., and I. Karagali, 2016: Sea Surface Temperature Climate Data Record for the North Sea and Baltic Sea. J. Climate, 29, 2529–2541, https://doi.org/10.1175/JCLI-D-15-0663.1.

68. Hughes K, Bellis MA, Hardcastle KA, Sethi D, Butchart A, Mikton C, Jones L, Dunne M.P. (2017). The effect of multiple adverse childhood experiences on health: a systematic review and meta-analysis. Lancet Public Health. Aug;2(8):e356-e366. doi: 10.1016/S2468-2667(17)30118-4. Epub 2017 Jul 31. PMID: 29253477.

69. Huthnance, J. et al. (2016). Recent Change—North Sea. In: Quante, M., Colijn, F. (eds) North Sea Region Climate Change Assessment. Regional Climate Studies. Springer, Cham. https://doi.org/10.1007/978-3-319-39745-0_3

70. ICES. (2020). Manual for the North Sea International Bottom Trawl Surveys. Series of ICES Survey Protocols SISP 10-IBTS 10, Revision 11. https://doi.org/10.17895/ices.pub.7562

71. ICES. (2021). Working Group for the Assessment of Demersal Stocks in the North Sea and Skagerrak (WGNSSK). ICES Scientific Reports. https://doi.org/10.17895/ices.pub.8211

72. ICES. (2022). Greater North Sea ecoregion – fisheries overview. ICES Advice: Fisheries Overviews. https://doi.org/10.17895/ices.advice.21641360.v1

73. ICES (2023). Working Group on the Assessment of Demersal Stocks in the North Sea and Skagerrak (WGNSSK). ICES Scientific Reports. Report. https://doi.org/10.17895/ices.pub.22643143.v1

74. IPCC (2022). Climate change 2022 impacts, adaptation and vulnerability: summary for policymakers. – Cambridge Univ.Press.

75. Isah RR, Enochs IC and San Diego-McGlone ML (2022). Sea surface carbonate dynamics at reefs of Bolinao, Philippines: Seasonal variation and fish mariculture-induced forcing. Front. Mar. Sci. 9:858853. doi: 10.3389/fmars.2022.858853

76. Jarnevich, C. S., Stohlgren, T. J., Kumar, S., Morisette, J. T. and Holcombe, T. R. (2015). Caveats for correlative species distribu- tion modeling. – Ecol. Inform. 29: 6–15.

77. Jickells, T. D. (1998). Nutrient biogeochemistry of the coastal zone. Science, 281(5374), 217–222.

78. Jones, M. C., Dye, S. R., Pinnegar, J. K., Warren, R., & Cheung, W. W. L. (2012). Modelling commercial fish distributions: Prediction and assessment using

doi:10.6342/NTU202500202

different approaches. Ecological Modelling, 225, 133–145. https://doi.org/10.1016/j.ecolmodel.2011.11.003

79. Kléparski L, Beaugrand G, Edwards M. (2021) Plankton biogeography in the North Atlantic Ocean and its adjacent seas: Species assemblages and environmental signatures. Ecol Evol; 11: 5135–5149. https://doi.org/10.1002/ece3.7406

80. Koenigstein, S., Mark, F.C., Gößling-Reisemann, S., Reuter, H. and Poertner, H.-O. (2016), Modelling climate change impacts on marine fish populations: process-based integration of ocean warming, acidification and other environmenal drivers. Fish Fish, 17: 972-1004. https://doi.org/10.1111/faf.12155

81. Lai, Y.-Z., Lin, Y.-C., & Ko, C.-Y. (2024). How would estimation of geographic range shifts of marine fishes be different when using occurrence and abundance data? Diversity and Distributions, 30, e13919. https://doi.org/10.1111/ddi.13919

82. Lange, S., Büchner, M., Volkholz, J., Wohland, J., Geiger, T., Akoğlu, E., & Frieler, K. (2020). ISIMIP3 simulation protocol. https://protocol.isimip.org

83. Lange, S., Volkholz, J., Geiger, T., Zhao, F., Vega, I., Veldkamp, T., et al. (2020). Projecting exposure to extreme climate impact events across six event categories and three spatial scales. Earth's Future, 11, e2020EF001616. https://doi.org/10.1029/2020EF001616

84. Laruelle, G. G., Cai, W. J., Hu, X., Gruber, N., Mackenzie, F. T., & Regnier, P. (2018). Continental shelves as a variable but increasing global sink for atmospheric carbon dioxide. Nature Communications, 9(1), 11. https://hdl.handle.net/10.1038/s41467-017-02738-z

85. Lasram F. B. R., Hattab T., Nogues Q. et. al. (2020). An open-source framework to model present and future marine species distributions at local scale, Ecological Informatics, Volume 59, 101130, ISSN 1574-9541, https://doi.org/10.1016/j.ecoinf.2020.101130.

86. Le Quesne, W.J.F. and Pinnegar, J.K. (2012). The potential impacts of ocean acidification: scaling from physiology to fisheries. Fish and Fisheries, 13: 333-344. https://doi.org/10.1111/j.1467-2979.2011.00423.x

87. Ma, D., Gregor, L., & Gruber, N. (2023). Four decades of trends and drivers of global surface ocean acidification. Global Biogeochemical Cycles, 37, e2023GB007765. https://doi.org/10.1029/2023GB007765

88. Martinez-Lopez, B., Quintanar, A. I., Cabos-Narvaez, W. D., & Moreles, E. (2024). On the non-linear nature of long-term sea surface temperature global trends. Earth and Space Science, 11, e2023EA003302. https://doi.org/10.1029/2023EA003302

89. Mathis M., Elizalde A., Mikolajewicz U., Pohlmann T. (2015). Variability patterns of the general circulation and sea water temperature in the North Sea, Progress in Oceanography, Volume 135, Pages 91-112, ISSN 0079-6611, https://doi.org/10.1016/j.pocean.2015.04.009.

90. Maynou, F., Sabatés, A., Ramirez-Romero, E. et al. (2020). Future distribution of early life stages of small pelagic fishes in the northwestern Mediterranean. Climatic Change161, 567–589. https://doi.org/10.1007/s10584-020-02723-4

doi:10.6342/NTU202500202

91. McHenry, J., Welch, H., Lester, S. E., & Saba, V. (2019). Projecting marine species range shifts from only temperature can mask climate vulnerability. Global Change Biology, 25(12), 4208–4221. https://doi. org/10.1111/gcb.14828

92. Meyer-Gutbrod, E., Kui, L., Miller, R., Nishimoto, M., Snook, L., & Love, M. (2021). Moving on up: Vertical distribution shifts in rocky reef fish species during climate-driven decline in dissolved oxygen from 1995 to 2009. Global Change Biology, 27, 6280–6293. https://doi.org/10.1111/gcb.15821

93. Meyer, J. and Riebesell, U. (2015). Reviews and Syntheses: Responses of coccolithophores to ocean acidification: a meta-analysis, Biogeosciences, 12, 1671–1682, https://doi.org/10.5194/bg-12-1671-2015.

94. Morée, A. L., Clarke, T. M., Cheung, W. W. L., and Frölicher, T. L. (2023). Impact of deoxygenation and warming on global marine species in the 21st century, Biogeosciences, 20, 2425–2454, https://doi.org/10.5194/bg-20-2425-2023

95. Nagelkerken I., Munday P.L. (2015). Animal behaviour shapes the ecological effects of ocean acidification and warming: moving from individual to community-level responses. Glob Chang Biol. 2016 Mar;22(3):974-89. doi: 10.1111/gcb.13167. Epub Dec 23. PMID: 26700211.

96. Nagelkerken, I., Russell, B., Gillanders, B. et al. (2016). Ocean acidification alters fish populations indirectly through habitat modification. Nature Clim Change 6, 89–93 https://doi.org/10.1038/nclimate275

97. Neuenfeldt, Stefan & Righton, David & Neat, Francis & Wright, Peter & Svedäng, Henrik & Michalsen, Kathrine & Subbey, Sam & P, Steingrund & V, Thorsteinsson & Pampoulie, Christophe & Andersen, Ken & Pedersen, Martin & Metcalfe, J. (2013). Analysing migrations of Atlantic cod Gadus morhua in the North-East Atlantic Ocean: then, now and the future. Journal of Fish Biology. 82. 741-763.10.1111/jfb.12043.

98. Nisin Mohamed K.M.N., Sreenath K.R., Miriam Paul Sreeram (2023). Change in habitat suitability of the invasive Snowflake coral (Carijoa riisei) during climate change: An ensemble modelling approach, Ecological Informatics, Volume 76, 102145, ISSN 1574-9541, https://doi.org/10.1016/j.ecoinf.2023.102145.

99. NOAA National Centers for Environmental Information. (2022). ETOPO 2022 15 Arc-Second Global Relief Model. https://doi.org/10.25921/fd45-gt74

100. NOAA National Ocean Service. (2024). What is the difference between latitude and longitude? National Oceanic and Atmospheric Administration, U.S. Department of Commerce. https://oceanservice.noaa.gov/facts/longitude.html

101. O'Neill, B. C., Tebaldi, C., van Vuuren, D. P., Eyring, V., Friedlingstein, P., Hurtt, G., Knutti, R., Kriegler, E., Lamarque, J.-F., Lowe, J., Meehl, G. A., Moss, R., Riahi, K., and Sanderson, B. M. (2016): The Scenario Model Intercomparison Project (ScenarioMIP) for CMIP6, Geosci. Model Dev., 9, 3461–3482, https://doi.org/10.5194/gmd-9-3461-2016.

102. Omstedt, A., et al. (2004). The Skagerrak and Kattegat. Deep Sea Research Part II, 51(21-22), 2645-2654.

103. OSPAR Commission. (2000). Quality Status Report 2000. OSPAR Commission.

doi:10.6342/NTU202500202

104. OSPAR Commission. (2023). Fish Thematic Assessment. In Quality Status Report 2023. https://oap.ospar.org/en/ospar-assessments/quality-status-reports/qsr-2023/thematic-assessments/fish/

105. Otto, L., Zimmerman, J. T. F., Furnes, G. K., Mork, M., Sætre, R., & Becker, G. (1990). Review of the physical oceanography of the North Sea. Netherlands Journal of Sea Research, 26 (2–4), 161–238. https://doi.org/10.1016/0077-7579(90)90091-T

106. Pauly, D. (2021). The gill-oxygen limitation theory (GOLT) and its critics. Science Advances, 7(2), eabc6050. https://doi.org/10.1126/sciadv. abc6050

107. Pauly, D., Christensen, V., Dalsgaard, J., Froese, R., & Torres, F. Jr. (1998). Trophic levels of marine consumers. Marine Ecology Progress Series, 171, 19-34.

108. Peck M. A., Pinnegar J., (2018). Impacts of climate change on fisheries and aquaculture: Synthesis of current knowledge, adaptation and mitigation options. FAO Fisheries and aquaculture technical paper, Chapter 5, P. 87-111, ISSN 2070-7010

109. Pérez Roda, M.A. (ed.), Gilman, E., Huntington, T., Kennelly, S.J., Suuronen, P., Chaloupka, M. and Medley, P. (2019) A third assessment of global marine fisheries discards. FAO Fisheries and Aquaculture Technical Paper No. 633. Rome, FAO. 78 pp.

110. Phillips, S. J., Anderson, R. P. and Schapire, R. E. (2006). Maximum entropy modeling of species geographic distributions. – Ecol. Model. 190: 231–259. DOI: 10.1016/j.ecolmodel.2005.03.026

111. Piet G. J., van Hal R., Greenstreet S. P. R. (2009) Modelling the direct impact of bottom trawling on the North Sea fish community to derive estimates of fishing mortality for non-target fish species, ICES Journal of Marine Science, Volume 66, Issue 9, Pages 1985–1998, https://doi.org/10.1093/icesjms/fsp162

112. Pingree, R. D., & Griffiths, D. K. (1978). Tidal fronts on the shelf seas around the British Isles. Journal of Geophysical Research, 83(C9), 4615-4622.

113. Pinsky, M. L., Eikeset, A. M., Helmerson, C., Bradbury, I. R., Bentzen, P., Morris, C., Gondek-Wyrozemska, A. T., Baalsrud, H. T., Brieuc, M. S. O., Kjesbu, O. S., Godiksen, J. A., Barth, J. M. I., Matschiner, M., Stenseth, N. C., Jakobsen, K. S., Jentoft, S., & Star, B. (2021). Genomic stability through time despite decades of exploitation in cod on both sides of the Atlantic. Proceedings of the National Academy of Sciences, 118 (15), https://doi.org/10.1073/pnas.2025453118

114. Pinsky, M. L., et al. (2018). Preparing ocean governance for species on the move. Science, 360(6394), 1189–1191. https://doi.org/10.1126/science.aat2360

115. Pinsky, M.L., Eikeset, A.M., McCauley, D.J. et al. (2019). Greater vulnerability to warming of marine versus terrestrial ectotherms. Nature 569, 108–111 https://doi.org/10.1038/s41586-019-1132-4

116. Poloczanska, E., Brown, C., Sydeman, W. et al. (2013). Global imprint of climate change on marine life. Nature Clim Change 3, 919–925. https://doi.org/10.1038/nclimate1958

doi:10.6342/NTU202500202

117. Pontius, R. G., & Millones, M. (2011). Death to Kappa: Birth of quantity disagreement and allocation disagreement for accuracy assessment. International Journal of Remote Sensing, 32(15), 4407-4429. https://doi.org/10.1080/01431161.2011.552923

118. Pörtner, H. O., & Knust, R. (2007). Climate change affects marine fishes through the oxygen limitation of thermal tolerance. Science, 315(5808), 95–97. https://doi.org/10.1126/science.1135471

119. Quante, M.; Colijn, F.; Bakker, J.P.; Härdtle, W.; Heinrich, H.; Lefebvre, C.; Nöhren, I.; Olesen, J.E.; Pohlmann, T.; Sterr, H.; Sündermann, J.; Tölle, M.H. (2016). Introduction to the assessment - characteristics of the region, in North Sea region climate change assessment. Regional Climate Studies: pp. 1-52. http://dx.doi.org/10.1007/978-3-319-39745-0_1

120. Radach, G., Pätsch, J. (2007). Variability of continental riverine freshwater and nutrient inputs into the North Sea for the years 1977–2000 and its consequences for the assessment of eutrophication. Estuaries and Coasts: J ERF 30, 66–81 https://doi.org/10.1007/BF02782968

121. Raftery, A. E., Zimmer, A., Frierson, D. M. W., Startz, R., & Liu, P. (2017). Less than 2 °C warming by 2100 unlikely. Nature Climate Change, 7, 637–641. https://doi.org/10.1038/nclimate3352

122. Salt, L. A., H. Thomas, A. E. F. Prowe, A. V. Borges, Y. Bozec, and H. J. W. de Baar (2013). Variability of North Sea pH and CO2 in response to North Atlantic Oscillation forcing, J. Geophys. Res. Biogeosci., 118, 1584–1592, doi:10.1002/2013JG002306.

123. Saraji, S., Akindipe, D. (2024). The Role of the Oil and Gas Industry in the Energy Transition. In: Walker, T., Barabanov, S., Michaeli, M., Kelly, V. (eds) Sustainability in the Oil and Gas Sector. Palgrave Macmillan, Cham. https://doi.org/10.1007/978-3-031-51586-6_3

124. Sarofim, M.C., Smith, C.J., Malek, P. et al. (2024). High radiative forcing climate scenario relevance analyzed with a ten-million-member ensemble. Nat Commun 15, 8185 https://doi.org/10.1038/s41467-024-52437-9

125. Schulte P. M., (2015). The effects of temperature on aerobic metabolism: Towards a mechanistic understanding of the responses of ectotherms to a changing environment. J. Exp. Biol. 218, 1856 –1866

126. Seo, C., Thorne, J., Hannah, L. and Thuiller, W. (2008). Scale effects in species distribution models: implications for conservation planning under climate change. – Biol. Lett. 5: 39–43.

127. Shelton, A. O., Thorson, J. T., Ward, E. J. and Feist, B. E. (2014). Spatial semiparametric models improve estimates of species abundance and distribution. – Can. J. Fish. Aquat. Sci. 71: 1655–1666.

128. Shiogama, H., Fujimori, S., Hasegawa, T. et al. (2023). Important distinctiveness of SSP3–7.0 for use in impact assessments. Nat. Clim. Chang. 13, 1276–1278 https://doi.org/10.1038/s41558-023-01883-2

129. Simon P.R. Greenstreet, Stuart I. Rogers, Indicators of the health of the North Sea fish community (2006): identifying reference levels for an ecosystem

doi:10.6342/NTU202500202

approach to management, ICES Journal of Marine Science, Volume 63, Issue 4, Pages 573–593, https://doi.org/10.1016/j.icesjms.2005.12.009

130. Smale, D.A., Wernberg, T., Oliver, E.C.J. et al. Marine heatwaves threaten global biodiversity and the provision of ecosystem services. Nat. Clim. Chang. 9, 306–312 (2019). https://doi.org/10.1038/s41558-019-0412-1

131. Smith, K. E., Burrows, M. T., Hobday, A. J., King, N. G., Moore, P. J., Sen Gupta, A., Thomsen, M. S., Wernberg, T., & Smale, D. A. (2023). Biological impacts of marine heatwaves. Annual Review of Marine Science, 15, 119–145. https://doi.org/10.1146/annurev-marine-032122-121437

132. Sofaer, H. R., Jarnevich, C. S. and Flather, C. H. (2018). Misleading prioritizations from modelling range shifts under climate change. – Global Ecol. Biogeogr. 27: 658–666

133. Stenberg, Claus & Støttrup, J.G. & Deurs, Mikael & Berg, C. & Dinesen, Grete & Mosegaard, Henrik & Grome, T. & Leonhard, S.(2015). Long-term effects of an offshore wind farm in the North Sea on fish communities. Marine Ecology Progress Series. 528. 257–265,10.3354/meps11261.

134. Sunday, J.M., Pecl, G.T., Frusher, S., Hobday, A.J., Hill, N., Holbrook, N.J., Edgar, G.J., Stuart-Smith, R., Barrett, N., Wernberg, T., Watson, R.A., Smale, D.A., Fulton, E.A., Slawinski, D., Feng, M., Radford, B.T., Thompson, P.A. and Bates, A.E. (2015), Species traits and climate velocity explain geographic range shifts in an ocean-warming hotspot. Ecol Lett, 18: 944-953. https://doi.org/10.1111/ele.12474

135. Sündermann, J., & Pohlmann, T. (2011). A brief analysis of North Sea physics. Oceanologia, 53 (3), 663–689. https://doi.org/10.5697/oc.53-3.663

136. Tai TC, Sumaila UR and Cheung WWL (2021) Ocean Acidification Amplifies Multi-Stressor Impacts on Global Marine Invertebrate Fisheries. Front. Mar. Sci. 8:596644. doi: 10.3389/fmars.2021.596644

137. Thuiller, W., Lafourcade, B., Engler, R. and Araújo, M.B. (2009), BIOMOD – a platform for ensemble forecasting of species distributions. Ecography, 32: 369-373. https://doi.org/10.1111/j.1600-0587.2008.05742.x

138. Thuiller, W., Damie, G., Robin, E., Frank, F. Biomod2: Ensemble Platform for Species Distribution Modeling (2016).

139. Thuiller, W., Georges, D., Gueguen, M., Engler, R., Breiner, F., Lafourcade, B., Patin, R., & Blancheteau, H. (2024). biomod2: Ensemble Platform for Species Distribution Modeling [R package]. https://doi.org/10.32614/CRAN.package.biomod2

140. Tishchenko P., et al. (2022) - Revisiting the Carbonate Chemistry of the Sea of Japan (East Sea): From Water Column to Sediment – Marine Science and Engineering, MDPI.

141. Tittensor, D. P., Novaglio, C., Harrison, C. S., et al. (2021). Next-generation ensemble projections reveal higher climate risks for marine ecosystems. Nature Climate Change, 11, 973–981. https://doi.org/10.1038/s41558-021-01173-9

doi:10.6342/NTU202500202

142. Townhill B. L., Couce E., Tinker J., Kay S., & Pinnegar, J. K. (2023). Climate change projections of commercial fish distribution and suitable habitat around northwestern Europe. Fish and Fisheries, 24, 848–862. https://doi.org/10.1111/faf.12773

143. Turrell, W. R., Henderson, E. W., Slesser, G., Payne, R., & Adams, R. D. (1992). Seasonal changes in the circulation of the northern North Sea. Continental Shelf Research, 12 (2–3), 257–286. https://doi.org/10.1016/0278-4343(92)90032-F

144. UNESCO. (2024). New UNESCO report: Rate of ocean warming doubled in 20 years, rate of sea level rise doubled in 30 years. https://www.unesco.org/en/articles/new-unesco-report-rate-ocean-warming-doubled-20-years-rate-sea-level-rise-doubled-30-years

145. Urban M.C.(2019). Projecting biological impacts from climate change like a climate scientist. WIREs Clim Change; 10:e585. https://doi.org/10.1002/wcc.585

146. Valavi, R., G. Guillera-Arroita, J. J. Lahoz-Monfort, and J. Elith. (2022). Predictive performance of presence-only species distribution models: a benchmark study with reproducible code. Ecological Monographs 92(1):e01486. 10.1002/ecm.1486

147. van Aken, H. M., G. J. van Heijst, and L. R. Maas. (1987). "Observations of fronts Journal of Marine Research 45, (3). https://elischolar.library.yale.edu/journal_of_marine_research/1862

148. van Leeuwen, S., P. Tett, D. Mills, and J. van der Molen (2015). Stratified and nonstratified areas in the North Sea: Long-term variability and biological and policy implications, J. Geophys. Res. Oceans, 120, 4670–4686, doi:10.1002/2014JC010485.

149. Van Vuuren et al. (2013). A new scenario framework for Climate Change Research: scenario matrix architecture, Climatic Change, volume 122, pages373–386(2014), doi:10.1007/s10584-013-0906-1

150. Vargas, C., Lagos, N., Lardies, M. et al. (2017). Species-specific responses to ocean acidification should account for local adaptation and adaptive plasticity. Nat Ecol Evol 1, 0084 https://doi.org/10.1038/s41559-017-0084

151. Vergés A., Doropoulos C., Malcolm H.A., Skye M., Garcia-Pizá M., Marzinelli E.M., Campbell A.H., Ballesteros E., Hoey A.S., Vila-Concejo A., Bozec Y., Steinberg P.D., (2016). Long-term empirical evidence of ocean warming leading to tropicalization of fish communities, increased herbivory, and loss of kelp, Proc. Natl. Acad. Sci. U.S.A. 113 (48) 13791-13796, https://doi.org/10.1073/pnas.1610725113

152. Wahl, T., Haigh, I., Albrecht, F., Dillingh, D., Jensen, J., Nicholls, R., Weisse, R., Woodworth, P.L., Wöppelmann, G. (2013). Observed mean sea level changes around the North Sea coastline from 1800 to present, Earth Science Reviews, 124, 51–67.

153. Wang, H., Hu, X., Cai, W.-J., Sterba-Boatwright, B. (2017). Decadal fCO2 trends in global ocean margins and adjacent boundary current-influenced areas. Geophysical Research Letters,44,8962–8970. https://doi.org/10.1002/2017GL074724

doi:10.6342/NTU202500202

154. Whittaker, R. J., Araújo, M. B., Jepson, P., Ladle, R. J., Watson, J.E. M. and Willis, K. J. (2005). Conservation biogeography: assessment and prospect. – Divers. Distrib. 11: 3–23.

155. Willis, K.J. and Bhagwat, S.A. (2009). Biodiversity and Climate Change. Science, 326, 806-807. http://dx.doi.org/10.1126/science.1178838

156. Wolff G. J. L. Sarmiento & N. Gruber (2006). Ocean Biogeochemical Dynamics. xiii + 503 pp. Princeton, Woodstock: Princeton University Press. Price £48.95 (hard covers). 0 691 01707 7. Geological Magazine. 2007;144(6):1034-1034. doi:10.1017/S0016756807003755

157. Woods PJ, Macdonald JI, Bárðarson H, et al. (2022). A review of adaptation options in fisheries management to support resilience and transition under socio-ecological change. ICES J Mar Sci.79(2):463-479. doi:10.1093/icesjms/fsab244.

158. Wright, P. J., Millar, C. P. & Gibb, F. M. (2011). Intra-stock differences in maturation schedules of Atlantic cod Gadus morhua in the North Sea. ICES Journal of Marine Science 86, 1918–1927.

159. Yates K.L., Bouchet P.J., Caley M.J. et al. (2018). Outstanding Challenges in the Transferability of Ecological Models. Trends Ecol Evol. Oct;33(10):790-802. doi: 10.1016/j.tree.2018.08.001. Epub 2018 Aug 27. PMID: 30166069.

160. Yates, L. A., Aandahl, Z., Richards, S. A. and Brook, B. W. (2023) – Cross validation for model selection: a primer with examples from ecology. Ecol. Monogr. 93: e1557.

161. Young, M. and Carr, M. H. (2015). Application of species distribution models to explain and predict the distribution, abundance and assemblage structure of nearshore temperate reef fishes. – Divers. Distrib. 21: 1428–1440.

162. Zangiabadi S., Zaremaivan H., Brotons L, Mostafavi H., Ranjbar H. (2021). Using climatic variables alone overestimate climate change impacts on predicting distribution of an endemic species. PLoS ONE 16(9): e0256918. https://doi.org/10.1371/journal.pone.0256918

163. Zhang S., Heck P.R., Meyer M.N., Chabris C.F., Goldstein D.G., Hofman J.M., (2023). An illusion of predictability in scientific results: Even experts confuse inferential uncertainty and outcome variability, Proc. Natl. Acad. Sci. U.S.A. 120 (33) e2302491120, https://doi.org/10.1073/pnas.2302491120

164. Zhu, Y., Lin, Y., Chu, J. et al. (2022). Modelling the variation of demersal fish distribution in Yellow Sea under climate change. J. Ocean. Limnol. 40, 1544–1555 https://doi.org/10.107/s00343-021-1126-6

doi:10.6342/NTU202500202

Illustrations

Table 1. Identification of trophic level, commercial value and functional group (demersal or pelagic) of selected filtered species.

	Family	Scientific name	Common Name	Trophic Level	Commercial	Functional Group
1	Anarhichadidae	***Anarhichas lupus***	Atlantic Wolffish	3.6 ± 0.0	No	Demersal
2	Argentinidae	***Argentina sphyraena***	Argentine Herring	3.5 ± 0.5	No	Pelagic
3	Bothidae	***Arnoglossus laterna***	Mediterranean Scaldfish	3.6 ± 0.3	No	Demersal
4	Callionymidae	***Callionymus maculatus***	Spotted Dragonet	3.3 ± 0.45	No	Demersal
5	Carangidae	***Trachurus trachurus***	Atlantic Horse Mackerel	3.7 ± 0.0	Yes	Pelagic
6	Clupeidae	***Sardina pilchardus***	European Pilchard	3.1 ± 0.1	Yes	Pelagic
7	Cottidae	***Myoxocephalus scorpius***	Shorthorn Sculpin	3.9 ± 0.0	No	Demersal
8	Cyclopteridae	***Cyclopterus lumpus***	Lumpfish	3.9 ± 0.0	No	Demersal
9	Engraulidae	***Engraulis encrasicolus***	European Anchovy	3.1 ± 0.36	Yes	Pelagic
10	Merlucciidae	***Merluccius merluccius***	European Hake	4.4 ± 0.0	Yes	Demersal
11	Mullidae	***Mullus surmuletus***	Red Mullet	3.5 ± 0.3	Yes	Demersal
12	Rajidae	***Amblyraja radiata***	Thorny Skate	4.2 ± 0.3	No	Demersal
13	Rajidae	***Raja montagui***	Spotted Ray	3.9 ± 0.2	Yes	Demersal
14	Scombridae	***Scomber scombrus***	Atlantic Mackerel	3.6 ± 0.2	Yes	Pelagic
15	Scyliorhinidae	***Scyliorhinus canicula***	Small-Spotted Catshark	3.8 ± 0.3	No	Demersal
16	Sebastidae	***Sebastes viviparus***	Norway Redfish	4.0 ± 0.67	No	Demersal
17	Soleidae	***Buglossidium luteum***	Solenette	3.3 ± 0.4	No	Demersal
18	Triakidae	***Mustelus asterias***	Starry Smooth-Hound	3.6 ± 0.3	No	Demersal
19	Triglidae	***Chelidonichthys cuculus***	Red Gurnard	3.8 ± 0.1	Yes	Demersal
20	Triglidae	***Chelidonichthys lucerna***	Tub Gurnard	4.0 ± 0.0	Yes	Demersal
21	Triglidae	***Eutrigla gurnardus***	Grey Gurnard	3.9 ± 0.0	Yes	Demersal

doi:10.6342/NTU202500202

Table 2. List of filtered species and their coefficients obtained from regression model. Triple Asterisk (***) indicate high significance (p-value ≤ 0.001). "Years" refers to years of observed occurrence of each species.

	Scientific name	R^2	Intercept	Slope	Significance	Years
1	***Amblyraja radiata***	0.603	1418.491	-0.682	***	42
2	***Anarhichas lupus***	0.779	1590.44	-0.787	***	42
3	***Argentina sphyraena***	0.609	-1021.243	0.527	***	42
4	***Arnoglossus laterna***	0.694	-1560.86	0.791	***	42
5	***Buglossidium luteum***	0.517	-1018.883	0.522	***	42
6	***Callionymus maculatus***	0.543	-1547.886	0.791	***	42
7	***Chelidonichthys cuculus***	0.854	-1373.777	0.693	***	41
8	***Chelidonichthys lucerna***	0.722	-895.777	0.451	***	32
9	***Cyclopterus lumpus***	0.348	1238.605	-0.604	***	42
10	***Engraulis encrasicolus***	0.676	-3122.853	1.573	***	35
11	***Eutrigla gurnardus***	0.605	-997.019	0.541	***	42
12	***Merluccius merluccius***	0.441	-1209.944	0.621	***	42
13	***Mullus surmuletus***	0.736	-2222.816	1.12	***	34
14	***Mustelus asterias***	0.803	-1265.599	0.637	***	31
15	***Myoxocephalus scorpius***	0.595	-1182.999	0.604	***	42
16	***Raja montagui***	0.79	-1047.771	0.53	***	42
17	***Sardina pilchardus***	0.701	-2106.776	1.06	***	31
18	***Scomber scombrus***	0.573	-1664.207	0.852	***	42
19	***Scyliorhinus canicula***	0.927	-2551.399	1.29	***	42
20	***Sebastes viviparus***	0.558	511.551	-0.252	***	41
21	***Trachurus trachurus***	0.427	-2621.308	1.335	***	42

doi:10.6342/NTU202500202

Table 3. List of models used to project species distributions.

Functional Group	Model Name	Abbreviation
Demersal (16)	Sea Bottom Temperature	**SBT**
	Sea Bottom Temperature + Bottom pH	**SBT + pH_bot**
	Sea Bottom Temperature + Bottom Dissolved Oxygen	**SBT + O2_bot**
	Bottom Dissolved Oxygen + Bottom pH	**O2_bot +pH_bot**
	Sea Bottom Temperature + Bottom Dissolved Oxygen +Bottom pH	**SBT + O2_bot +pH_bot**
Pelagic (5)	Sea Surface Temperature	**SST**
	Sea Surface Temperature + Surface pH	**SST + pH_surf**
	Sea Surface Temperature + Surface Dissolved Oxygen	**SST + O2_surf**
	Surface Dissolved Oxygen + Surface pH	**O2_surf + pH_surf**
	Sea Surface temperature + Surface Dissolved Oxygen + Surface pH	**SST + O2_surf + pH_surf**

doi:10.6342/NTU202500202

Table 4. Best Performance of Evaluation Metric (TSS) by Experiment for 16 Demersal Species (A) and for 5 Pelagic Species (B). The "winning" experiment based on the highest value of the model performance is in bold and underlined. "E" refers to the "Ensemble" model that combines 6 different SDMs, "CTA" and "RF" refer to the types of SDMs. Each column represents the certain experiment, containing different environmental variables combinations.

Scientific Name	pH_bot+O2_bot	SBT	SBT+O2_bot	SBT+pH_bot	SBT+pH_bot +O2_bot
Amblyraja radiata	E:0.900	**E:0.951**	E:0.932	E:0.900	E:0.880
Anarhichas lupus	E:0.899	**E:0.948**	E:0.933	E:0.901	E:0.873
Arnoglossus laterna	E:0.932	**E:0.950**	E:0.941	E:0.923	E:0.922
Buglossidium luteum	E:0.930	**E:0.951**	E:0.949	E:0.923	E:0.926
Callionymus maculatus	E:0.904	**E:0.951**	E:0.910	E:0.906	E:0.865
Chelidonichthys cuculus	E:0.910	**E:0.948**	E:0.939	E:0.912	E:0.901
Chelidonichthys lucerna	E:0.900	**E:0.945**	E:0.911	E:0.895	E:0.869
Cyclopterus lumpus	E:0.913	**E:0.951**	E:0.933	E:0.911	E:0.900
Eutrigla gurnardus	E:0.888	**E:0.955**	E:0.927	E:0.909	E:0.900
Merluccius merluccius	E:0.915	**E:0.955**	E:0.935	E:0.902	E:0.890
Mullus surmuletus	E:0.921	**E:0.953**	E:0.925	E:0.916	RF:0.902
Mustelus asterias	E:0.893	**E:0.950**	E:0.926	E:0.897	E:0.872
Myoxocephalus scorpius	E:0.910	**CTA:0.949**	E:0.925	CTA:0.908	E:0.891
Raja montagui	E:0.906	**E:0.954**	E:0.923	E:0.902	E:0.880
Scyliorhinus canicula	E:0.902	**E:0.951**	E:0.919	E:0.903	E:0.889
Sebastes viviparus	E:0.899	**E:0.946**	E:0.914	E:0.891	E:0.878

doi:10.6342/NTU202500202

Table 5. Best Performance of Evaluation Metric (TSS) by Experiment for 5 Pelagic Species. The "winning" experiment based on the highest value of the model performance is in bold and underlined. "E" refers to the "Ensemble" model that combines 6 different SDMs. Each column represents the certain experiment, containing different environmental variables combinations.

Scientific Name	pH_surf+O2_surf	SST	SST+O2_surf	SST+pH_surf	SST+pH_surf+ O2_surf
Argentina sphyraena	E:0.919	**E:0.949**	E:0.938	E:0.913	E:0.896
Engraulis encrasicolus	E:0.938	**E:0.951**	E:0.937	E:0.925	E:0.916
Sardina pilchardus	E:0.937	**E:0.949**	E:0.924	E:0.933	E:0.924
Scomber scombrus	E:0.923	**E:0.951**	E:0.929	E:0.915	E:0.899
Trachurus trachurus	E:0.923	**E:0.951**	E:0.930	E:0.908	E:0.866

doi:10.6342/NTU202500202

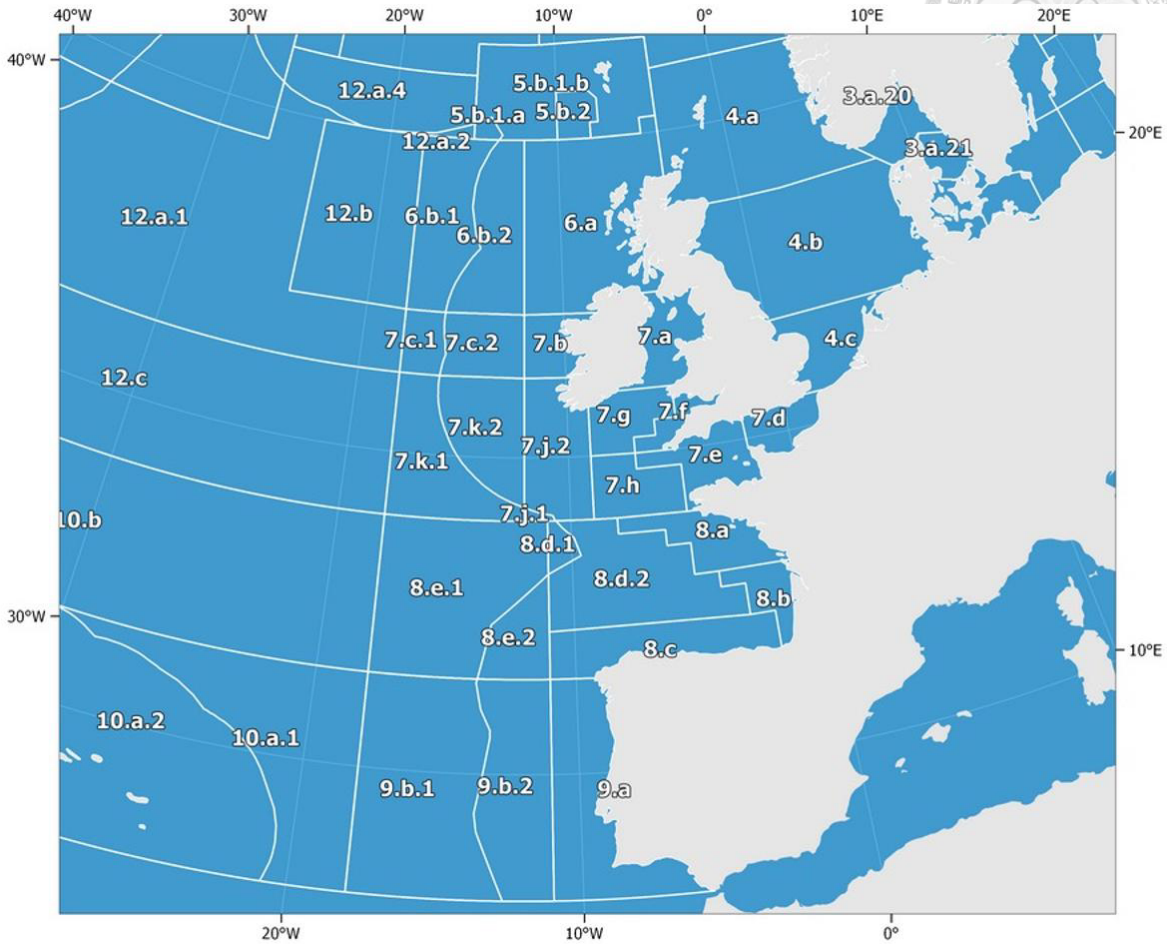

Figure 1. Atlantic, Northeast (Major Fishing Area 27) Here are the detailed boundaries of the ICES subareas 27.4, 27.5, 27.6, 27.7, 27.8, 27.9. North Sea refer to 4.a, 4.b, 4.c. (FAO, 2024).

doi:10.6342/NTU202500202

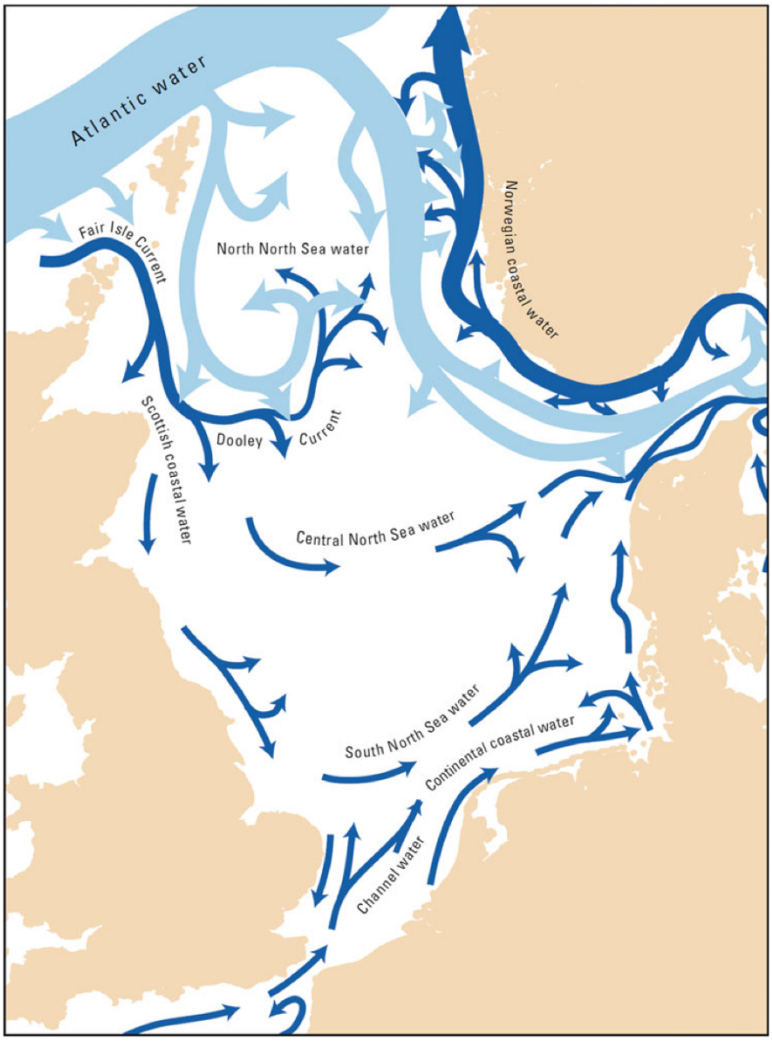

Figure 2. Circulation system of the North Sea (OSPAR, 2000). The width of arrows is indicative of the magnitude of volume transport. Light blues arrows indicate relatively pure Atlantic water, blue arrows indicate surface currents.

doi:10.6342/NTU202500202

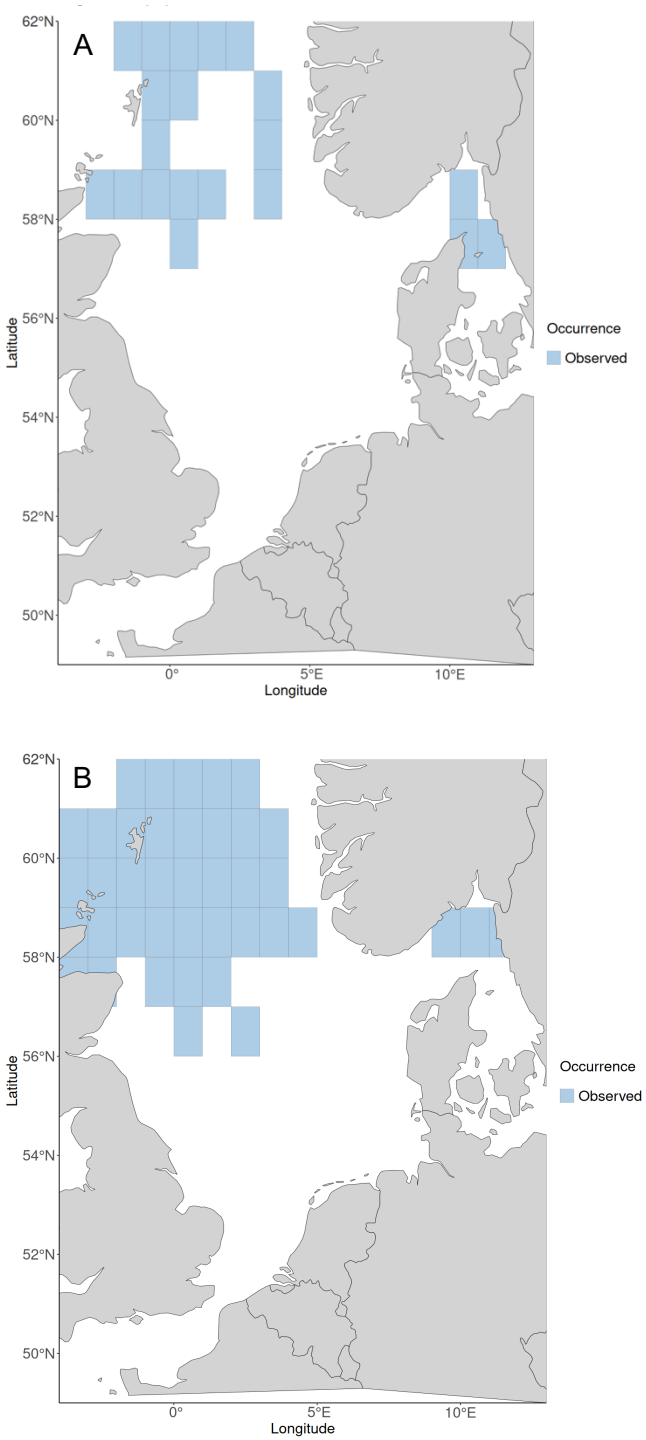

Figure 3. Original data visualization of occurrence maps for *Argentina sphyraena* in Q1 (Jan-Mar) season in1983 (A) and 2024 (B). The blue rectangles represent the observed occurrence of the fish in the exact 1°x1° grid area from the trawling data.

doi:10.6342/NTU202500202

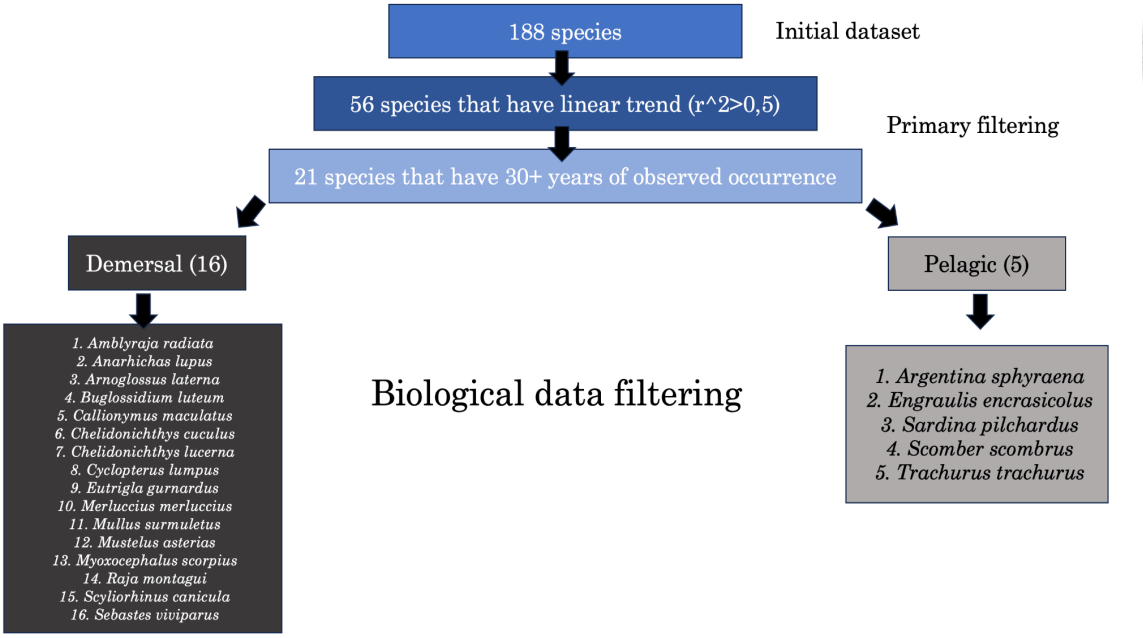

Figure 4. Chart for biological data filtering. Scientific species names refer to the ones used in this research

doi:10.6342/NTU202500202

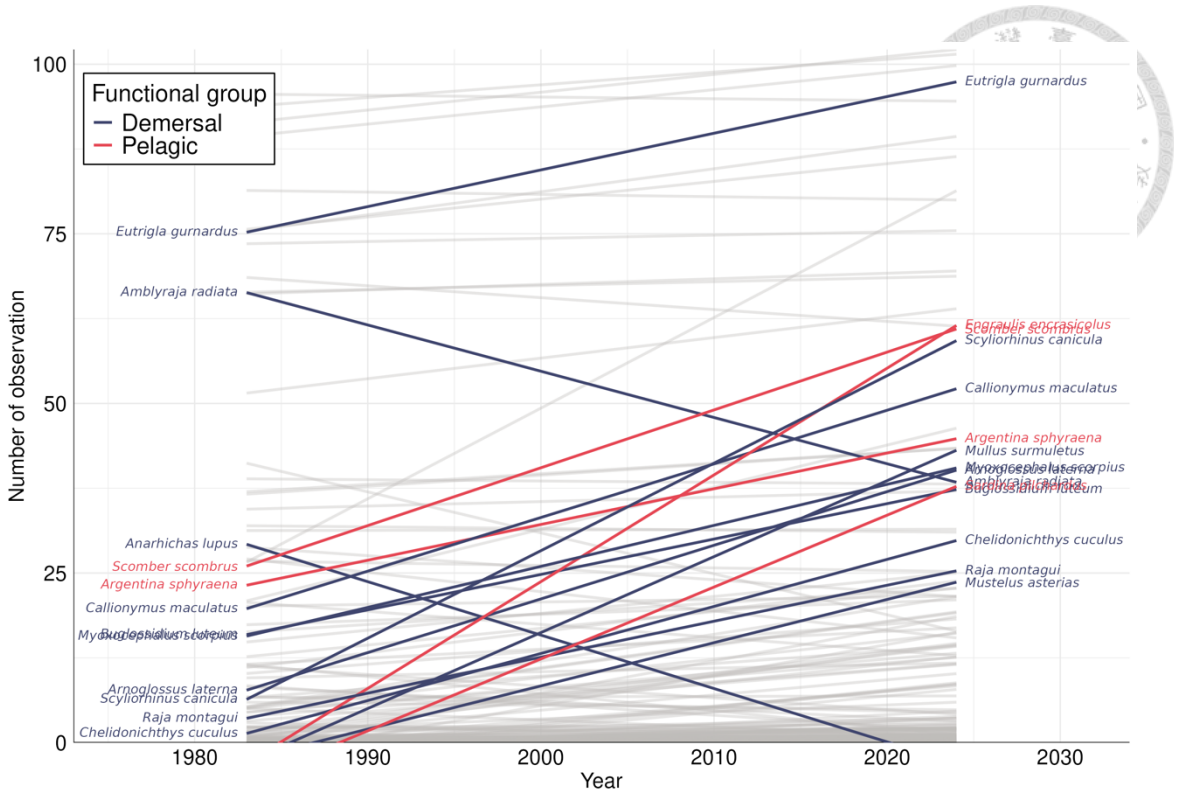

Figure 5. Combined changes (linear regression lines) in Demersal and Pelagic Species Distribution in the North Sea (1983-2024) based on observed grids per year. X-axis indicate years, y-axis indicate number of grids in which species were observed in each year during the 1983-2024 period. Red colors refer to pelagic species, Blue - to demersal and grey to those species that were not included in the research as they did not meet the requirements.

doi:10.6342/NTU202500202

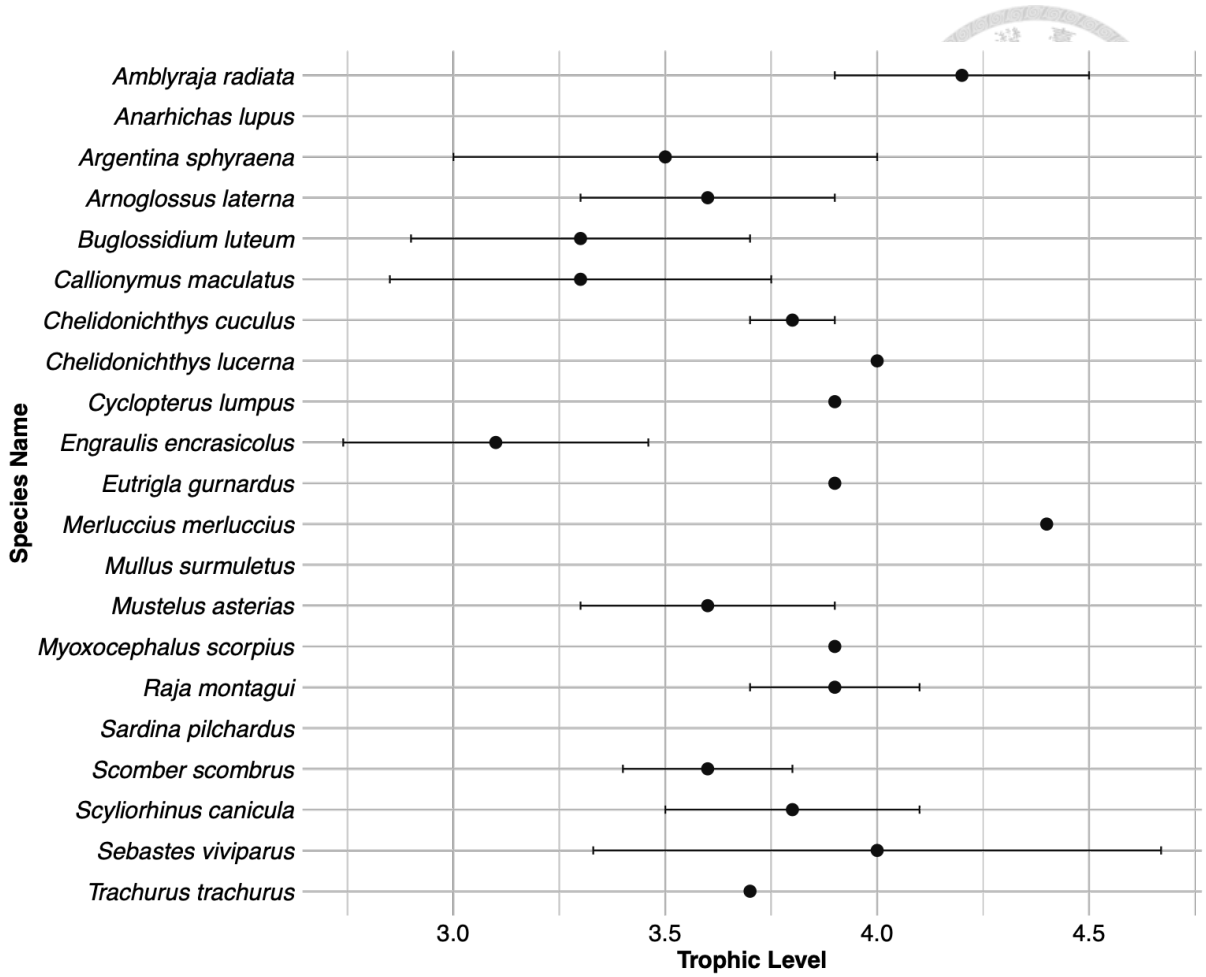

Figure 6. Selected species trophic levels based on the data from FishBase. The x-axis indicates trophic level, y-axis show fish speceis' scientific names. The thresholds explain the range of the trophic level for each species.

doi:10.6342/NTU202500202

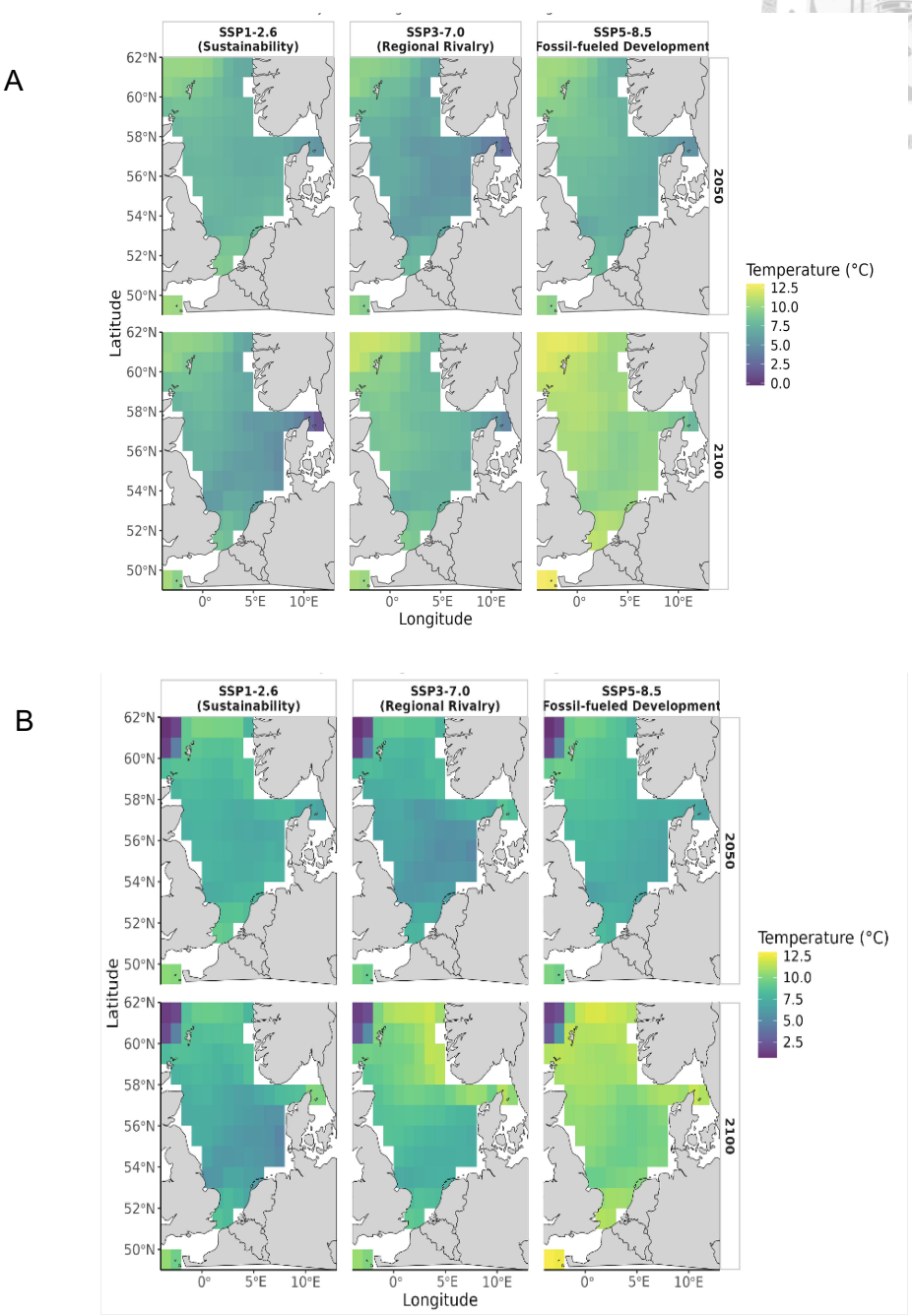

.

Figure 7. Projections of Sea Surface Temperature (A) and Sea Bottom Temperature (B) under 3 climate scenarios (SSP1-2.6, SSP3-7.0, and SSP5-8.5) across two time periods: 2050 (top row) and 2100 (bottom row). 1 gird resolution is 60 arcmin. Colors indicate temperature range.

doi:10.6342/NTU202500202

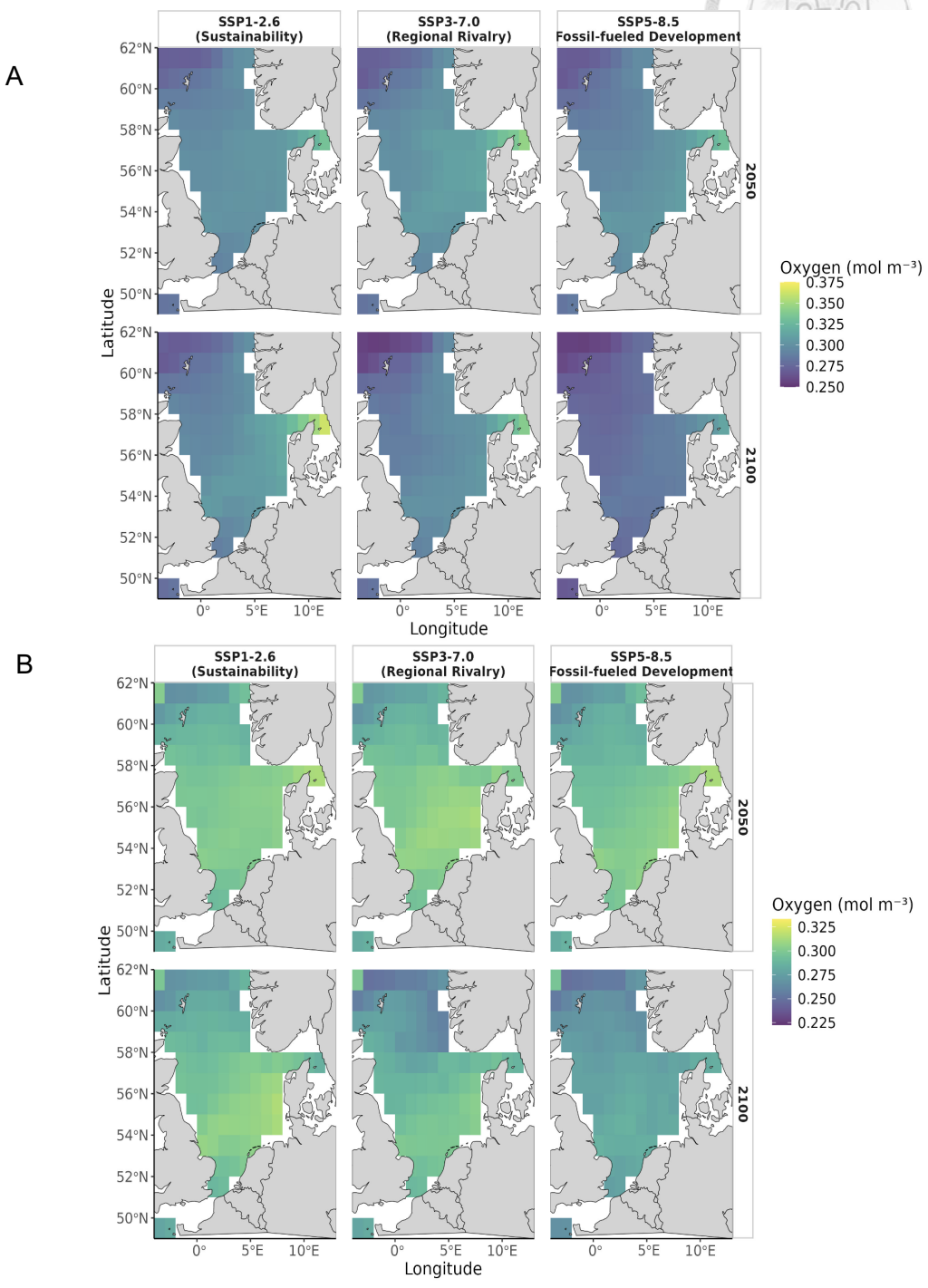

Figure 8. Projections of Surface Dissolved Oxygen Concentrations (A) and Bottom Dissolved Oxygen Concentrations (B) under 3 climate scenarios (SSP1-2.6, SSP3-7.0, and SSP5-8.5 across two time periods: 2050 (top row) and 2100 (bottom row). 1 gird resolution is 60 arcmin. Colors indicate dissolved oxygen range.

doi:10.6342/NTU202500202

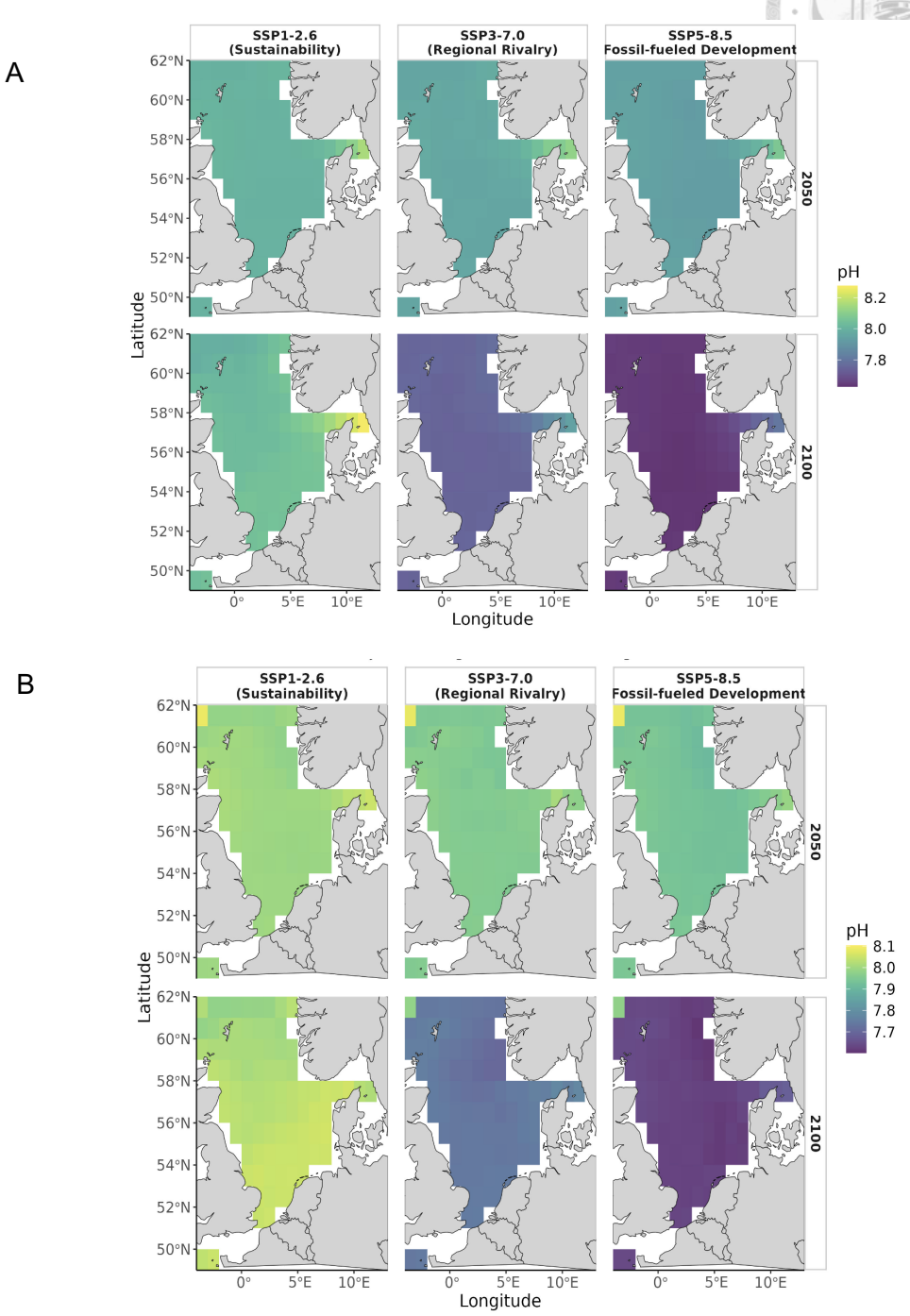

Figure 9. Projections of Surface pH (A) and Bottom Surface pH (B) under 3 climate scenarios (SSP1-2.6, SSP3-7.0, and SSP5-8.5) across two time periods: 2050 (top row) and 2100 (bottom row). 1 gird resolution is 60 arcmin. Colors indicate pH range.

doi:10.6342/NTU202500202

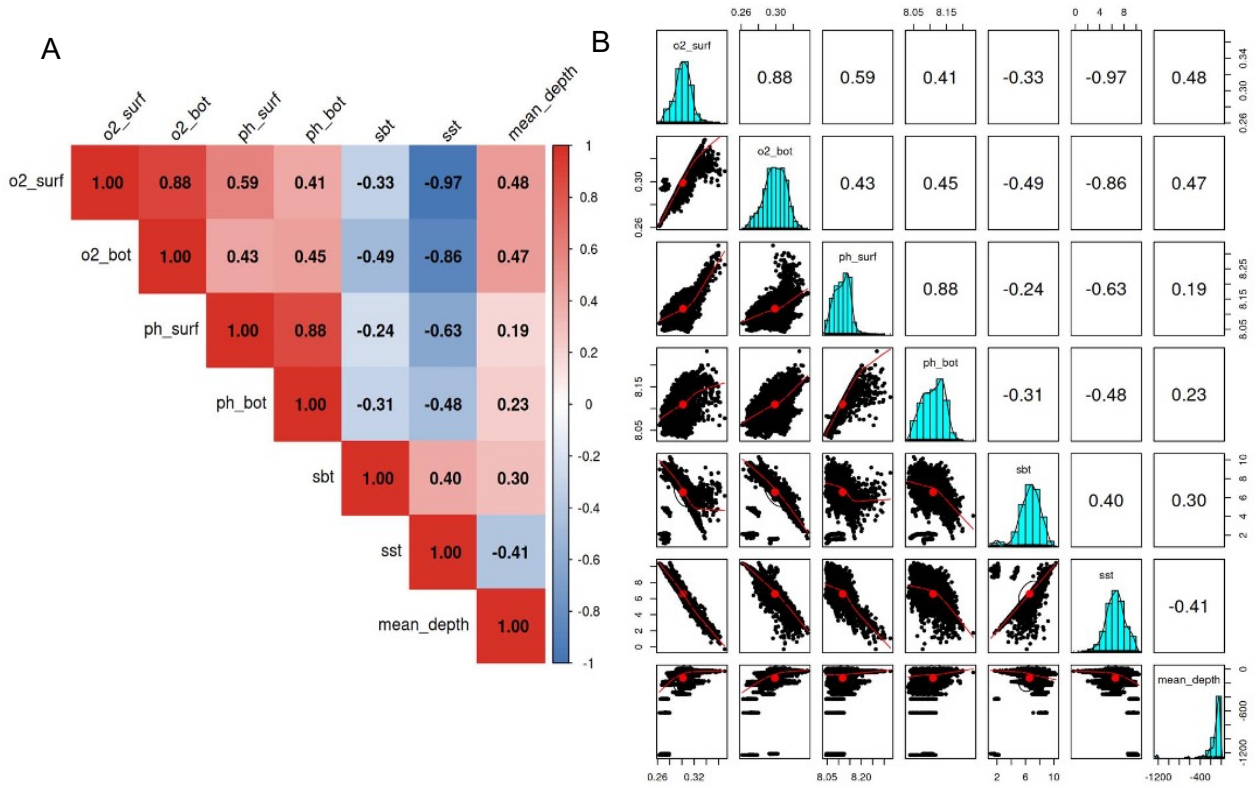

Figure 10A. Correlation Matrix of Environmental Variables. Values ranging from -1 (strong negative correlation) is colored in blue, to 1 (strong positive correlation) is colored in red. o2_surf is Surface Dissolved Oxygen, o2_bot is Bottom Dissolved Oxygen, ph_surf is surface pH level, ph_bot is bottom pH level, mean_depth is the mean depth at each grid on 60 arcmin.

Figure 10B. Pairwise Relationships and Distributions of Environmental Variables (The off-diagonal scatter plots depict pairwise relationships between variables. A red regression line indicates the direction and strength of the relationship. Points in the scatterplots represent data observations. The histograms represent the distribution between the variables.

doi:10.6342/NTU202500202

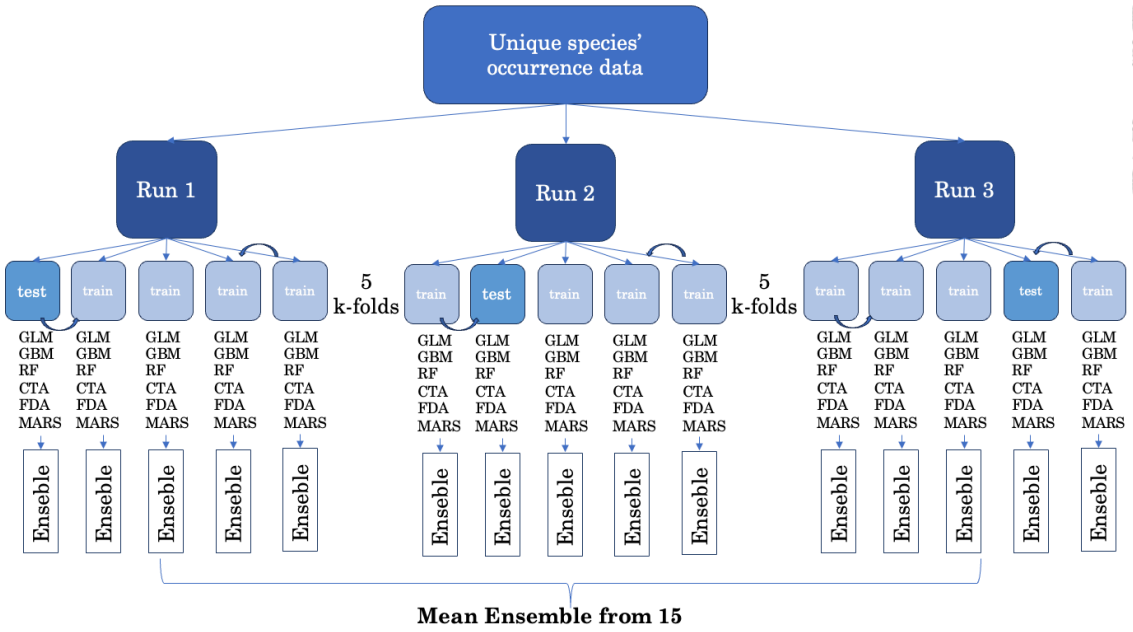

Figure 11. Algorithm of SDM validation process. Schematic representation of the modeling workflow showing three independent runs (Run 1-3), each employing 5-fold cross-validation. Each run processes unique species occurrence data through six modeling algorithms (GLM, GBM, RF, CTA, FDA, and MARS) with five training-testing data integrations.

doi:10.6342/NTU202500202

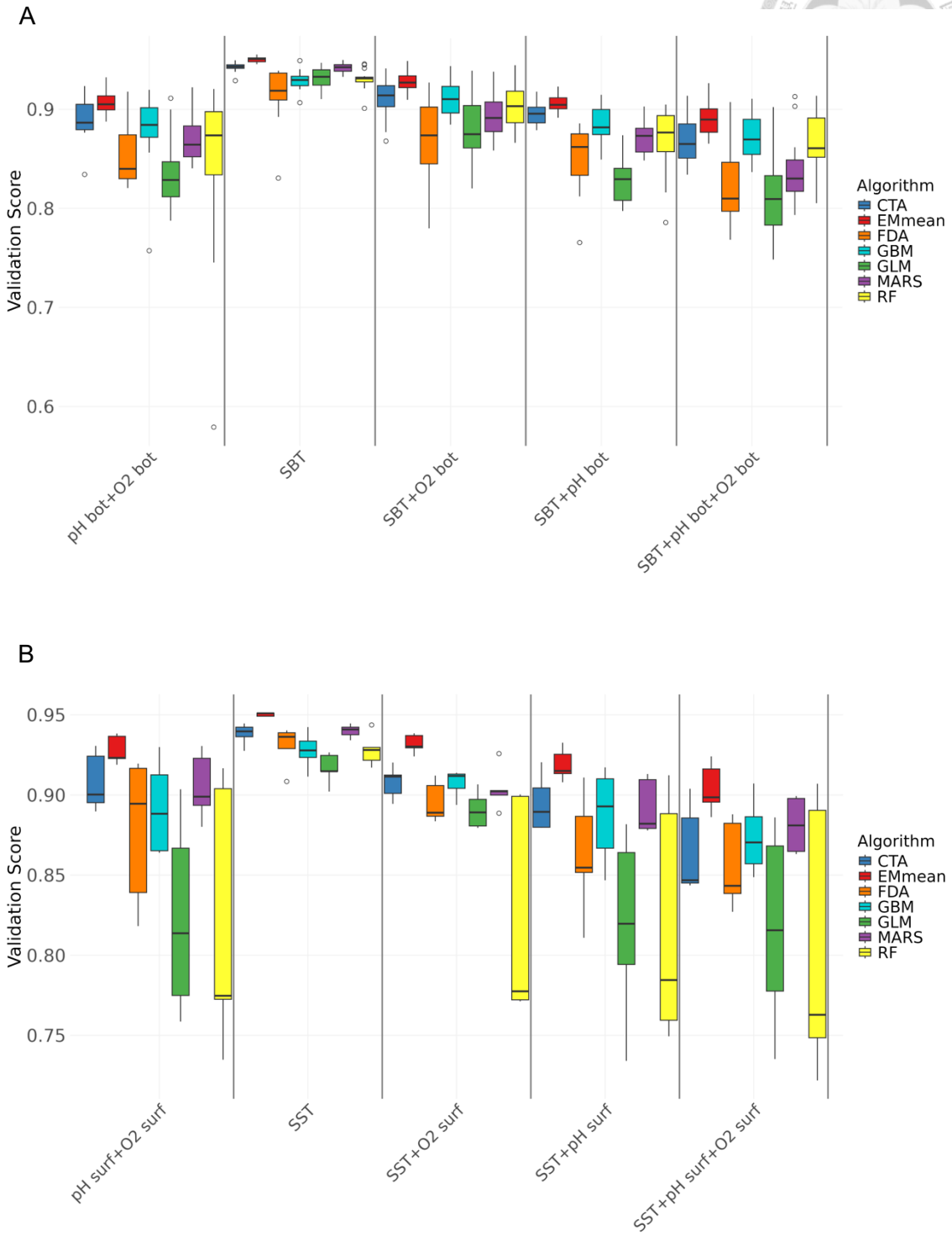

Figure 12. Comparison of models' performance metric (TSS) for demersal species (A) and for pelagic species (B). Boxplots represent the distribution of validation score of 6 different SDMs across different model experiments.

doi:10.6342/NTU202500202

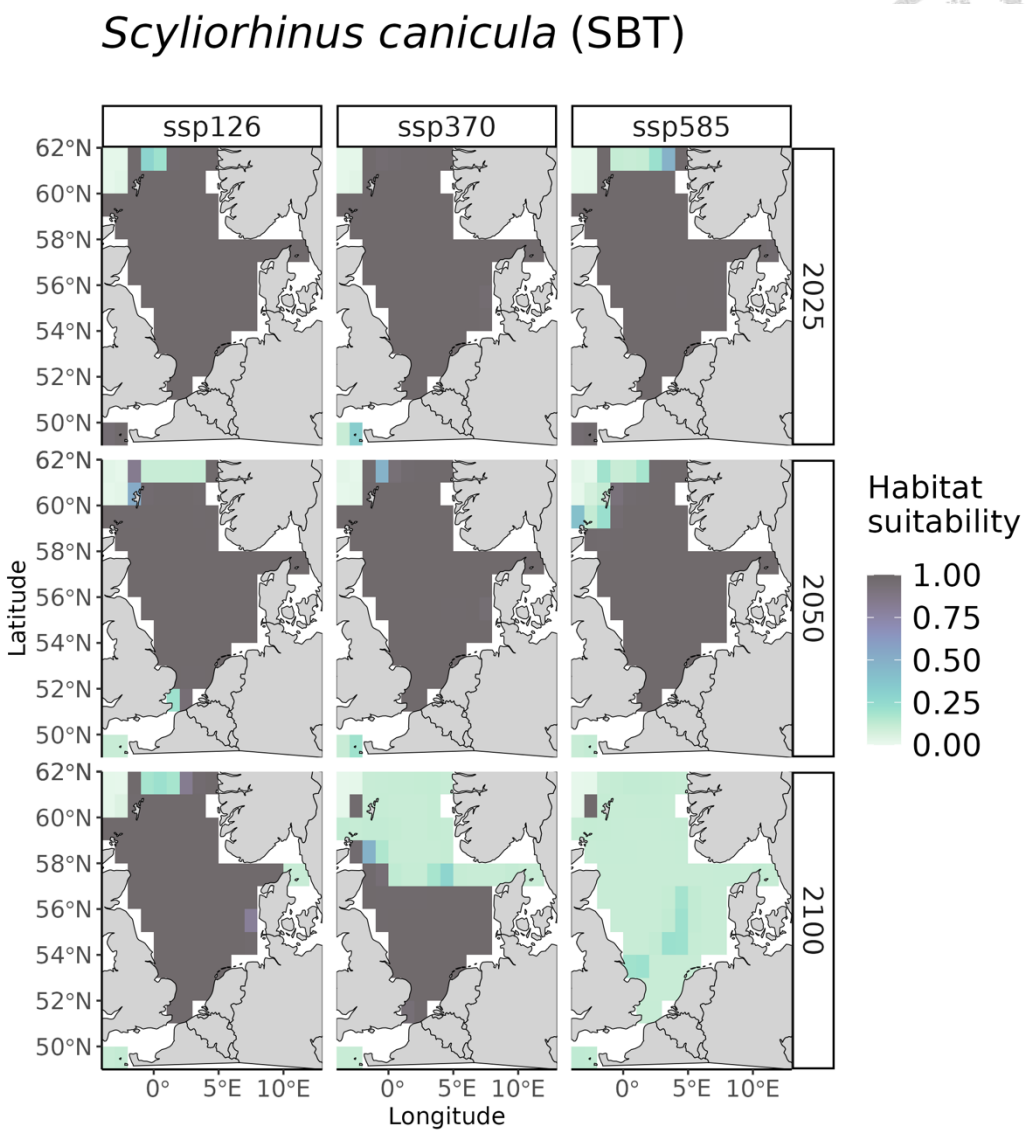

Figure 13. Projected distributional shifts of *Scyliorhinus canicula* in 2025 (top), 2050 (middle) and 2100 (bottom) under 3 climate scenarios (SSP1-2.6, SSP3-7.0, SSP5-8.5). Color shading indicate probability of species occurrence (0-1). Color-shading stands for probability of occurrence (0-1). Each grid refers to resolution 60 arcmin.

doi:10.6342/NTU202500202

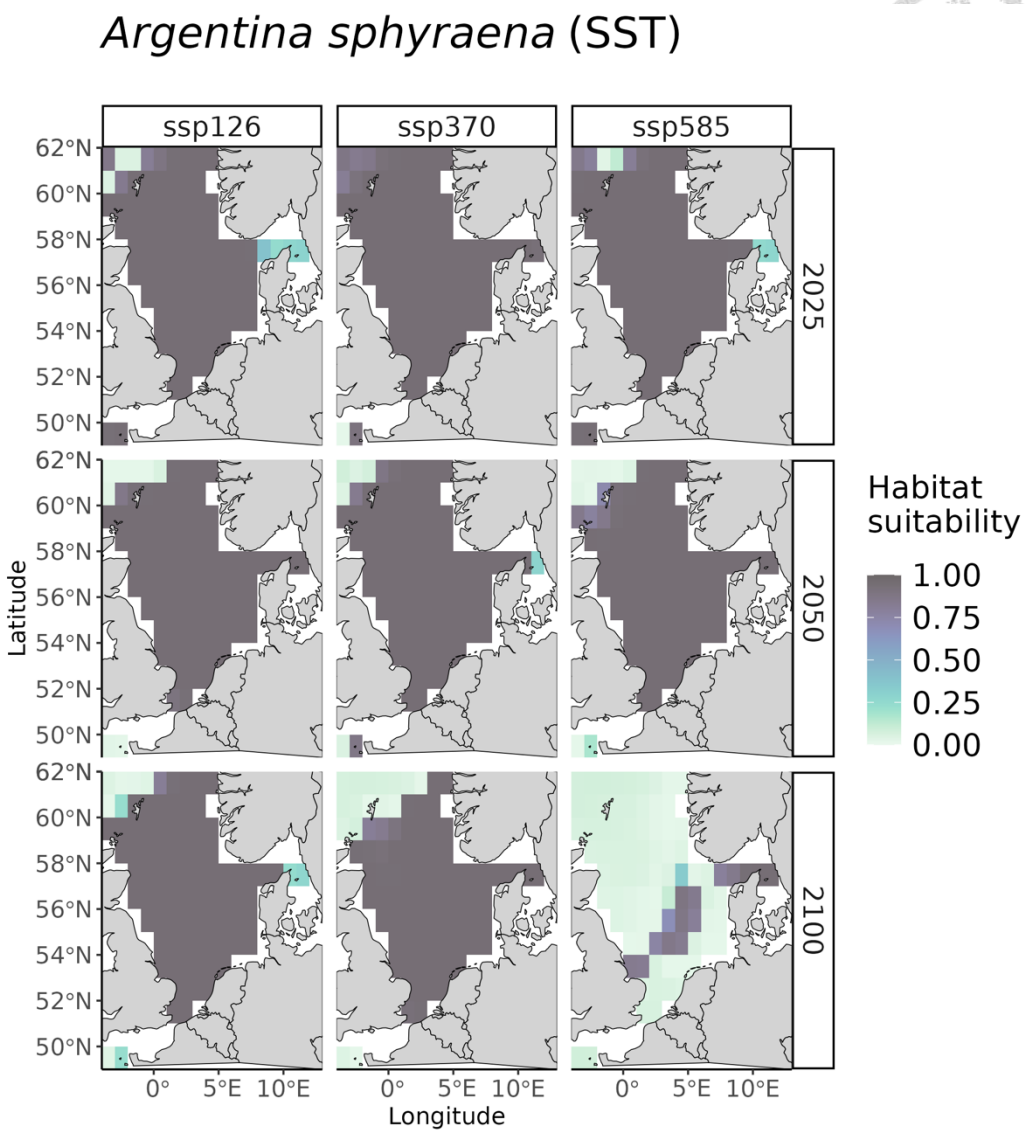

Figure 14. Projected distributional shifts of *Argentina sphyraena* in 2025 (top), 2050 (middle) and 2100 (bottom) under 3 climate scenarios (SSP1-2.6, SSP3-7.0, SSP5-8.5). Color shading indicate probability of species occurrence (0-1). Color-shading stands for probability of occurrence (0-1). Each grid refers to resolution 60 arcmin

doi:10.6342/NTU202500202

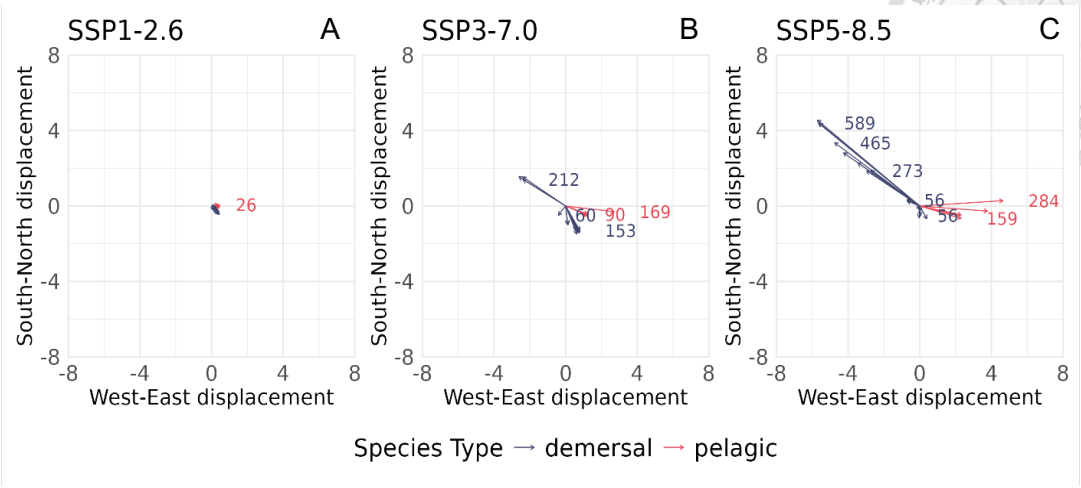

Figure 15. Distributional centroids vectors under temperature-based models. Mean shifts change from 2024 to 2100 under 3 climate scenarios. The three panels illustrate arrows that are species' movement vectors (direction and magnitude) under SSP1-2.6 (A), SSP3-7.0 (B), and SSP5-8.5 (C). Blue arrows: represent demersal species. Red arrows: indicate pelagic species. The length of the arrows indicates the magnitude of the response. Longer arrows reflect greater shifts in species distributions or probabilities of presence. Numbers represent the distance in kilometers (km). Resolution of 1 grid is 60 arcmin. Each horizontal cell is 1 degree in longitude (West-East displacement) and each vertical cell is 1 degree in latitude (South-North displacement).

doi:10.6342/NTU202500202

Supplementary materials

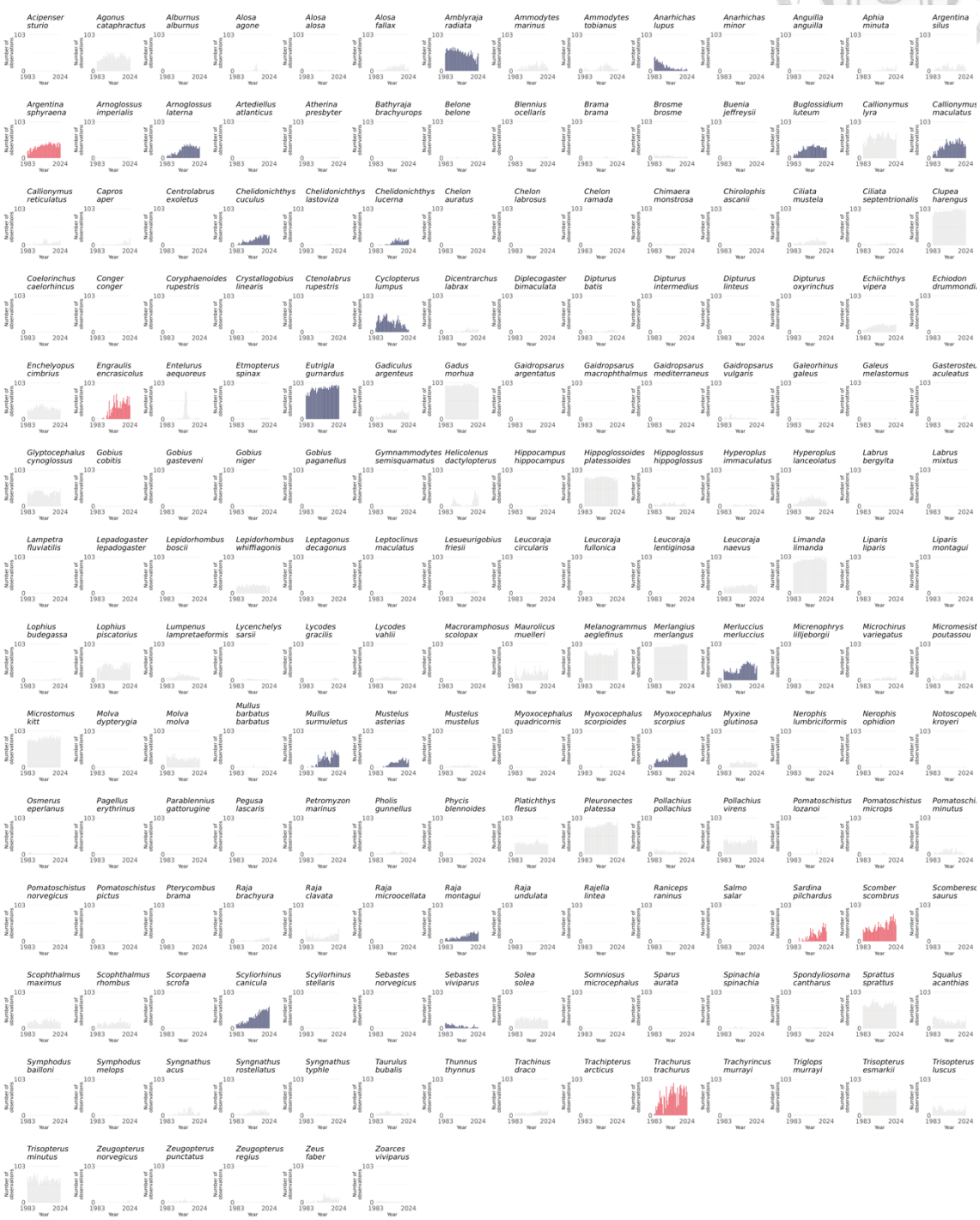

S.1. All species (188) occurrence record for the entire period 1983-2024 from the trawling surveys. The x-axis represents the year during the 1983-2024 period, while the y-axis (0-103 – max number of observed grids per year) indicates observed grids in the study area per each year. Blue histograms correspond to the selected demersal species and red histograms indicate pelagic species. Grey histograms refer to those species that were not included in the research, as they did not meet the thresholds. Scientific names of species are above the corresponding histograms.

doi:10.6342/NTU202500202

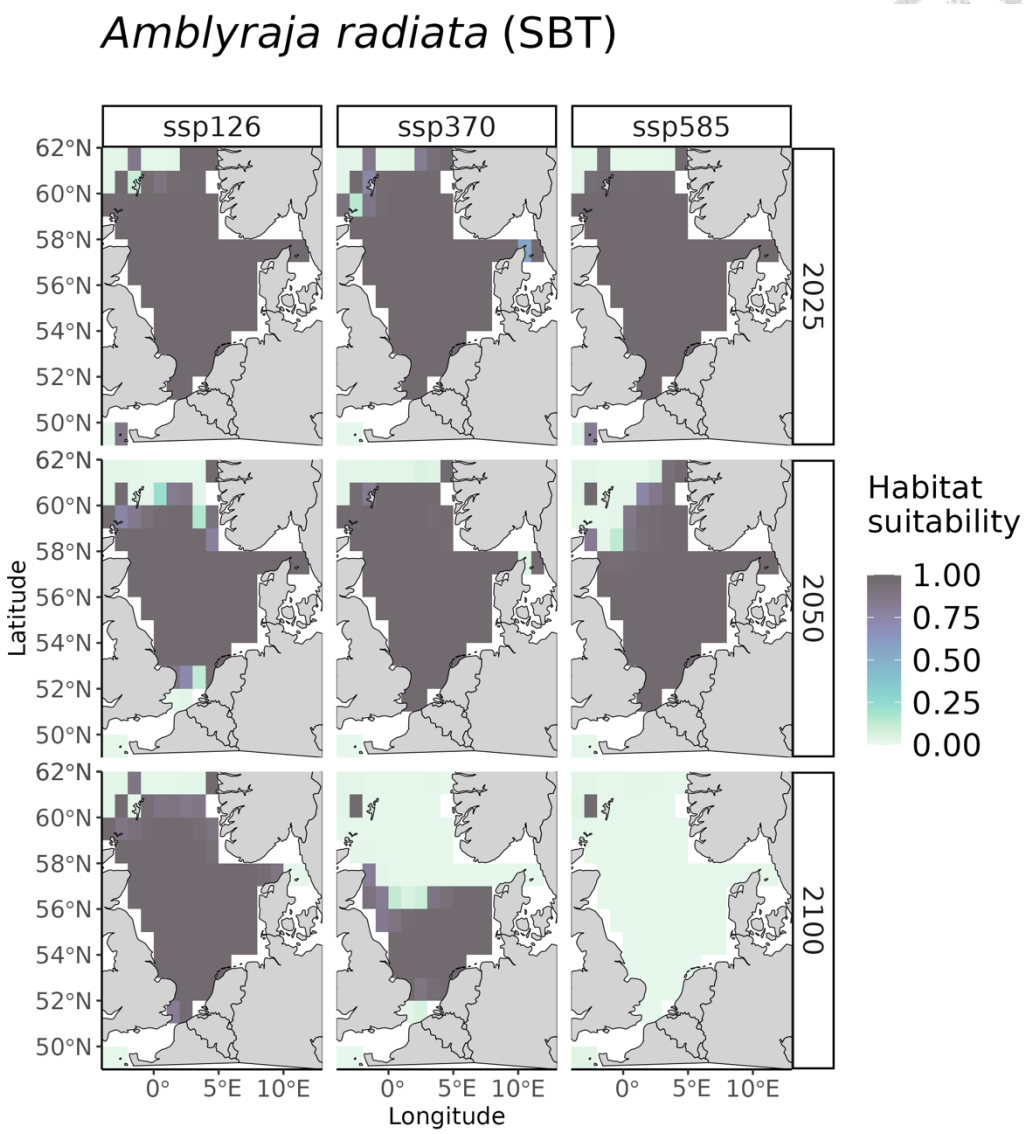

S.2.Projected distributional shifts of *Amblyraja radiata* (based on habitat suitability) in 2025 (top), 2050 (middle) and 2100 (bottom) under 3 climate scenarios (SSP1-2.6, SSP3-7.0, SSP5-8.5). Color shading indicate probability of species occurrence in a grid of habitat suitability (0-1). Color-shading stands for potential habitat suitability, where 1 – suitable, 0 – unsuitable conditions. Each grid refers to resolution 60 arcmin. Applied model is indicated in the heading of each figure.

doi:10.6342/NTU202500202

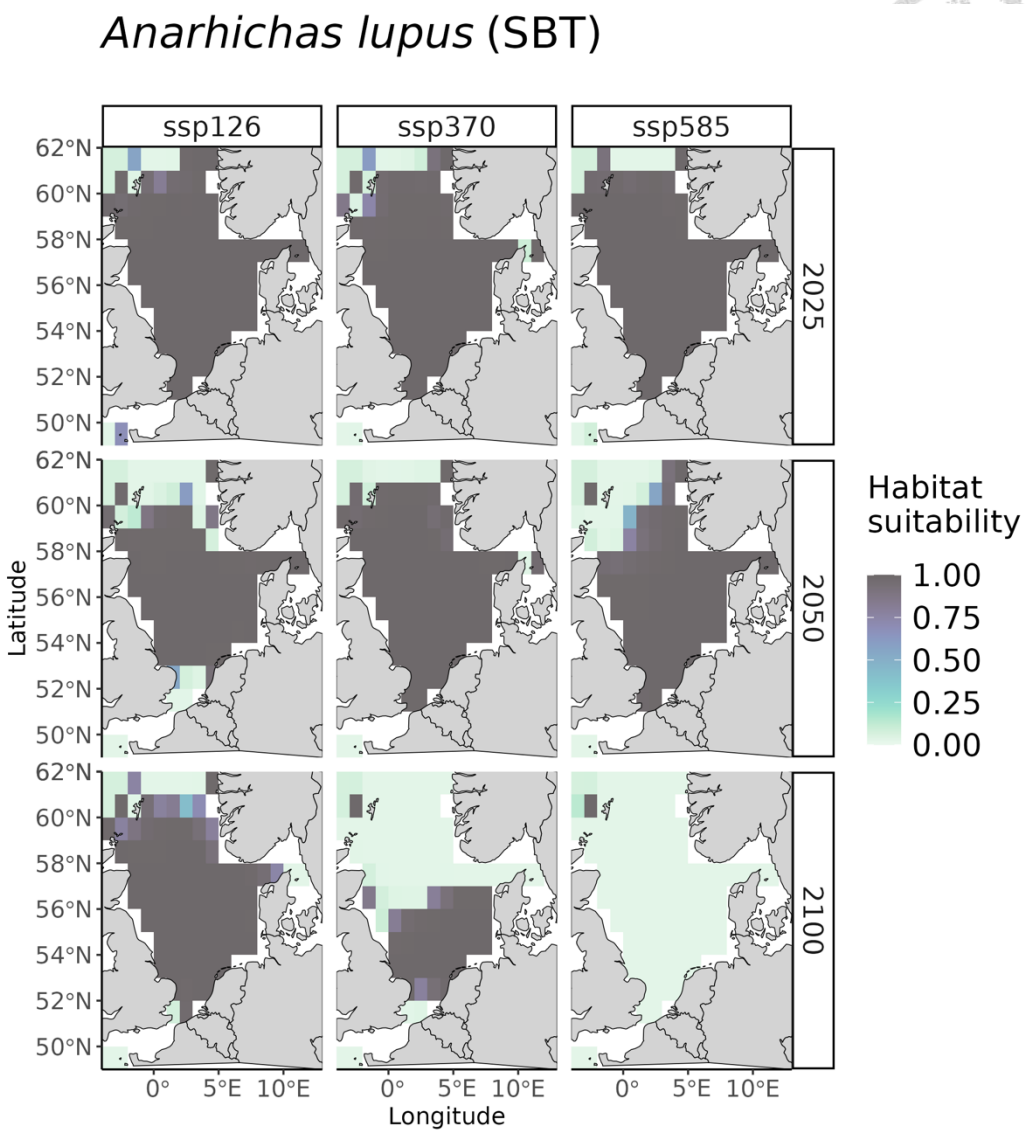

S.3. Projected distributional shifts of *Anarhichas lupus radiata* (based on habitat suitability) in 2025 (top), 2050 (middle) and 2100 (bottom) under 3 climate scenarios (SSP1-2.6, SSP3-7.0, SSP5-8.5). Color shading indicate probability of species occurrence in a grid of habitat suitability (0-1). Color-shading stands for potential habitat suitability, where 1 – suitable, 0 – unsuitable conditions. Each grid refers to resolution 60 arcmin. Applied model is indicated in the heading of each figure.

doi:10.6342/NTU202500202

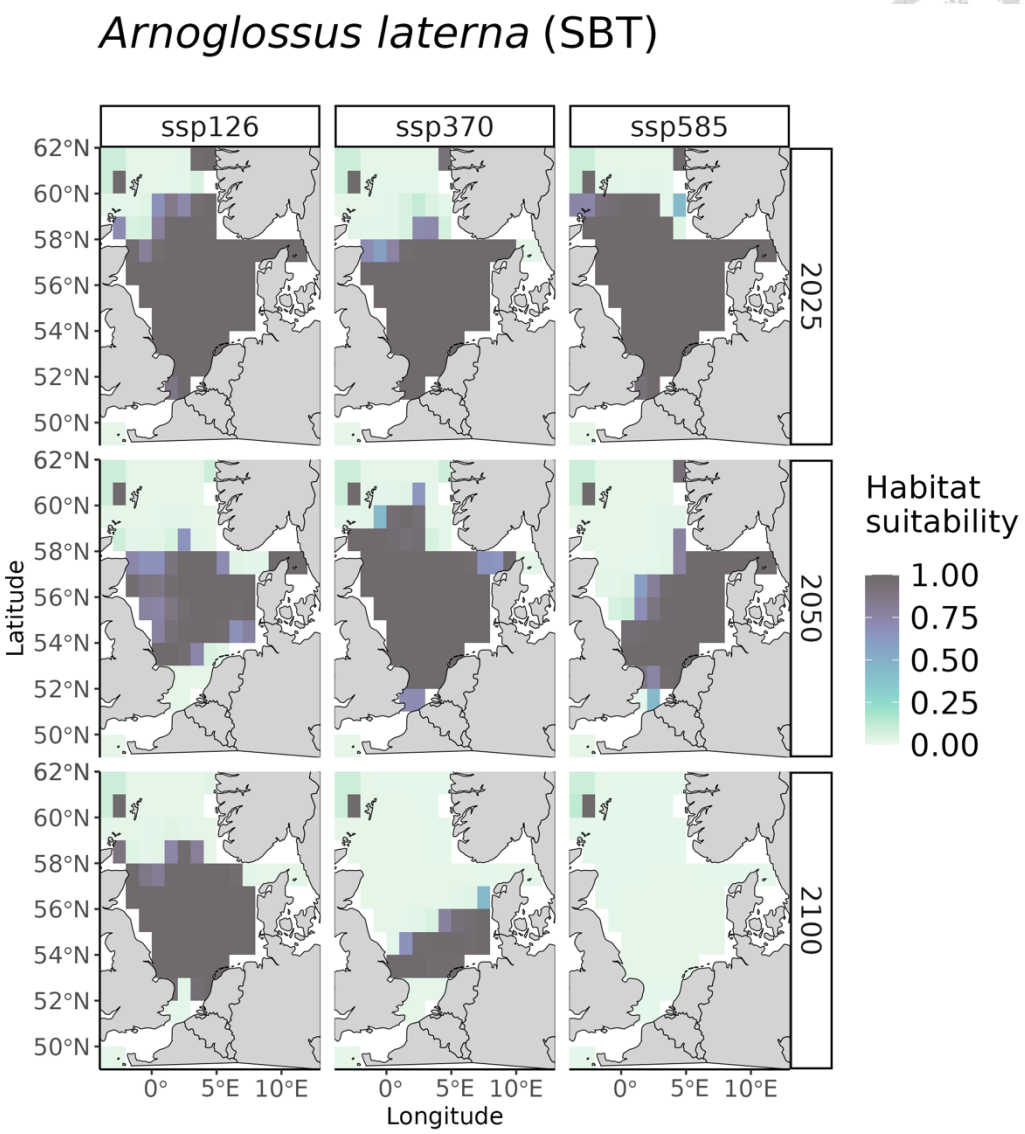

S.4. Projected distributional shifts of *Arnoglossus laterna radiata* (based on habitat suitability) in 2025 (top), 2050 (middle) and 2100 (bottom) under 3 climate scenarios (SSP1-2.6, SSP3-7.0, SSP5-8.5). Color shading indicate probability of species occurrence in a grid of habitat suitability (0-1). Color-shading stands for potential habitat suitability, where 1 – suitable, 0 – unsuitable conditions. Each grid refers to resolution 60 arcmin. Applied model is indicated in the heading of each figure.

doi:10.6342/NTU202500202

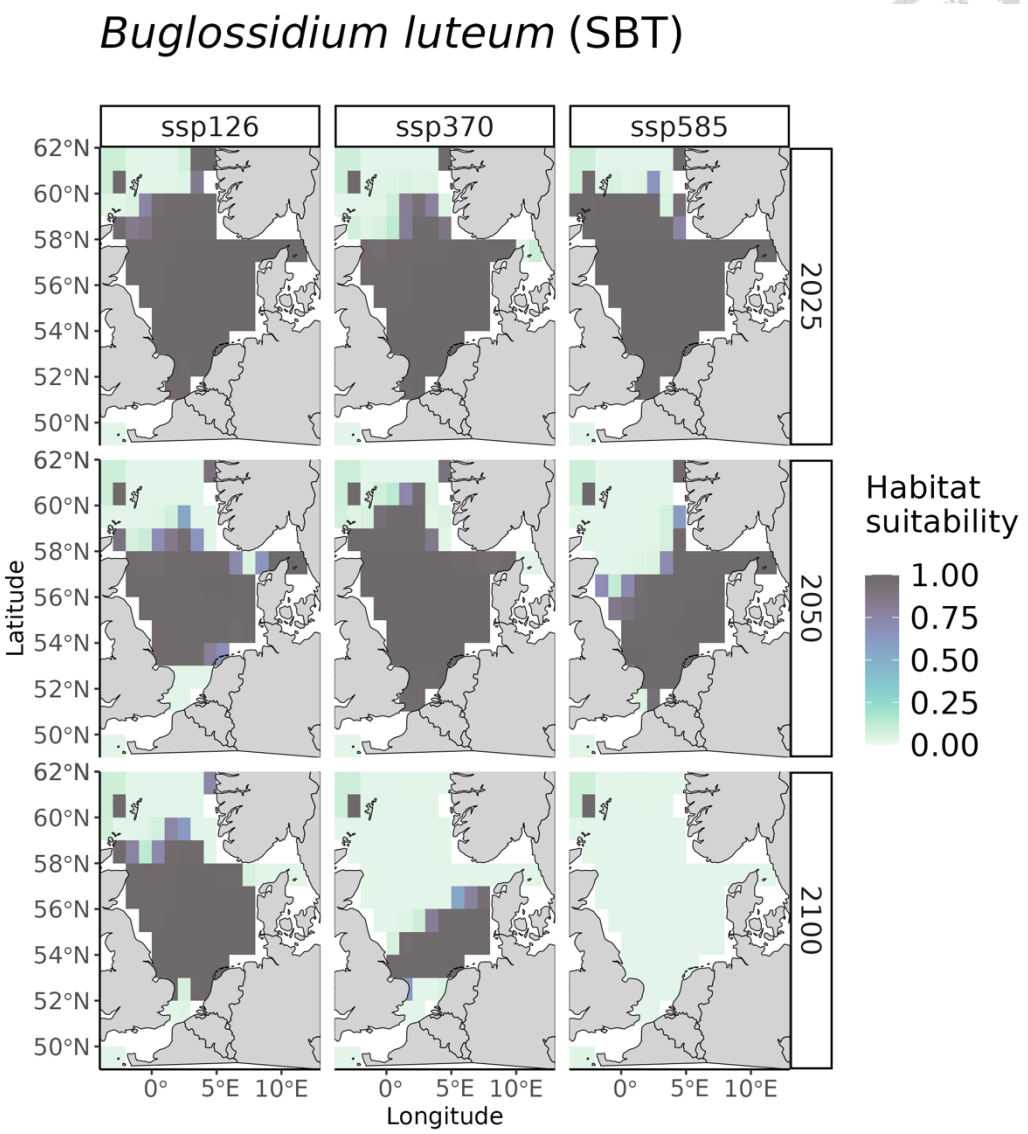

S.5. Projected distributional shifts of *Buglossidium luteum radiata* (based on habitat suitability) in 2025 (top), 2050 (middle) and 2100 (bottom) under 3 climate scenarios (SSP1-2.6, SSP3-7.0, SSP5-8.5). Color shading indicate probability of species occurrence in a grid of habitat suitability (0-1). Color-shading stands for potential habitat suitability, where 1 – suitable, 0 – unsuitable conditions. Each grid refers to resolution 60 arcmin. Applied model is indicated in the heading of each figure.

doi:10.6342/NTU202500202

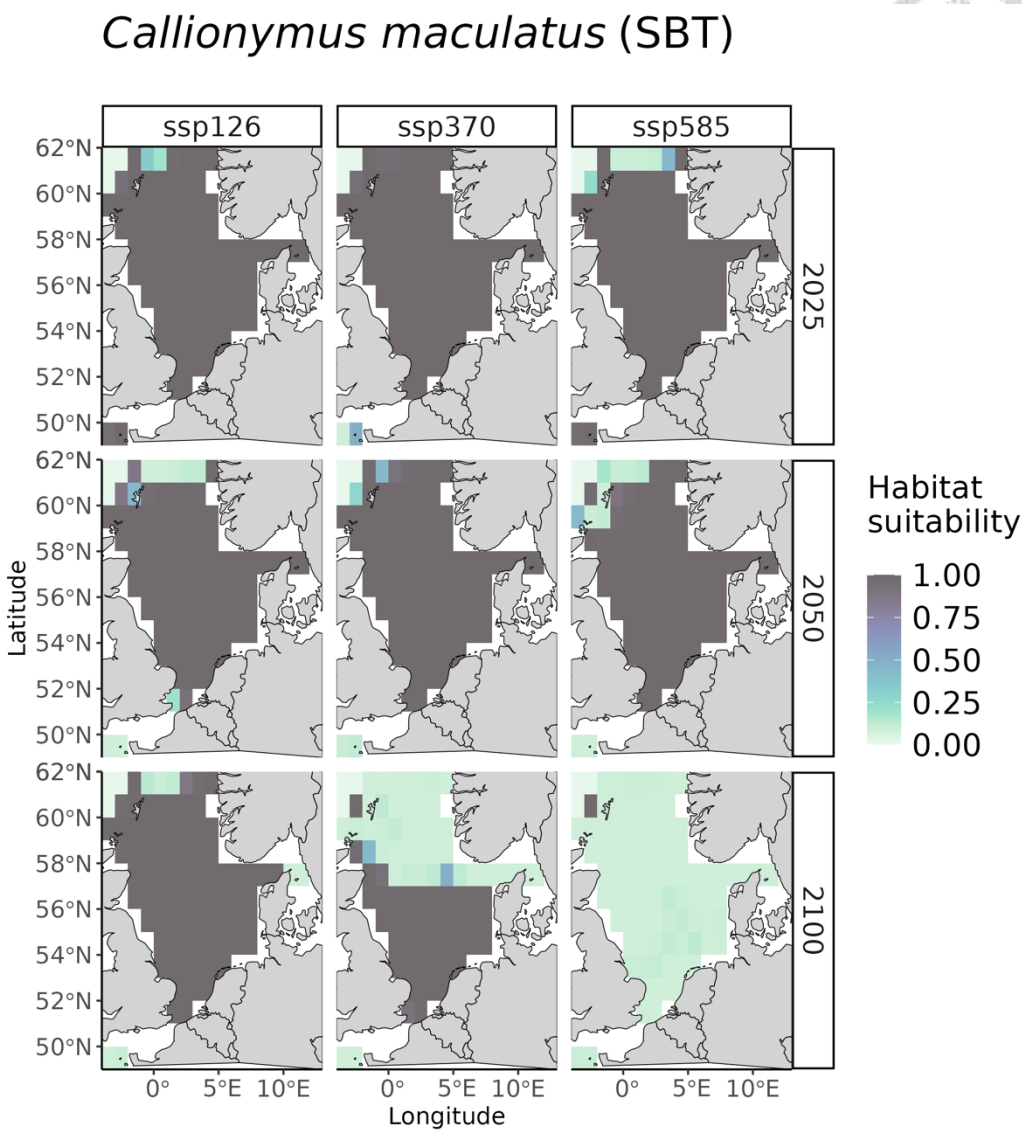

S.6. Projected distributional shifts of *Callionymus maculatus radiata* (based on habitat suitability) in 2025 (top), 2050 (middle) and 2100 (bottom) under 3 climate scenarios (SSP1-2.6, SSP3-7.0, SSP5-8.5). Color shading indicate probability of species occurrence in a grid of habitat suitability (0-1). Color-shading stands for potential habitat suitability, where 1 – suitable, 0 – unsuitable conditions. Each grid refers to resolution 60 arcmin. Applied model is indicated in the heading of each figure.

doi:10.6342/NTU202500202

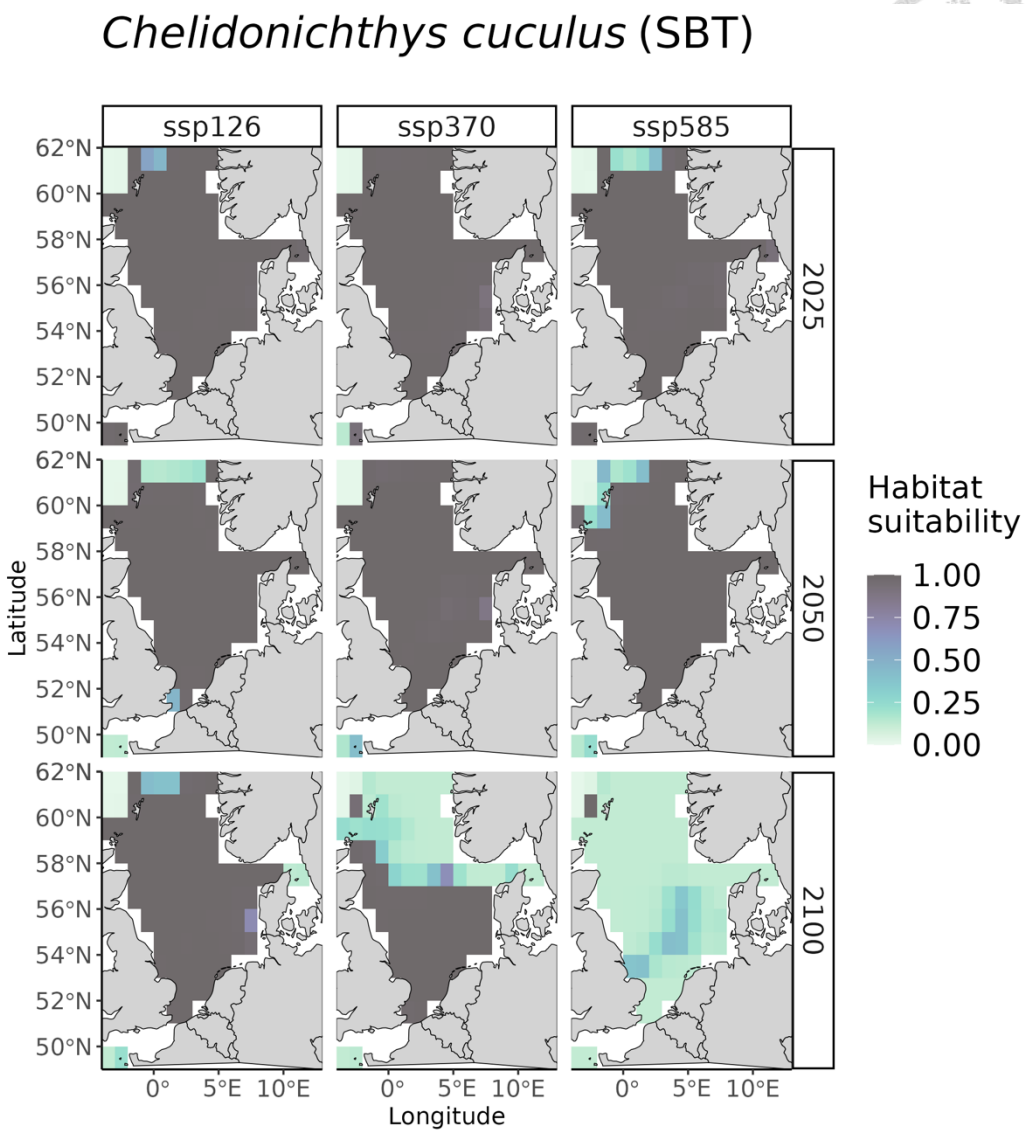

S.7. Projected distributional shifts of *Chelidonichtys cuculus radiata* (based on habitat suitability) in 2025 (top), 2050 (middle) and 2100 (bottom) under 3 climate scenarios (SSP1-2.6, SSP3-7.0, SSP5-8.5). Color shading indicate probability of species occurrence in a grid of habitat suitability (0-1). Color-shading stands for potential habitat suitability, where 1 – suitable, 0 – unsuitable conditions. Each grid refers to resolution 60 arcmin. Applied model is indicated in the heading of each figure.

doi:10.6342/NTU202500202

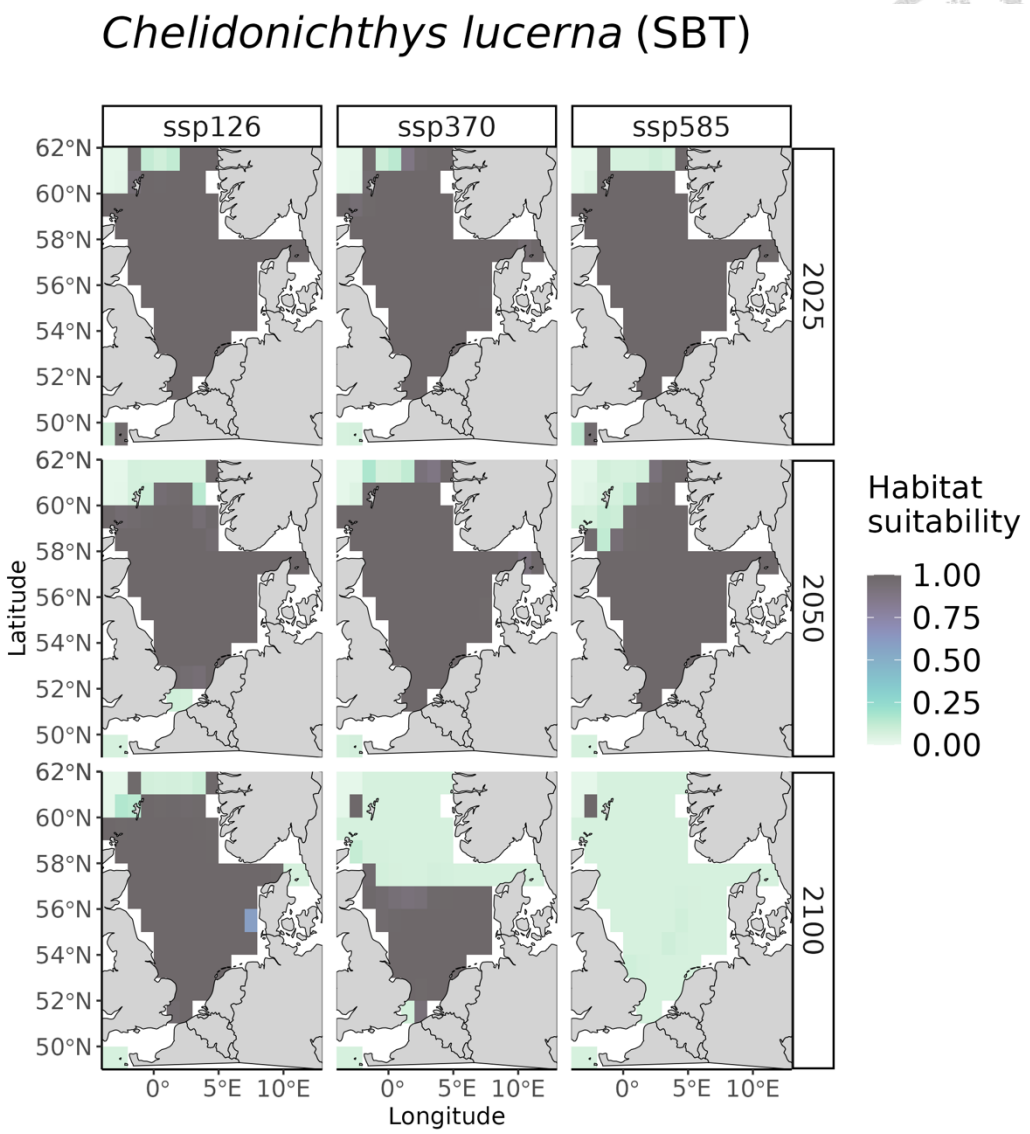

S.8. Projected distributional shifts of *Chelidonichthys lucerna radiata* (based on habitat suitability) in 2025 (top), 2050 (middle) and 2100 (bottom) under 3 climate scenarios (SSP1-2.6, SSP3-7.0, SSP5-8.5). Color shading indicate probability of species occurrence in a grid of habitat suitability (0-1). Color-shading stands for potential habitat suitability, where 1 – suitable, 0 – unsuitable conditions. Each grid refers to resolution 60 arcmin. Applied model is indicated in the heading of each figure.

doi:10.6342/NTU202500202

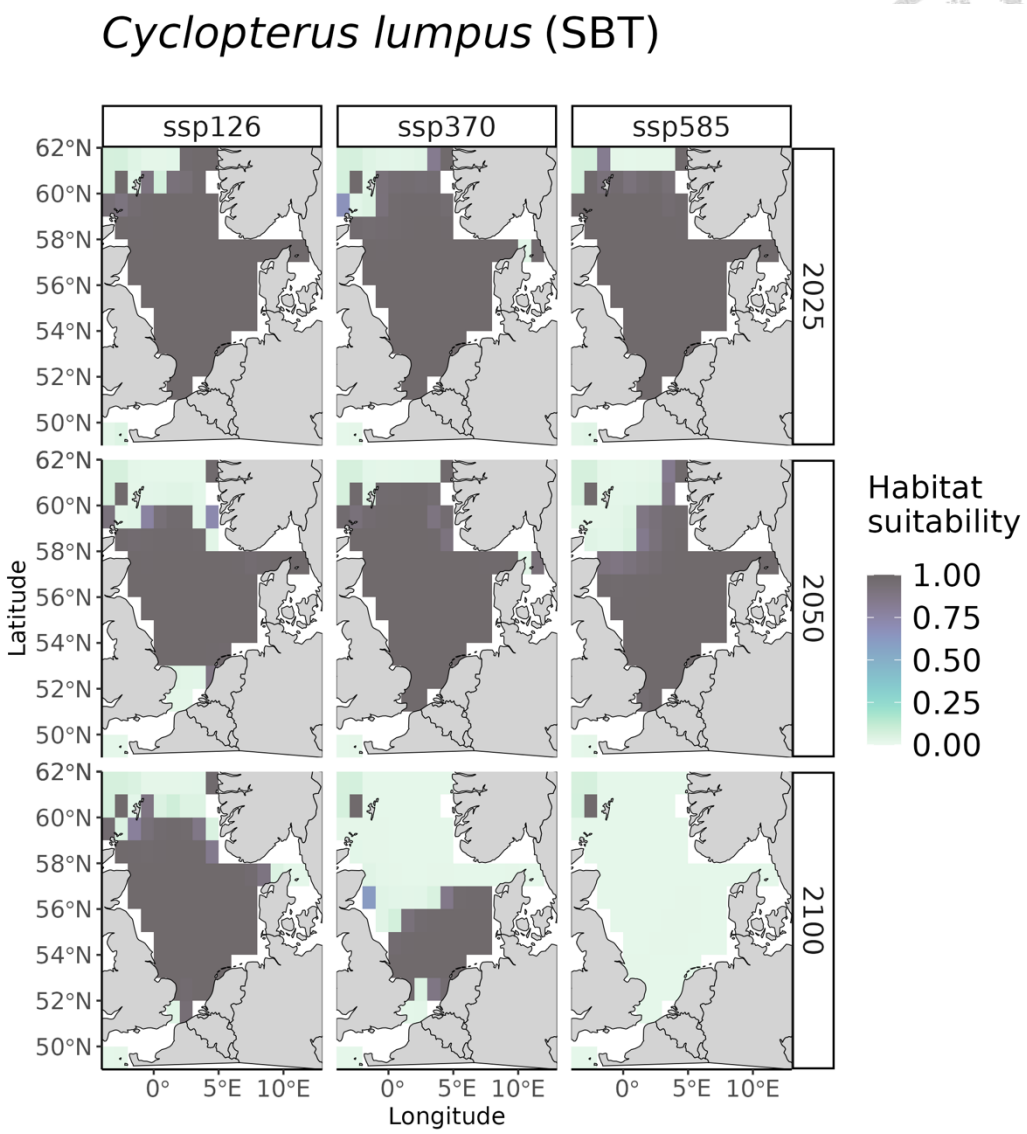

S.9. Projected distributional shifts of Cyclopterus lumpus radiata (based on habitat suitability) in 2025 (top), 2050 (middle) and 2100 (bottom) under 3 climate scenarios (SSP1-2.6, SSP3-7.0, SSP5-8.5). Color shading indicate probability of species occurrence in a grid of habitat suitability (0-1). Color-shading stands for potential habitat suitability, where 1 – suitable, 0 – unsuitable conditions. Each grid refers to resolution 60 arcmin. Applied model is indicated in the heading of each figure.

doi:10.6342/NTU202500202

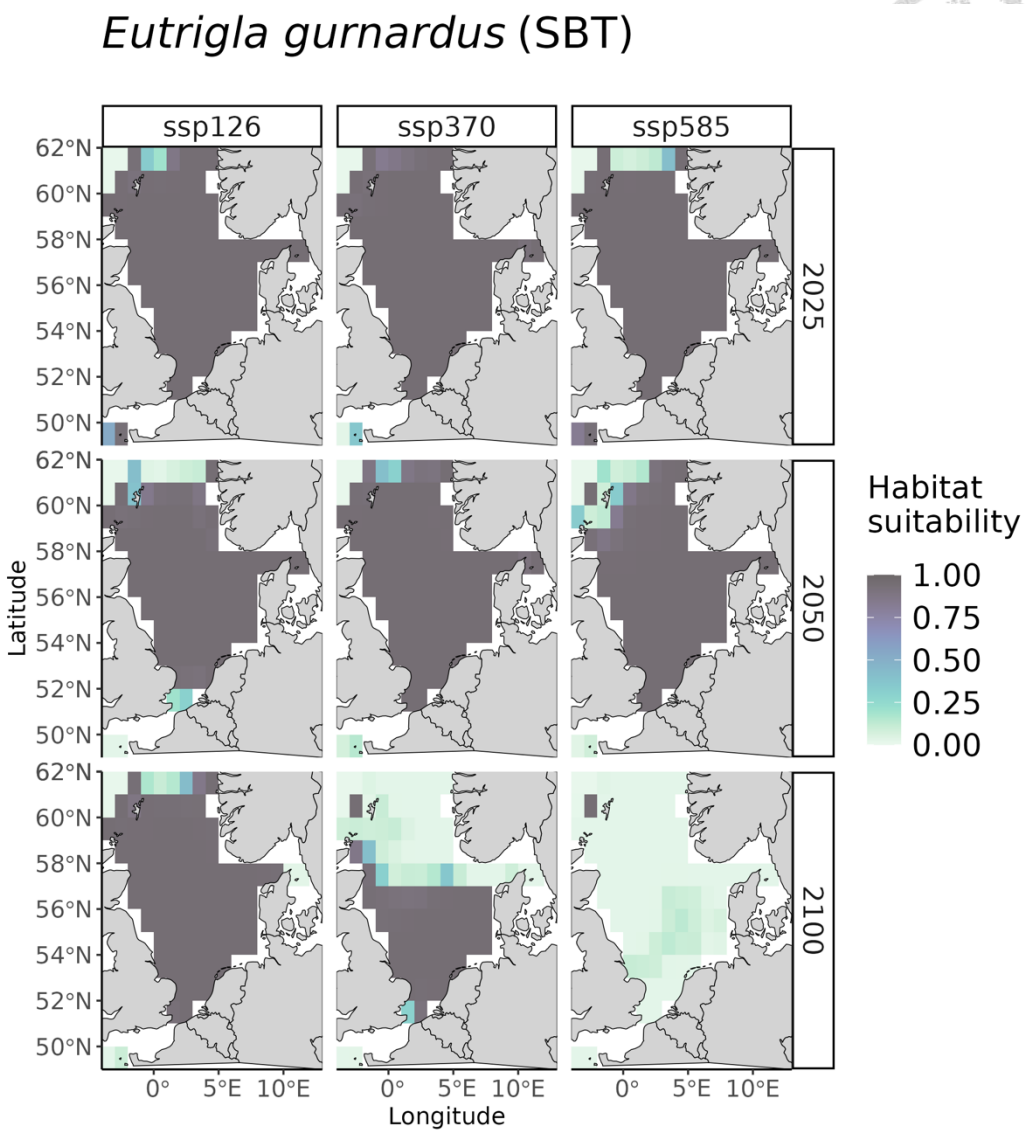

S.10. Projected distributional shifts of *Eutrigla radiata* (based on habitat suitability) in 2025 (top), 2050 (middle) and 2100 (bottom) under 3 climate scenarios (SSP1-2.6, SSP3-7.0, SSP5-8.5). Color shading indicate probability of species occurrence in a grid of habitat suitability (0-1). Color-shading stands for potential habitat suitability, where 1 – suitable, 0 – unsuitable conditions. Each grid refers to resolution 60 arcmin. Applied model is indicated in the heading of each figure.

doi:10.6342/NTU202500202

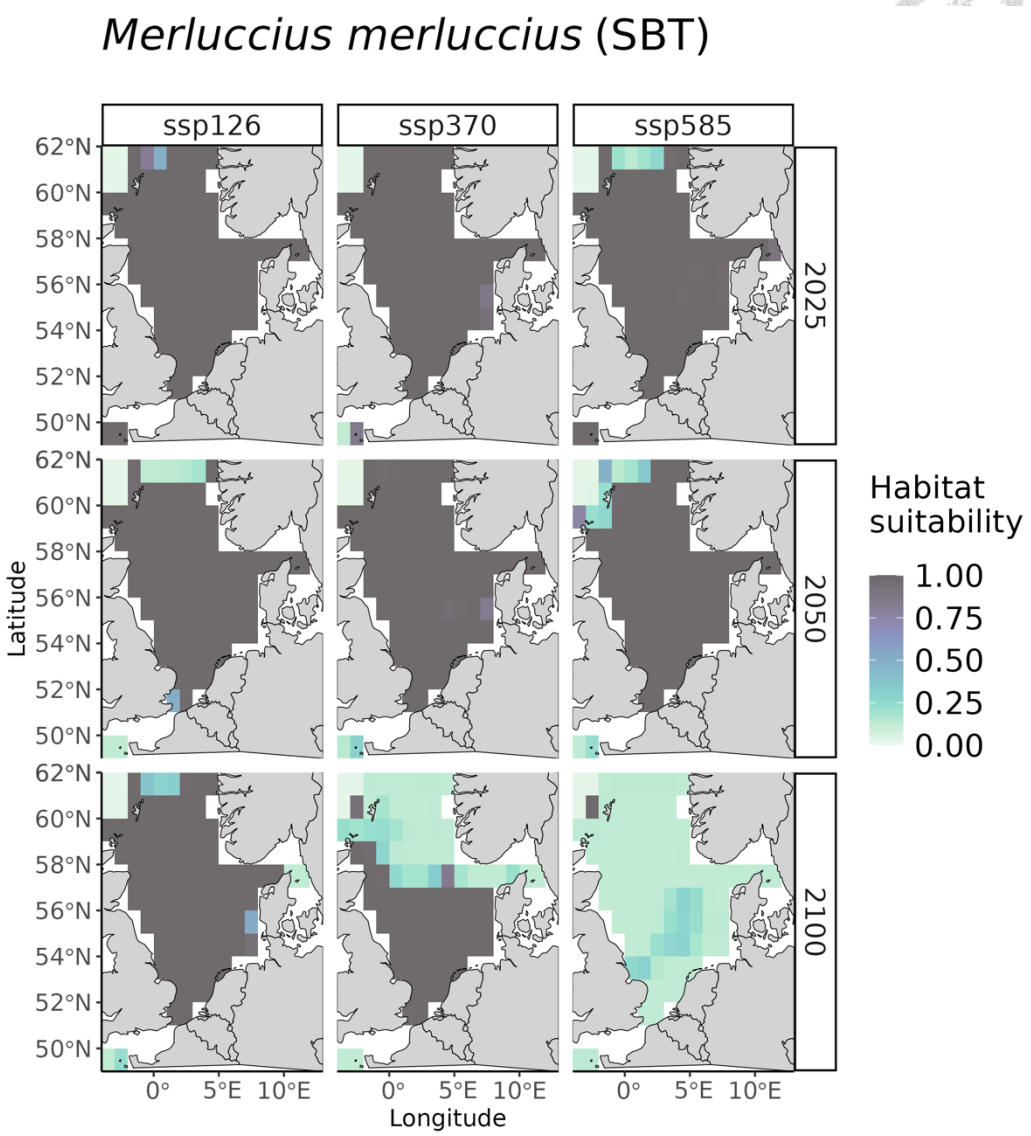

S.11. Projected distributional shifts of *Merluccius merluccies radiata* (based on habitat suitability) in 2025 (top), 2050 (middle) and 2100 (bottom) under 3 climate scenarios (SSP1-2.6, SSP3-7.0, SSP5-8.5). Color shading indicate probability of species occurrence in a grid of habitat suitability (0-1). Color-shading stands for potential habitat suitability, where 1 – suitable, 0 – unsuitable conditions. Each grid refers to resolution 60 arcmin. Applied model is indicated in the heading of each figure.

doi:10.6342/NTU202500202

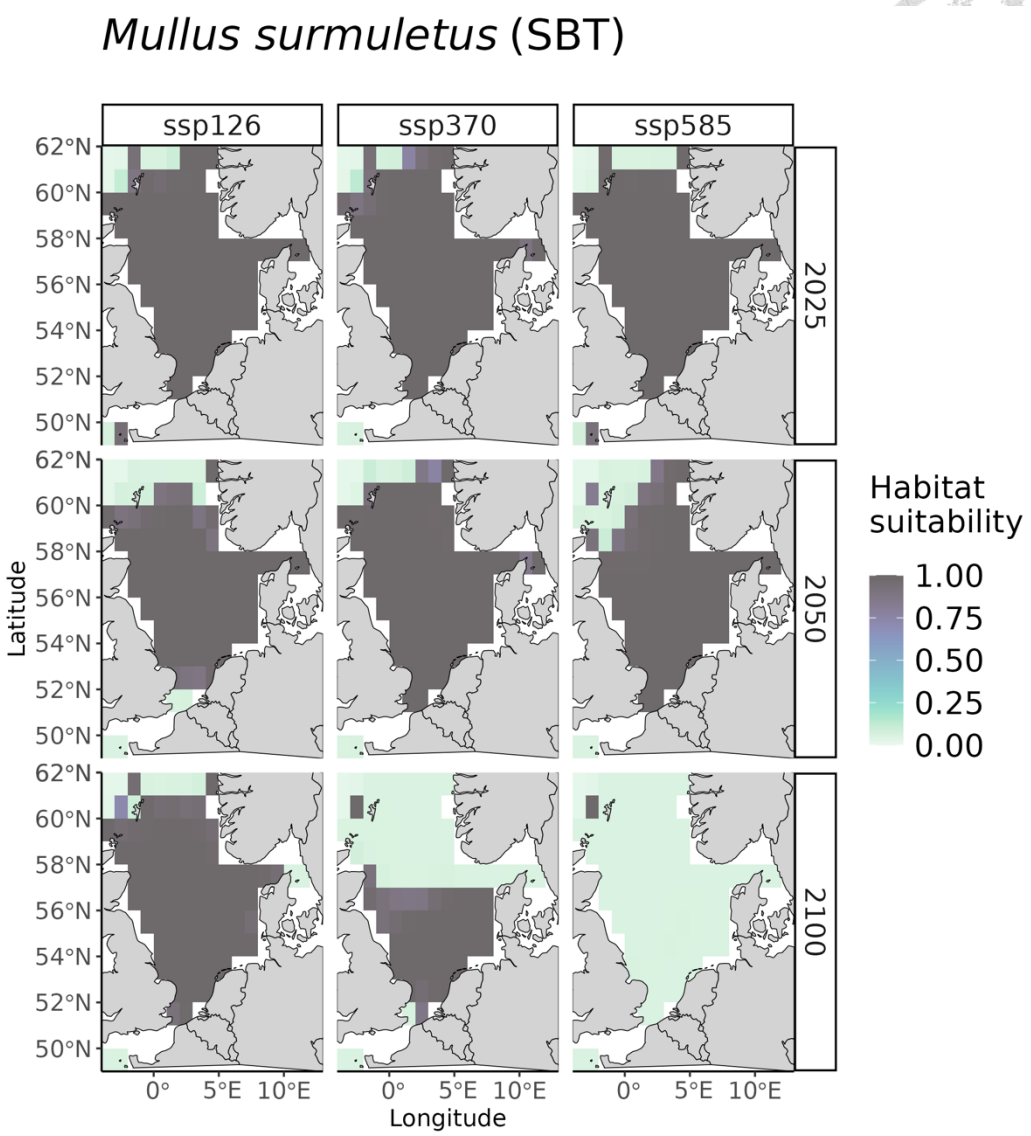

S.12. Projected distributional shifts of *Mullus surmuletus radiata* (based on habitat suitability) in 2025 (top), 2050 (middle) and 2100 (bottom) under 3 climate scenarios (SSP1-2.6, SSP3-7.0, SSP5-8.5). Color shading indicate probability of species occurrence in a grid of habitat suitability (0-1). Color-shading stands for potential habitat suitability, where 1 – suitable, 0 – unsuitable conditions. Each grid refers to resolution 60 arcmin. Applied model is indicated in the heading of each figure.

doi:10.6342/NTU202500202

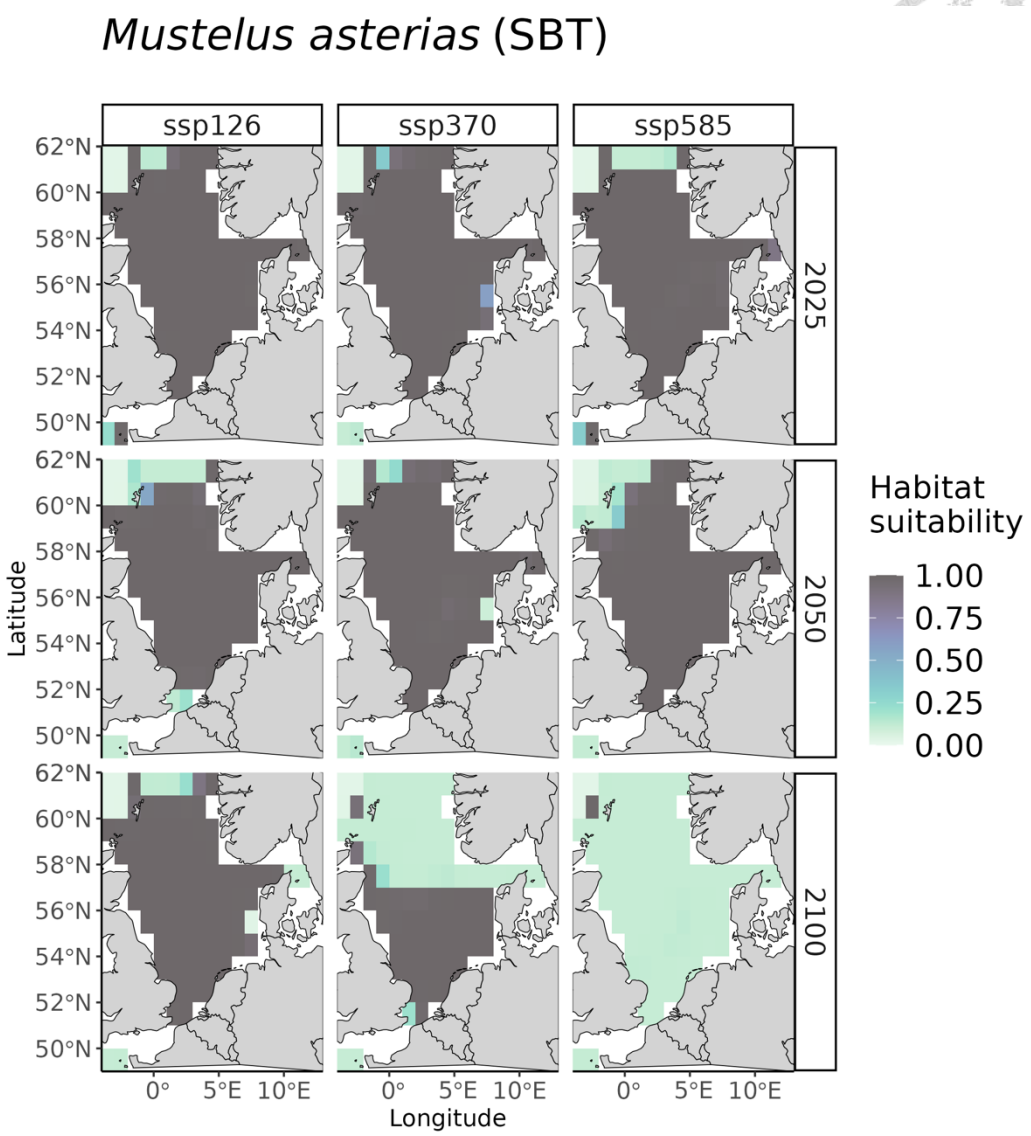

S.13. Projected distributional shifts of *Mustelus asterias radiata* (based on habitat suitability) in 2025 (top), 2050 (middle) and 2100 (bottom) under 3 climate scenarios (SSP1-2.6, SSP3-7.0, SSP5-8.5). Color shading indicate probability of species occurrence in a grid of habitat suitability (0-1). Color-shading stands for potential habitat suitability, where 1 – suitable, 0 – unsuitable conditions. Each grid refers to resolution 60 arcmin. Applied model is indicated in the heading of each figure.

doi:10.6342/NTU202500202

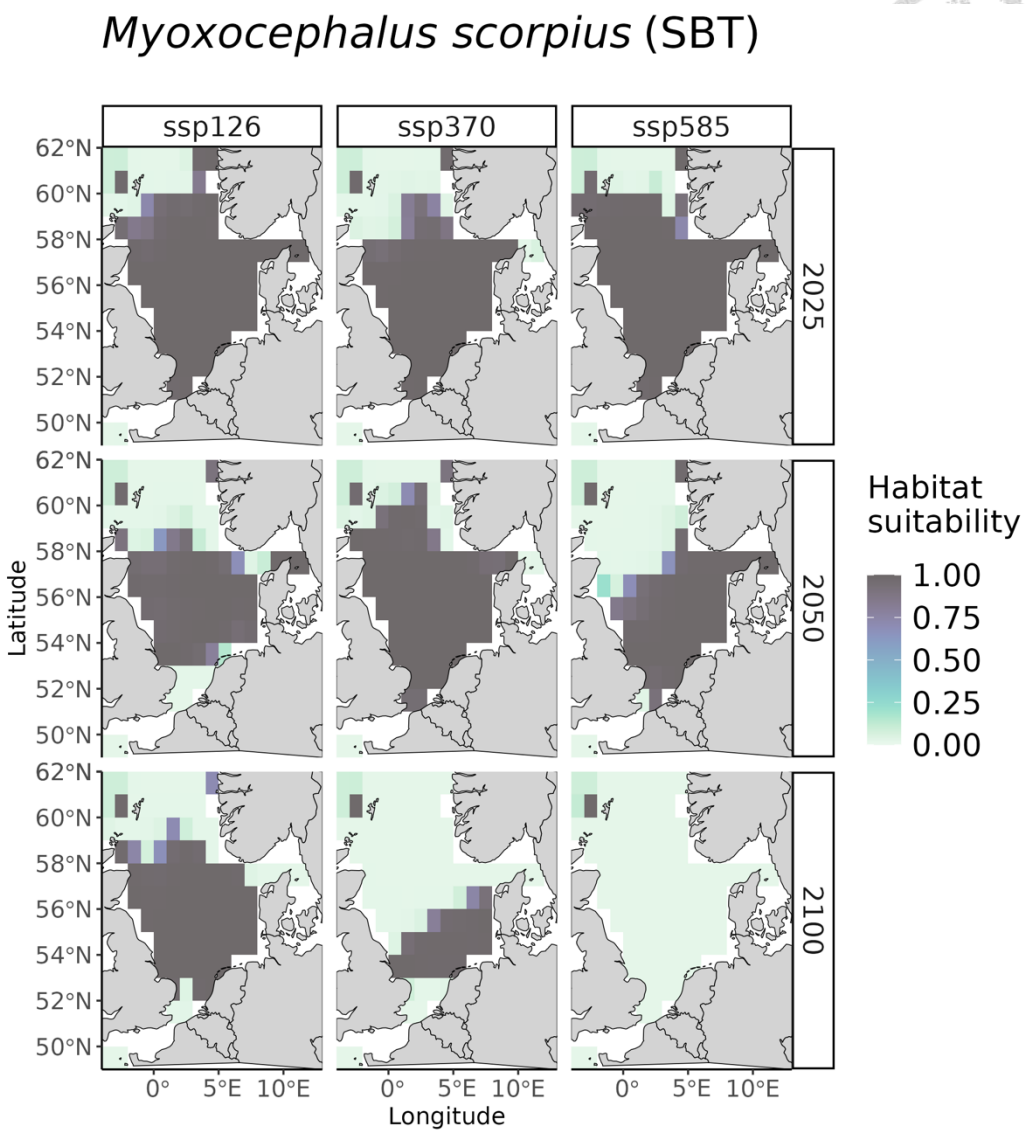

S.14. Projected distributional shifts of *Myoxocephalus scorpius radiata* (based on habitat suitability) in 2025 (top), 2050 (middle) and 2100 (bottom) under 3 climate scenarios (SSP1-2.6, SSP3-7.0, SSP5-8.5). Color shading indicate probability of species occurrence in a grid of habitat suitability (0-1). Color-shading stands for potential habitat suitability, where 1 – suitable, 0 – unsuitable conditions. Each grid refers to resolution 60 arcmin. Applied model is indicated in the heading of each figure.

doi:10.6342/NTU202500202

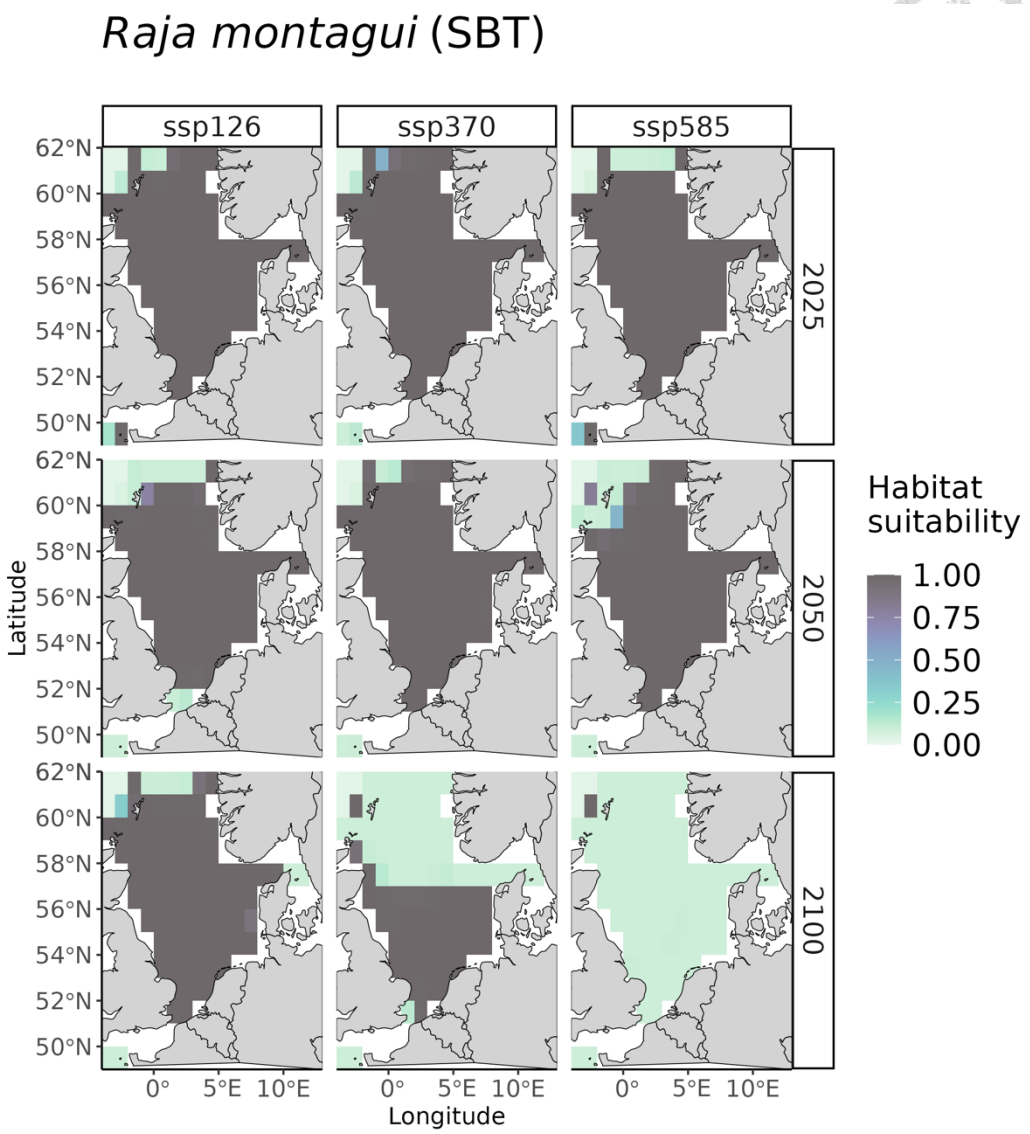

S.15. Projected distributional shifts of *Raja montagui radiata* (based on habitat suitability) in 2025 (top), 2050 (middle) and 2100 (bottom) under 3 climate scenarios (SSP1-2.6, SSP3-7.0, SSP5-8.5). Color shading indicate probability of species occurrence in a grid of habitat suitability (0-1). Color-shading stands for potential habitat suitability, where 1 – suitable, 0 – unsuitable conditions. Each grid refers to resolution 60 arcmin. Applied model is indicated in the heading of each figure.

doi:10.6342/NTU202500202

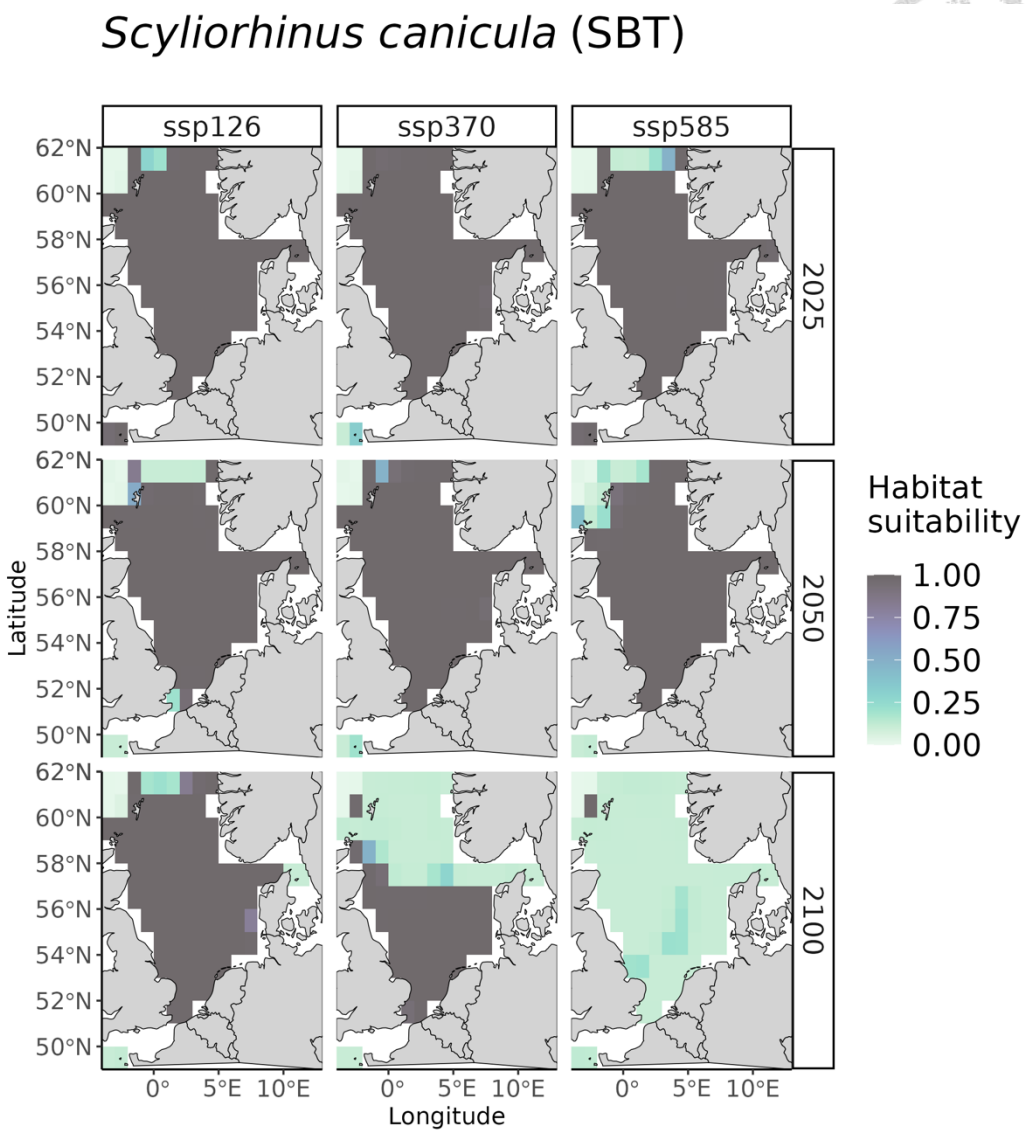

S.16. Projected distributional shifts of *Scyliorhunus canicula radiata* (based on habitat suitability) in 2025 (top), 2050 (middle) and 2100 (bottom) under 3 climate scenarios (SSP1-2.6, SSP3-7.0, SSP5-8.5). Color shading indicate probability of species occurrence in a grid of habitat suitability (0-1). Color-shading stands for potential habitat suitability, where 1 – suitable, 0 – unsuitable conditions. Each grid refers to resolution 60 arcmin. Applied model is indicated in the heading of each figure.

doi:10.6342/NTU202500202

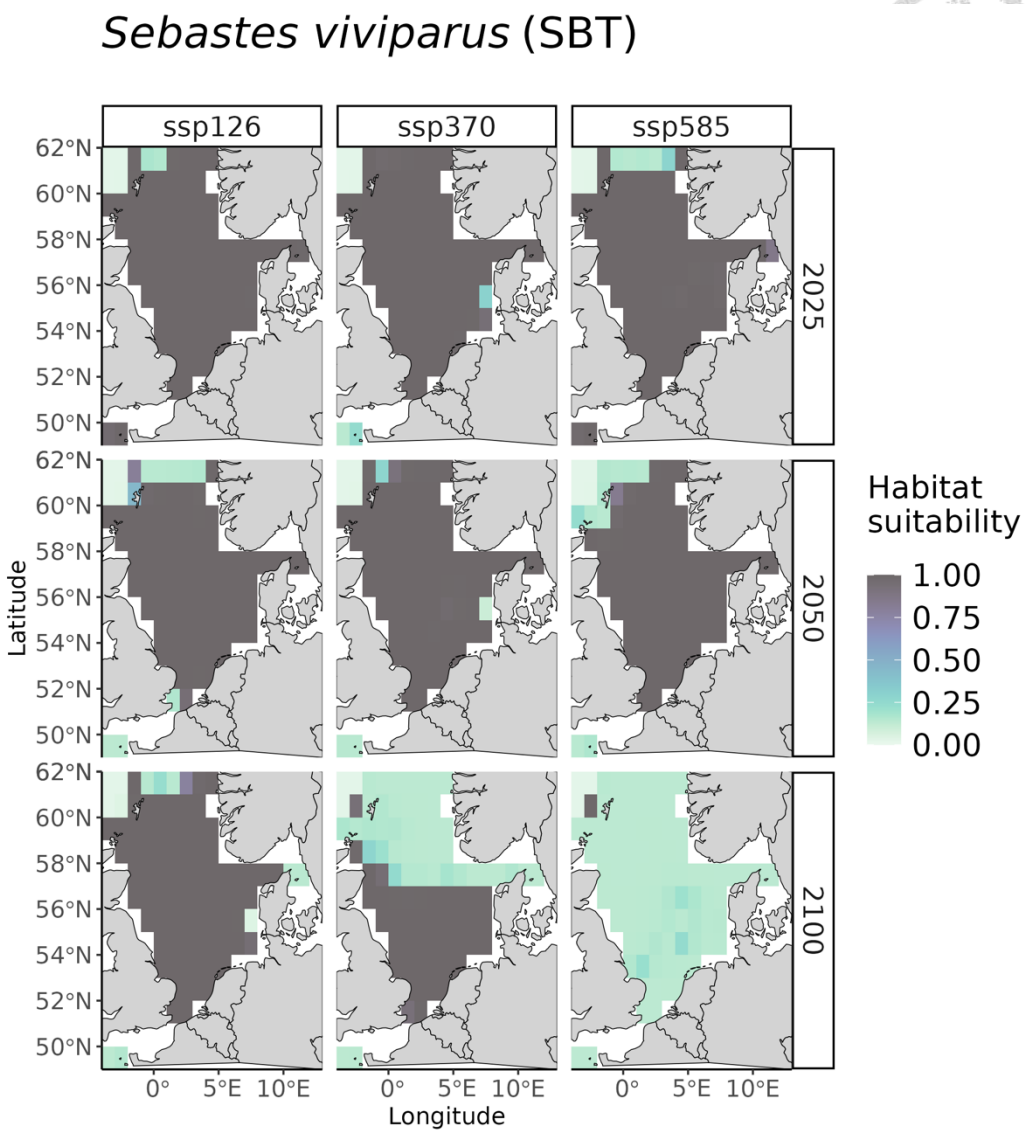

S.17. Projected distributional shifts of *Sebastes viviparus radiata* (based on habitat suitability) in 2025 (top), 2050 (middle) and 2100 (bottom) under 3 climate scenarios (SSP1-2.6, SSP3-7.0, SSP5-8.5). Color shading indicate probability of species occurrence in a grid of habitat suitability (0-1). Color-shading stands for potential habitat suitability, where 1 – suitable, 0 – unsuitable conditions. Each grid refers to resolution 60 arcmin. Applied model is indicated in the heading of each figure.

doi:10.6342/NTU202500202

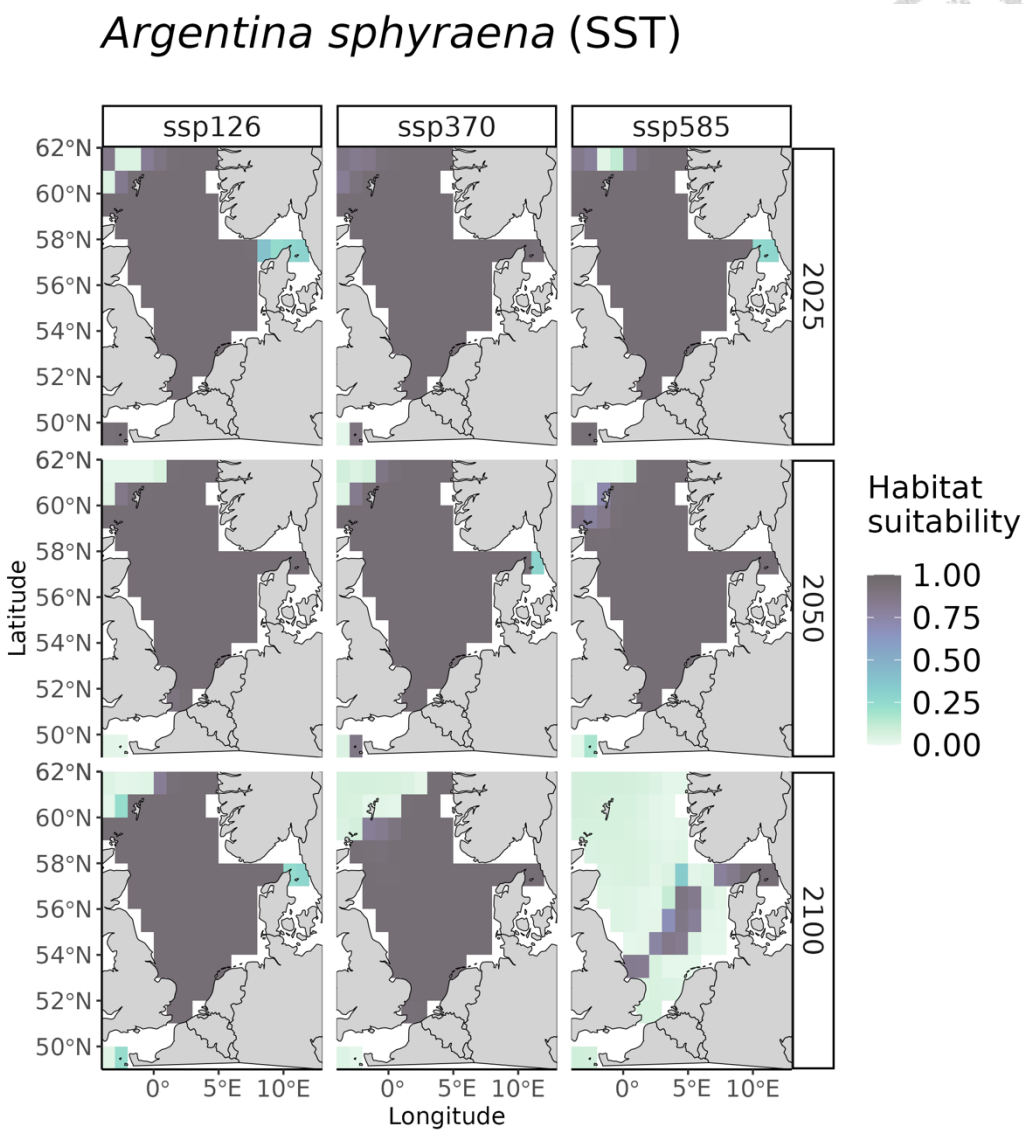

S.18. Projected distributional shifts of *Argentina sphyraena radiata* (based on habitat suitability) in 2025 (top), 2050 (middle) and 2100 (bottom) under 3 climate scenarios (SSP1-2.6, SSP3-7.0, SSP5-8.5). Color shading indicate probability of species occurrence in a grid of habitat suitability (0-1). Color-shading stands for potential habitat suitability, where 1 – suitable, 0 – unsuitable conditions. Each grid refers to resolution 60 arcmin. Applied model is indicated in the heading of each figure.

doi:10.6342/NTU202500202

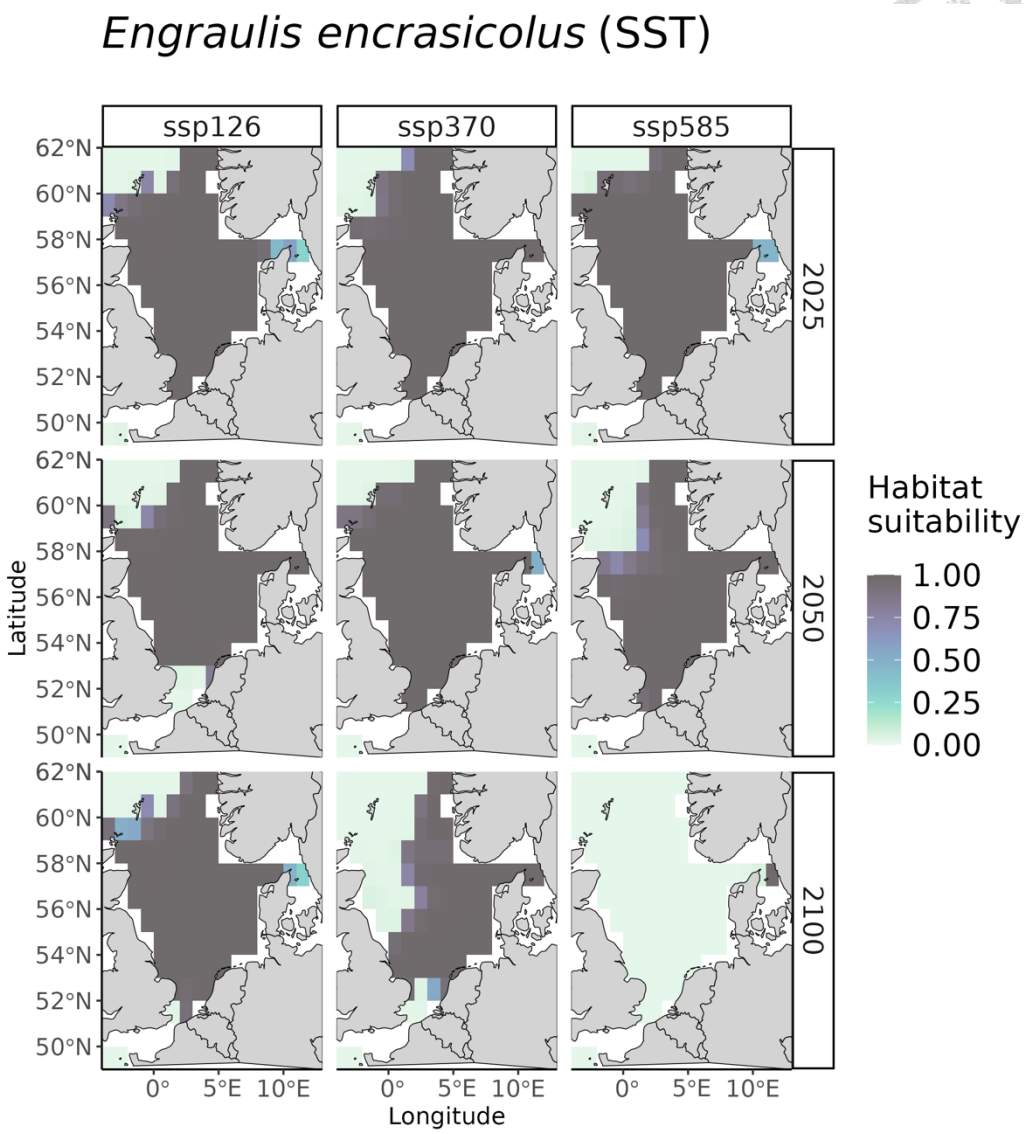

S.19. Projected distributional shifts of *Engraulis encrasicolus radiata* (based on habitat suitability) in 2025 (top), 2050 (middle) and 2100 (bottom) under 3 climate scenarios (SSP1-2.6, SSP3-7.0, SSP5-8.5). Color shading indicate probability of species occurrence in a grid of habitat suitability (0-1). Color-shading stands for potential habitat suitability, where 1 – suitable, 0 – unsuitable conditions. Each grid refers to resolution 60 arcmin. Applied model is indicated in the heading of each figure.

doi:10.6342/NTU202500202

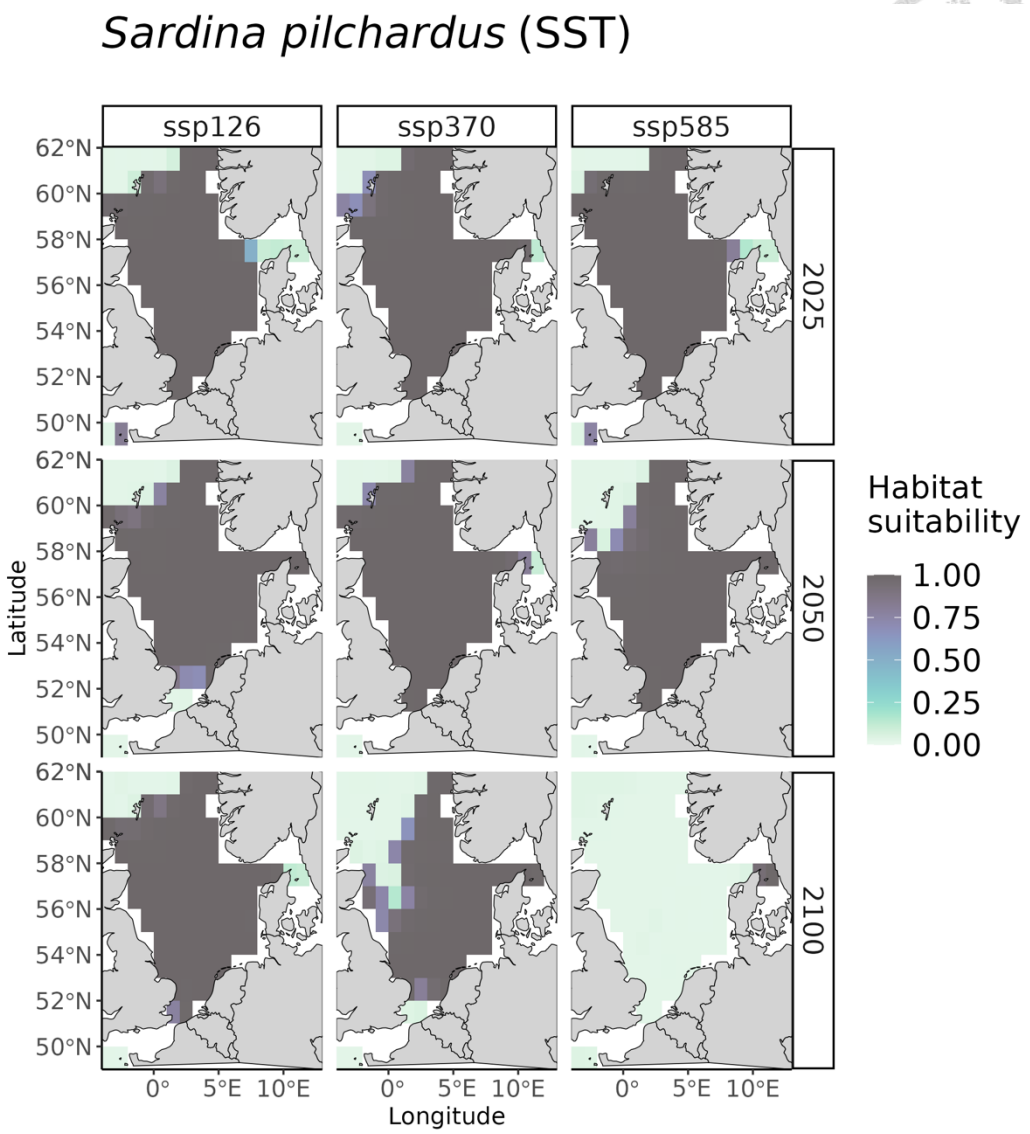

S.20. Projected distributional shifts of *Sardina pilchardus* 2 *radiata* (based on habitat suitability) in 2025 (top), 2050 (middle) and 2100 (bottom) under 3 climate scenarios (SSP1-2.6, SSP3-7.0, SSP5-8.5). Color shading indicate probability of species occurrence in a grid of habitat suitability (0-1). Color-shading stands for potential habitat suitability, where 1 – suitable, 0 – unsuitable conditions. Each grid refers to resolution 60 arcmin. Applied model is indicated in the heading of each figure.

doi:10.6342/NTU202500202

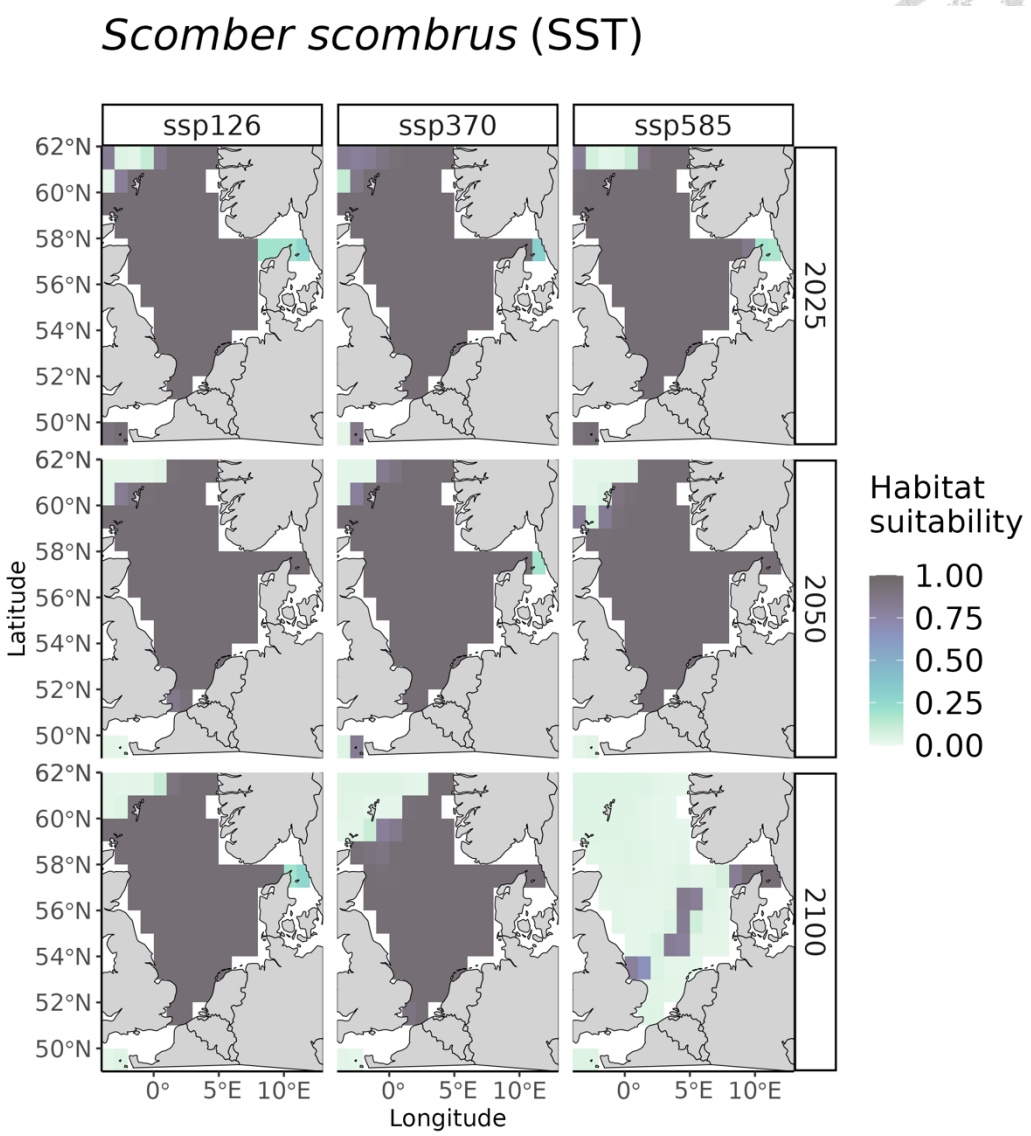

S.21. Projected distributional shifts of *Scomber scombrus radiata* (based on habitat suitability) in 2025 (top), 2050 (middle) and 2100 (bottom) under 3 climate scenarios (SSP1-2.6, SSP3-7.0, SSP5-8.5). Color shading indicate probability of species occurrence in a grid of habitat suitability (0-1). Color-shading stands for potential habitat suitability, where 1 – suitable, 0 – unsuitable conditions. Each grid refers to resolution 60 arcmin. Applied model is indicated in the heading of each figure.

doi:10.6342/NTU202500202

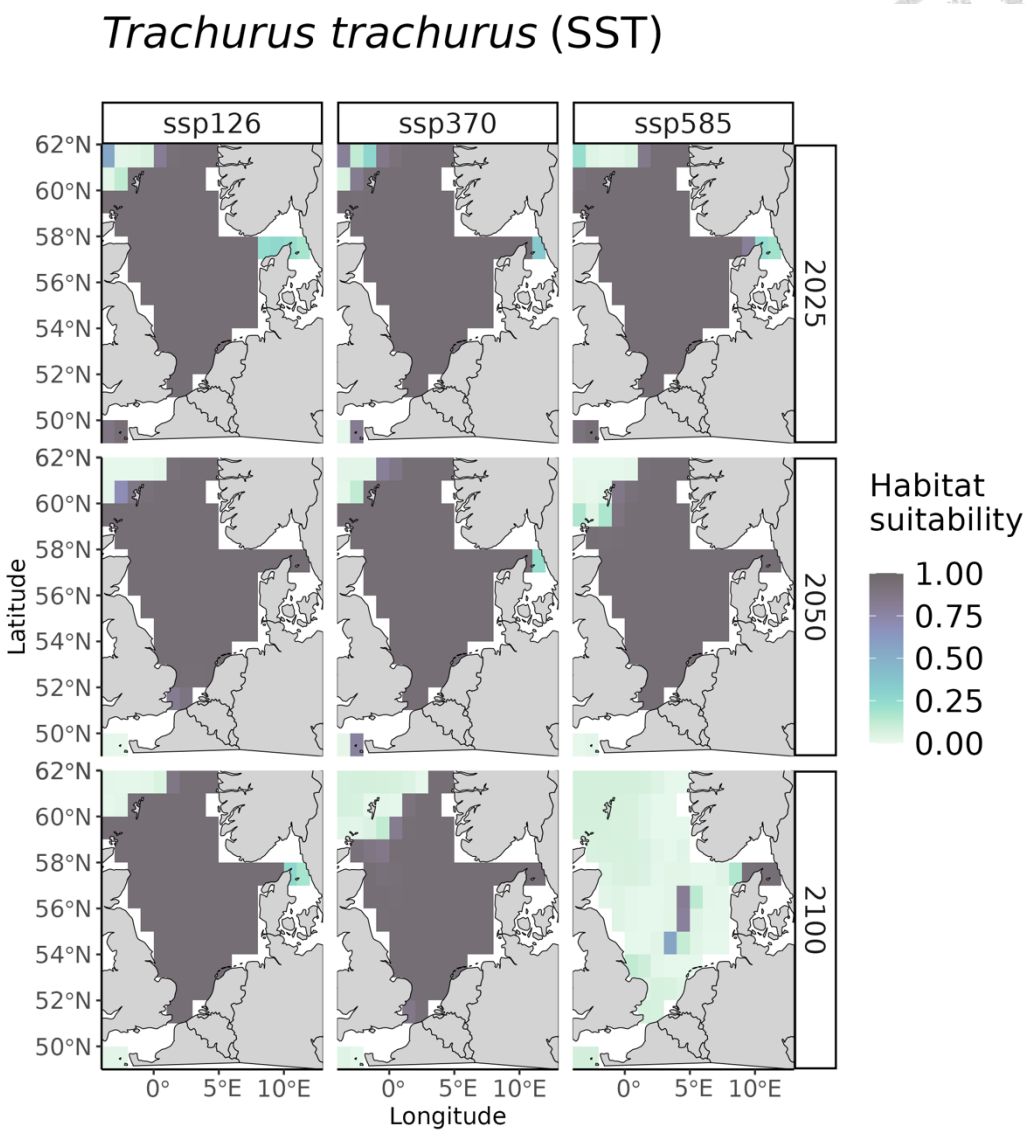

S.22. Projected distributional shifts of *Trachurus trachurus radiata* (based on habitat suitability) in 2025 (top), 2050 (middle) and 2100 (bottom) under 3 climate scenarios (SSP1-2.6, SSP3-7.0, SSP5-8.5). Color shading indicate probability of species occurrence in a grid of habitat suitability (0-1). Color-shading stands for potential habitat suitability, where 1 – suitable, 0 – unsuitable conditions. Each grid refers to resolution 60 arcmin. Applied model is indicated in the heading of each figure.

doi:10.6342/NTU202500202

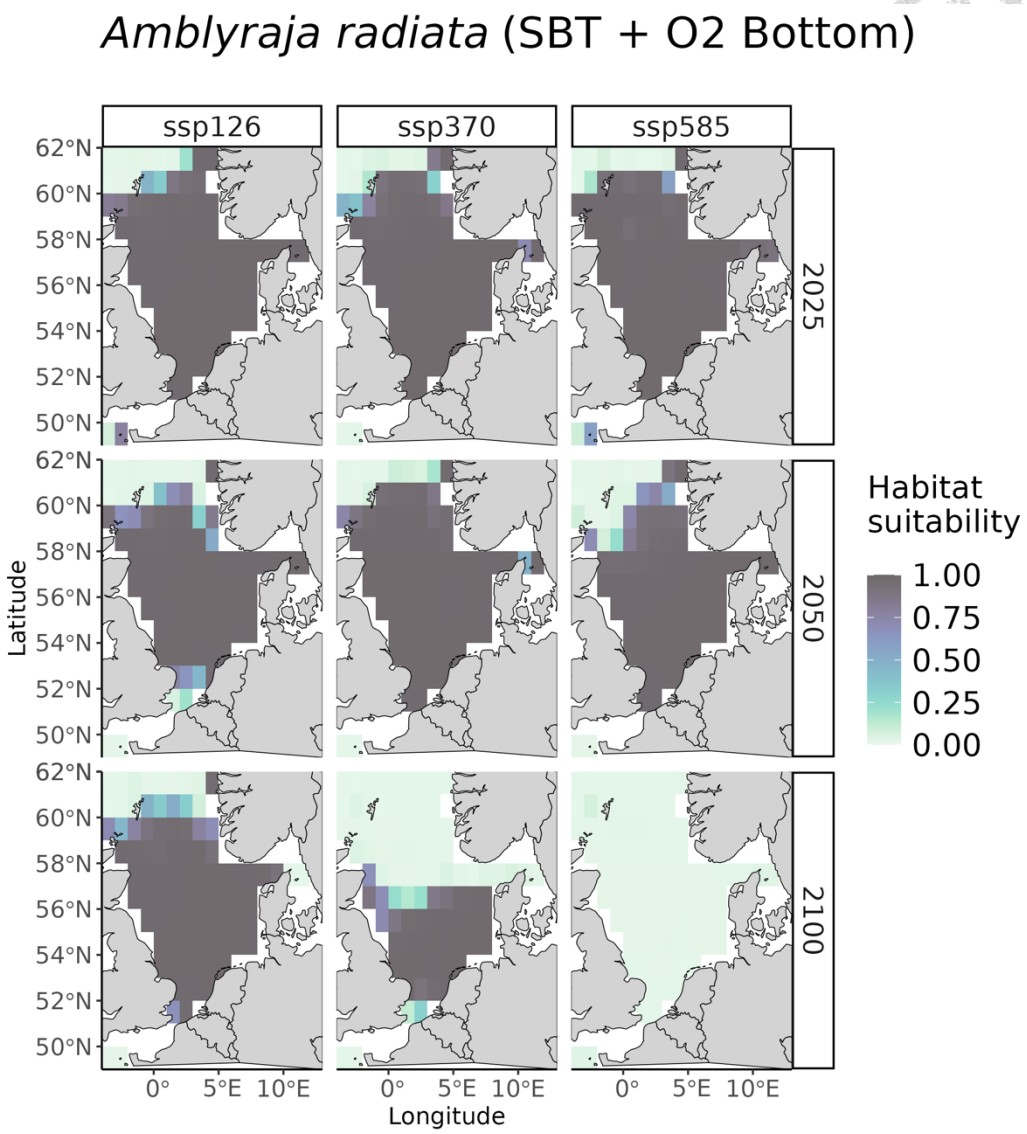

S.23. Projected distributional shifts of *Amblyraja radiata radiata* (based on habitat suitability) in 2025 (top), 2050 (middle) and 2100 (bottom) under 3 climate scenarios (SSP1-2.6, SSP3-7.0, SSP5-8.5). Color shading indicate probability of species occurrence in a grid of habitat suitability (0-1). Color-shading stands for potential habitat suitability, where 1 – suitable, 0 – unsuitable conditions. Each grid refers to resolution 60 arcmin. Applied model is indicated in the heading of each figure.

doi:10.6342/NTU202500202

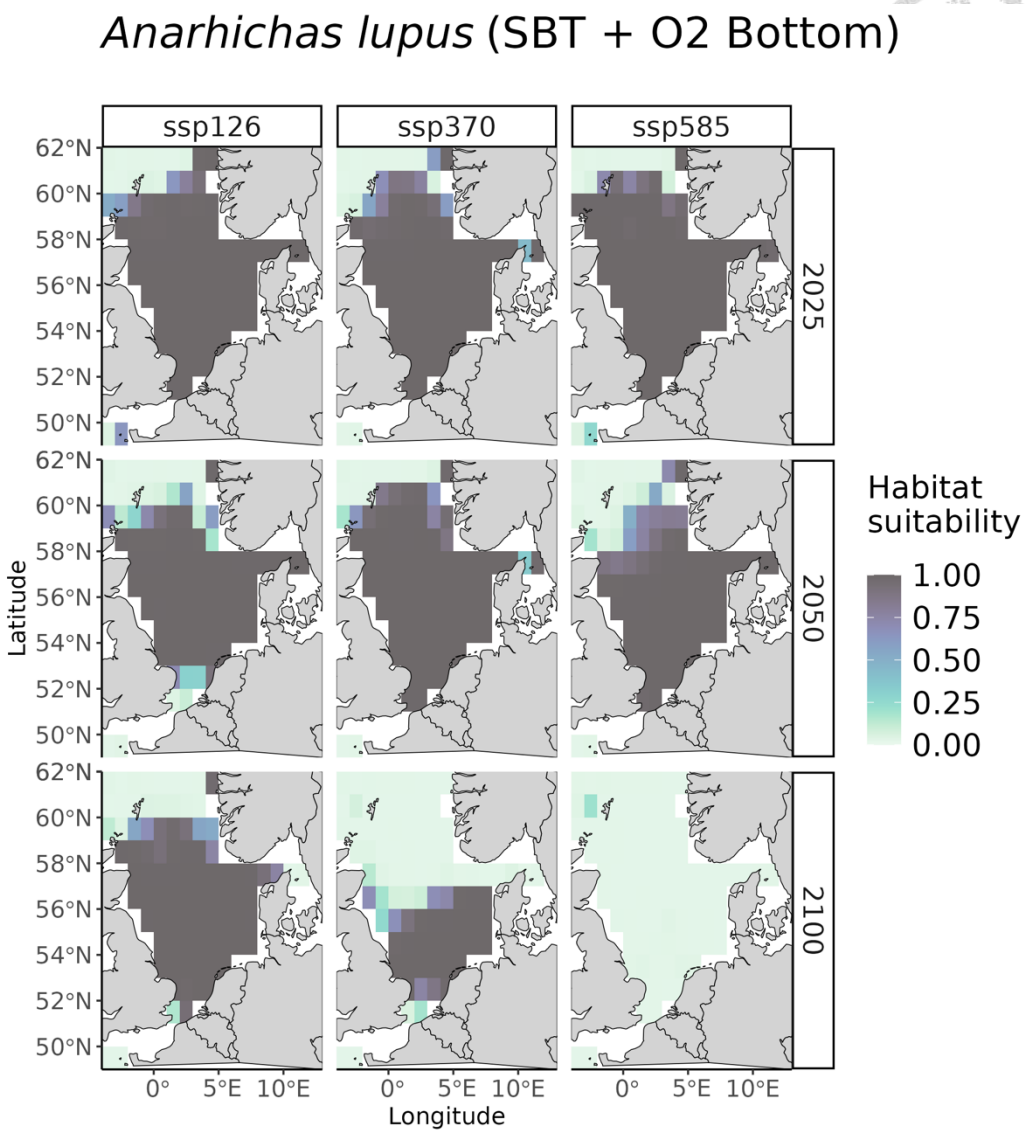

S.24. Projected distributional shifts of *Anarhichas lupus radiata* (based on habitat suitability) in 2025 (top), 2050 (middle) and 2100 (bottom) under 3 climate scenarios (SSP1-2.6, SSP3-7.0, SSP5-8.5). Color shading indicate probability of species occurrence in a grid of habitat suitability (0-1). Color-shading stands for potential habitat suitability, where 1 – suitable, 0 – unsuitable conditions. Each grid refers to resolution 60 arcmin. Applied model is indicated in the heading of each figure.

doi:10.6342/NTU202500202

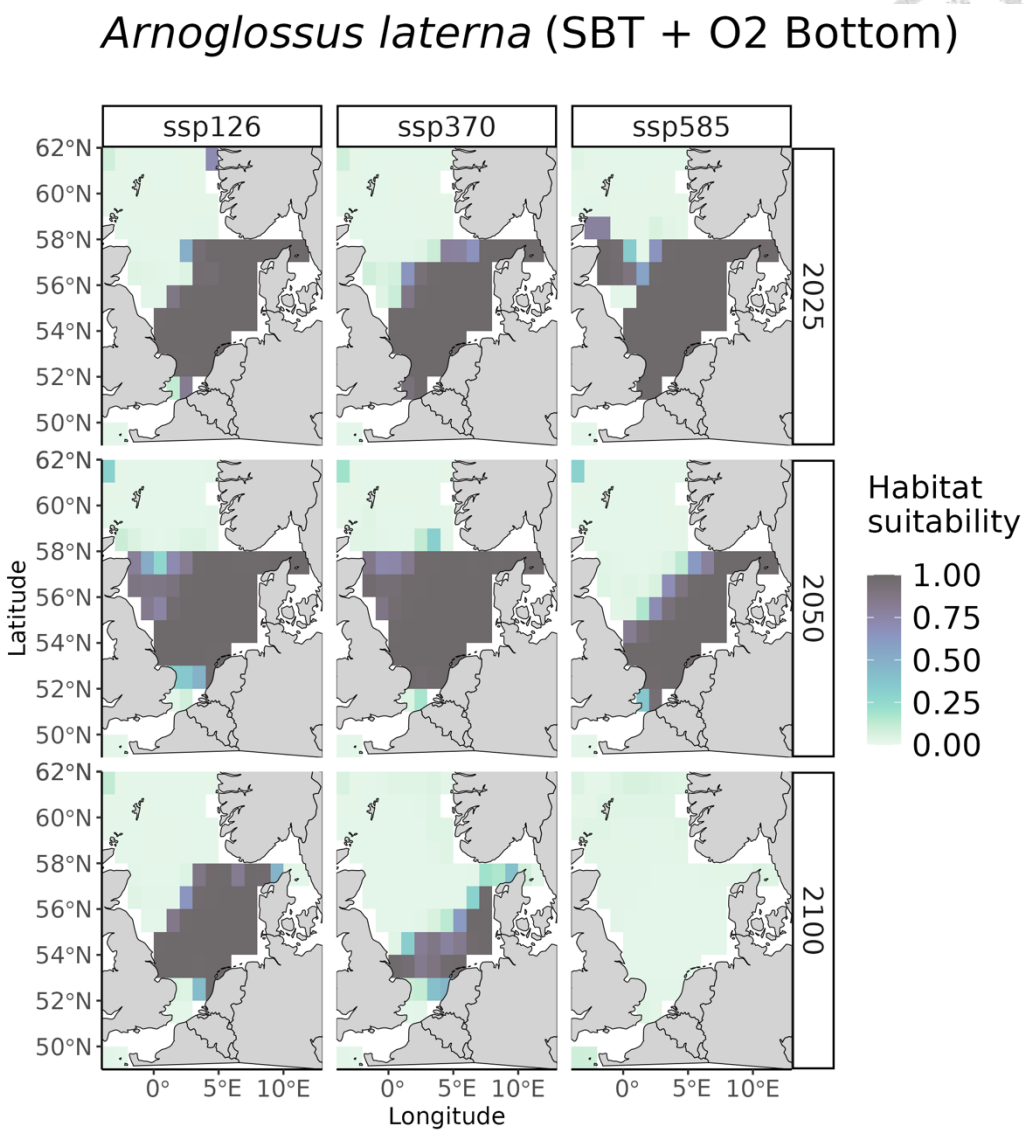

S.25. Projected distributional shifts of *Arnoglossus laterna radiata* (based on habitat suitability) in 2025 (top), 2050 (middle) and 2100 (bottom) under 3 climate scenarios (SSP1-2.6, SSP3-7.0, SSP5-8.5). Color shading indicate probability of species occurrence in a grid of habitat suitability (0-1). Color-shading stands for potential habitat suitability, where 1 – suitable, 0 – unsuitable conditions. Each grid refers to resolution 60 arcmin. Applied model is indicated in the heading of each figure.

doi:10.6342/NTU202500202

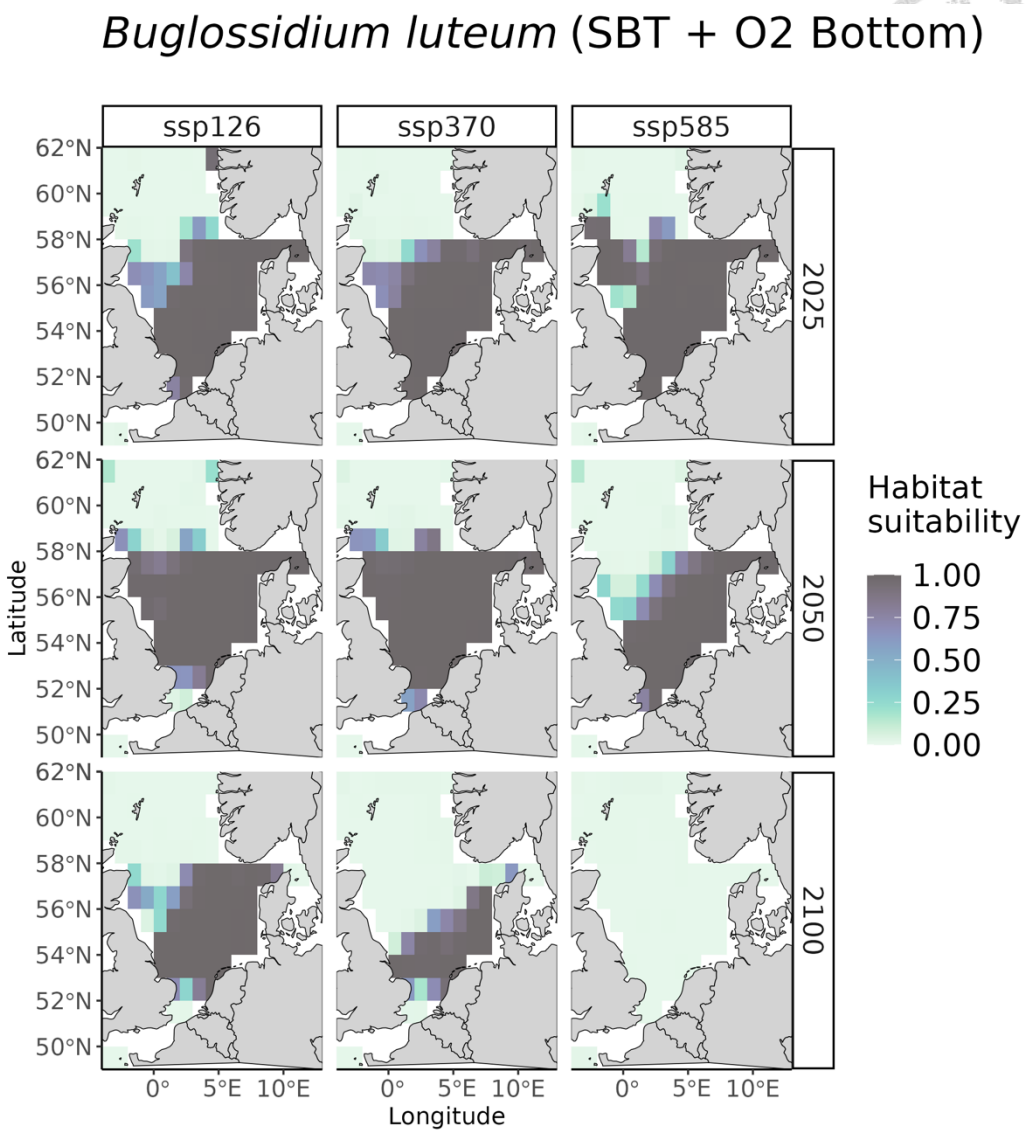

S.26. Projected distributional shifts of *Buglossidium luteum* (based on habitat suitability) 2025 (top), 2050 (middle) and 2100 (bottom) under 3 climate scenarios (SSP1-2.6, SSP3-7.0, SSP5-8.5). Color shading indicate probability of species occurrence (0-1). Color-shading stands for habitat suitability (0-1). Each grid refers to resolution 60 arcmin. Applied model is indicated in the heading of each figure.

doi:10.6342/NTU202500202

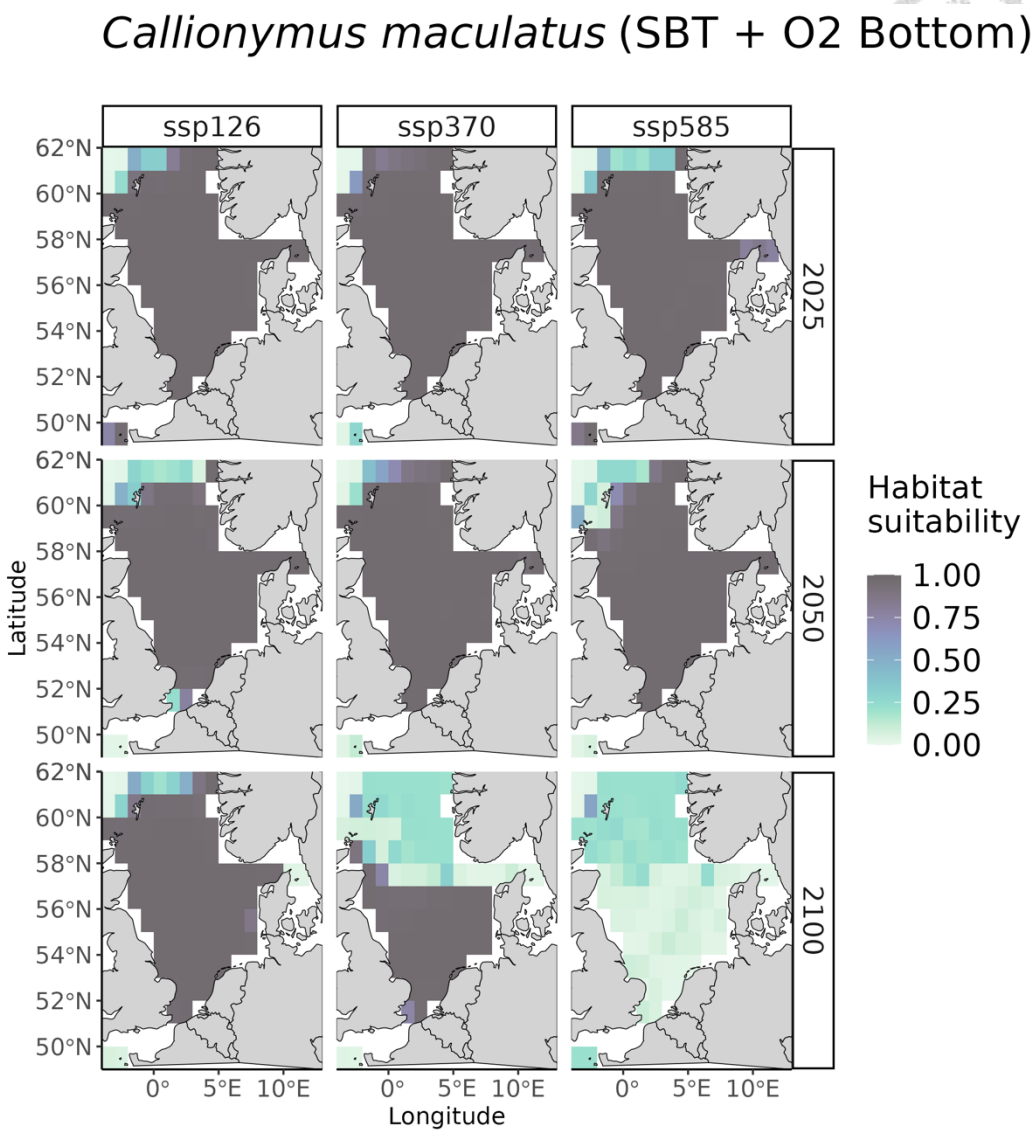

S.27. Projected distributional shifts of *Callionymus maculatus* (based on habitat suitability) 2025 (top), 2050 (middle) and 2100 (bottom) under 3 climate scenarios (SSP1-2.6, SSP3-7.0, SSP5-8.5). Color shading indicate probability of species occurrence (0-1). Color-shading stands for habitat suitability (0-1). Each grid refers to resolution 60 arcmin. Applied model is indicated in the heading of each figure.

doi:10.6342/NTU202500202

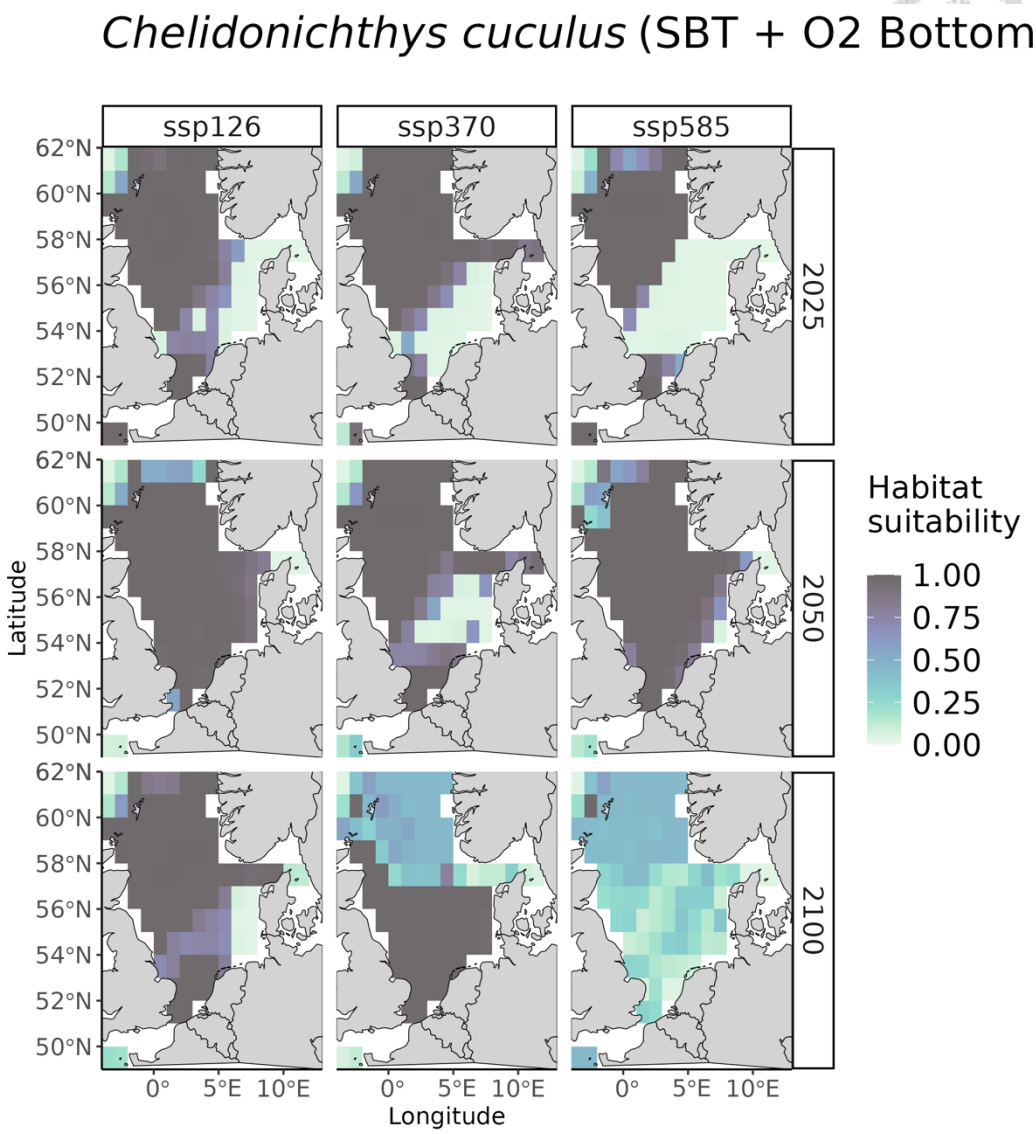

S.28. Projected distributional shifts of *Chelidonichtys cuculus radiata* (based on habitat suitability) in 2025 (top), 2050 (middle) and 2100 (bottom) under 3 climate scenarios (SSP1-2.6, SSP3-7.0, SSP5-8.5). Color shading indicate probability of species occurrence in a grid of habitat suitability (0-1). Color-shading stands for potential habitat suitability, where 1 – suitable, 0 – unsuitable conditions. Each grid refers to resolution 60 arcmin. Applied model is indicated in the heading of each figure.

doi:10.6342/NTU202500202

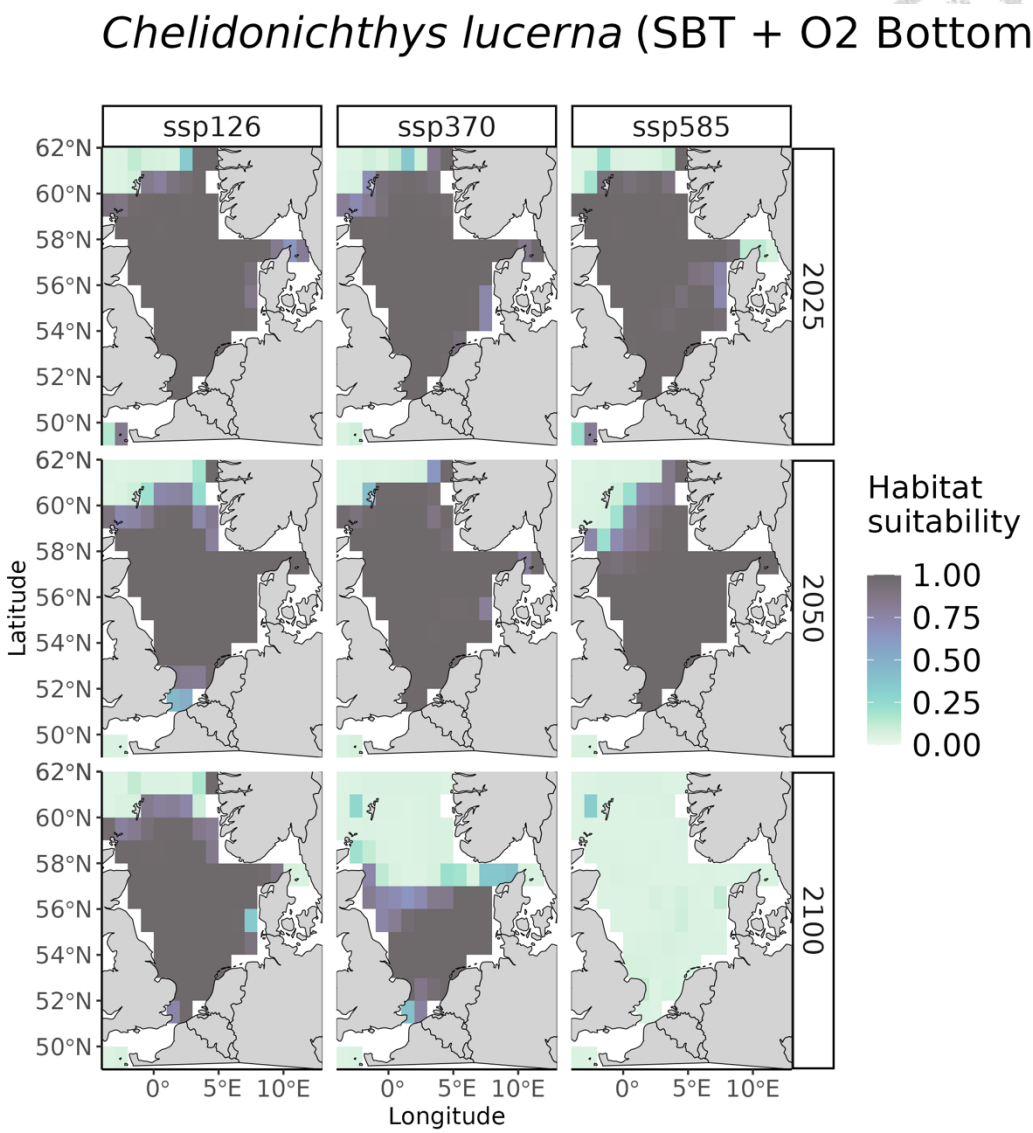

S.29. Projected distributional shifts of *Chelidonichthys lucerna radiata* (based on habitat suitability) in 2025 (top), 2050 (middle) and 2100 (bottom) under 3 climate scenarios (SSP1-2.6, SSP3-7.0, SSP5-8.5). Color shading indicate probability of species occurrence in a grid of habitat suitability (0-1). Color-shading stands for potential habitat suitability, where 1 – suitable, 0 – unsuitable conditions. Each grid refers to resolution 60 arcmin. Applied model is indicated in the heading of each figure.

doi:10.6342/NTU202500202

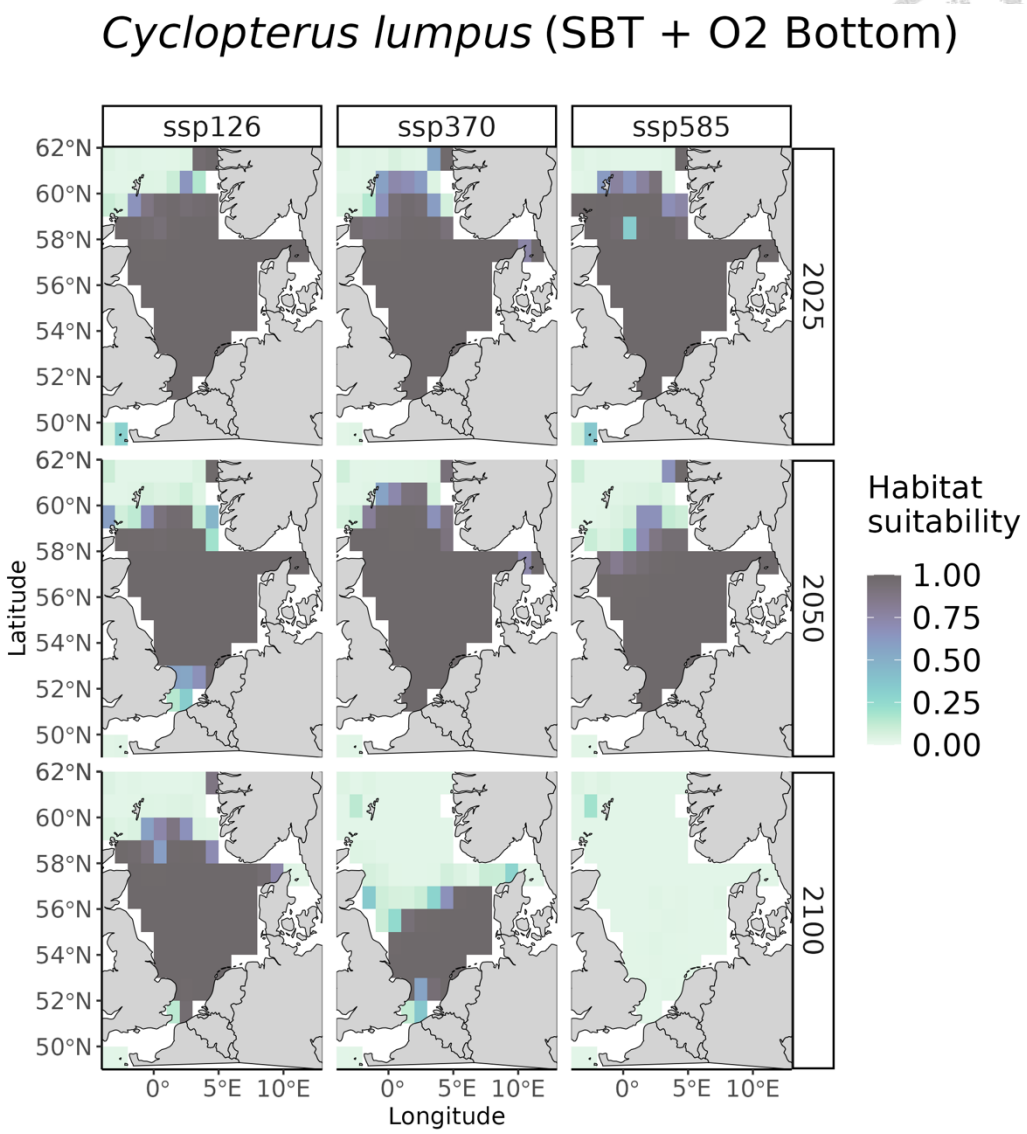

S.30. Projected distributional shifts of *Cyclopterus lumpus radiata* (based on habitat suitability) in 2025 (top), 2050 (middle) and 2100 (bottom) under 3 climate scenarios (SSP1-2.6, SSP3-7.0, SSP5-8.5). Color shading indicate probability of species occurrence in a grid of habitat suitability (0-1). Color-shading stands for potential habitat suitability, where 1 – suitable, 0 – unsuitable conditions. Each grid refers to resolution 60 arcmin. Applied model is indicated in the heading of each figure.

doi:10.6342/NTU202500202

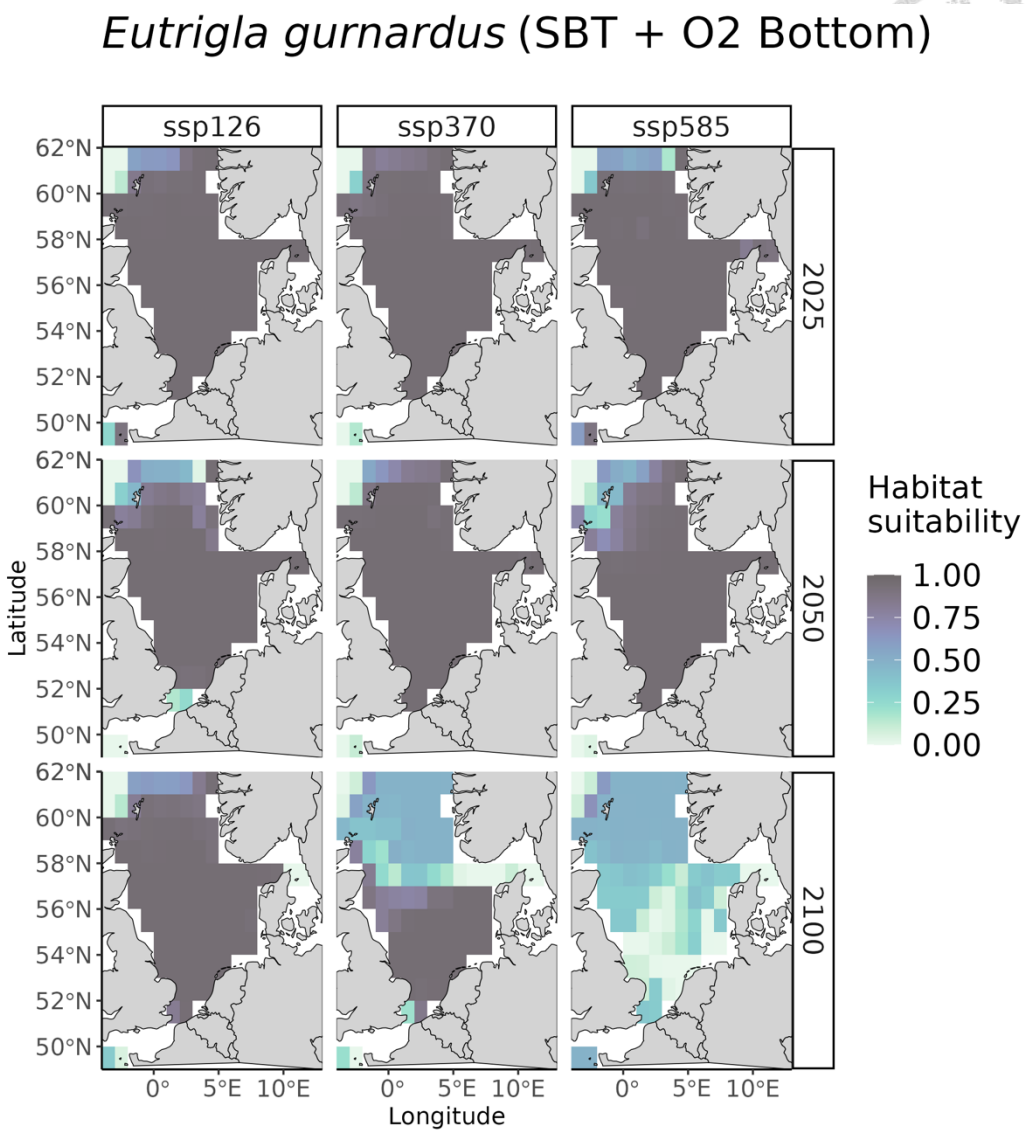

S.31. Projected distributional shifts of *Eutrigla gurnardus radiata* (based on habitat suitability) in 2025 (top), 2050 (middle) and 2100 (bottom) under 3 climate scenarios (SSP1-2.6, SSP3-7.0, SSP5-8.5). Color shading indicate probability of species occurrence in a grid of habitat suitability (0-1). Color-shading stands for potential habitat suitability, where 1 – suitable, 0 – unsuitable conditions. Each grid refers to resolution 60 arcmin. Applied model is indicated in the heading of each figure.

doi:10.6342/NTU202500202

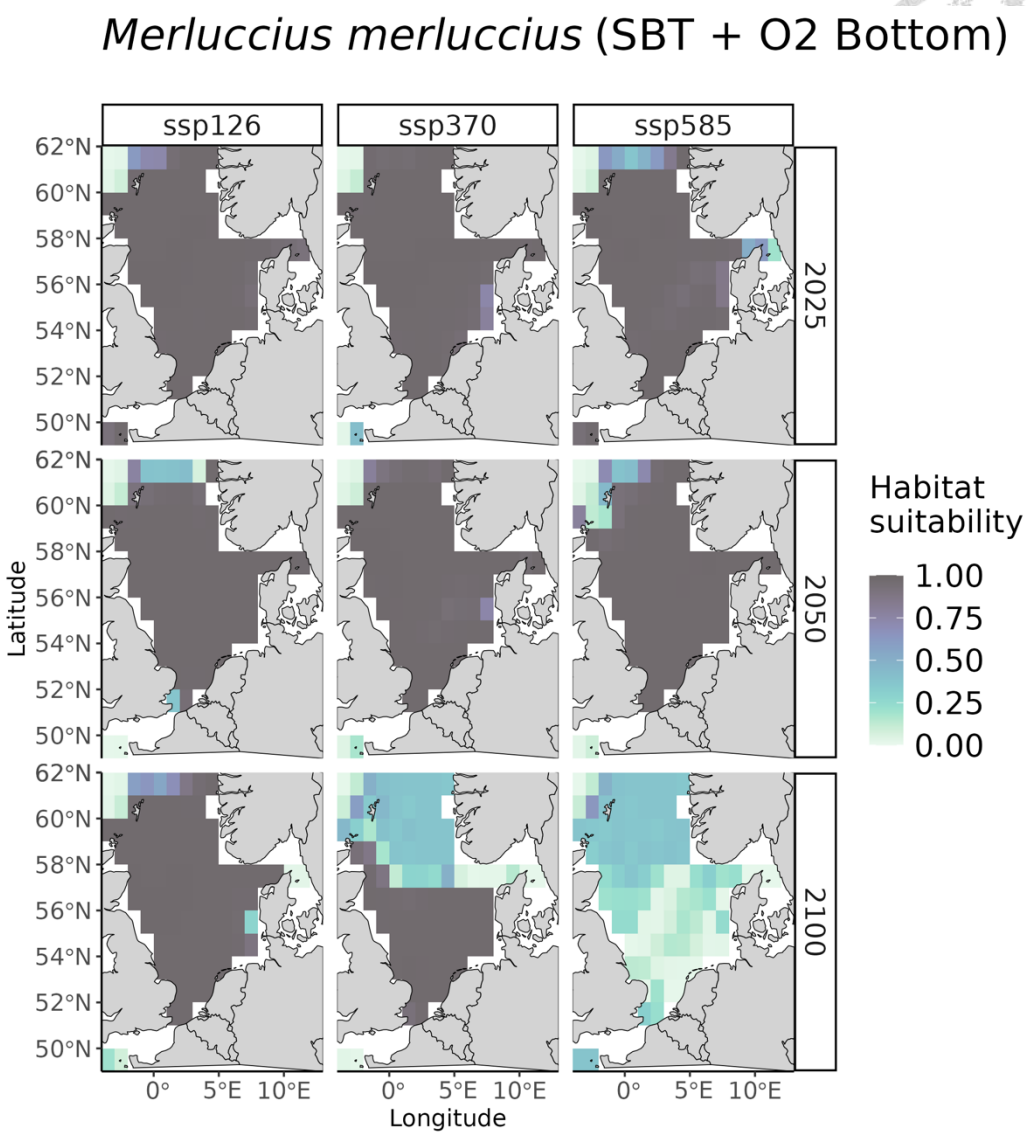

S.32. Projected distributional shifts of *Merluccius merluccius radiata* (based on habitat suitability) in 2025 (top), 2050 (middle) and 2100 (bottom) under 3 climate scenarios (SSP1-2.6, SSP3-7.0, SSP5-8.5). Color shading indicate probability of species occurrence in a grid of habitat suitability (0-1). Color-shading stands for potential habitat suitability, where 1 – suitable, 0 – unsuitable conditions. Each grid refers to resolution 60 arcmin. Applied model is indicated in the heading of each figure.

doi:10.6342/NTU202500202

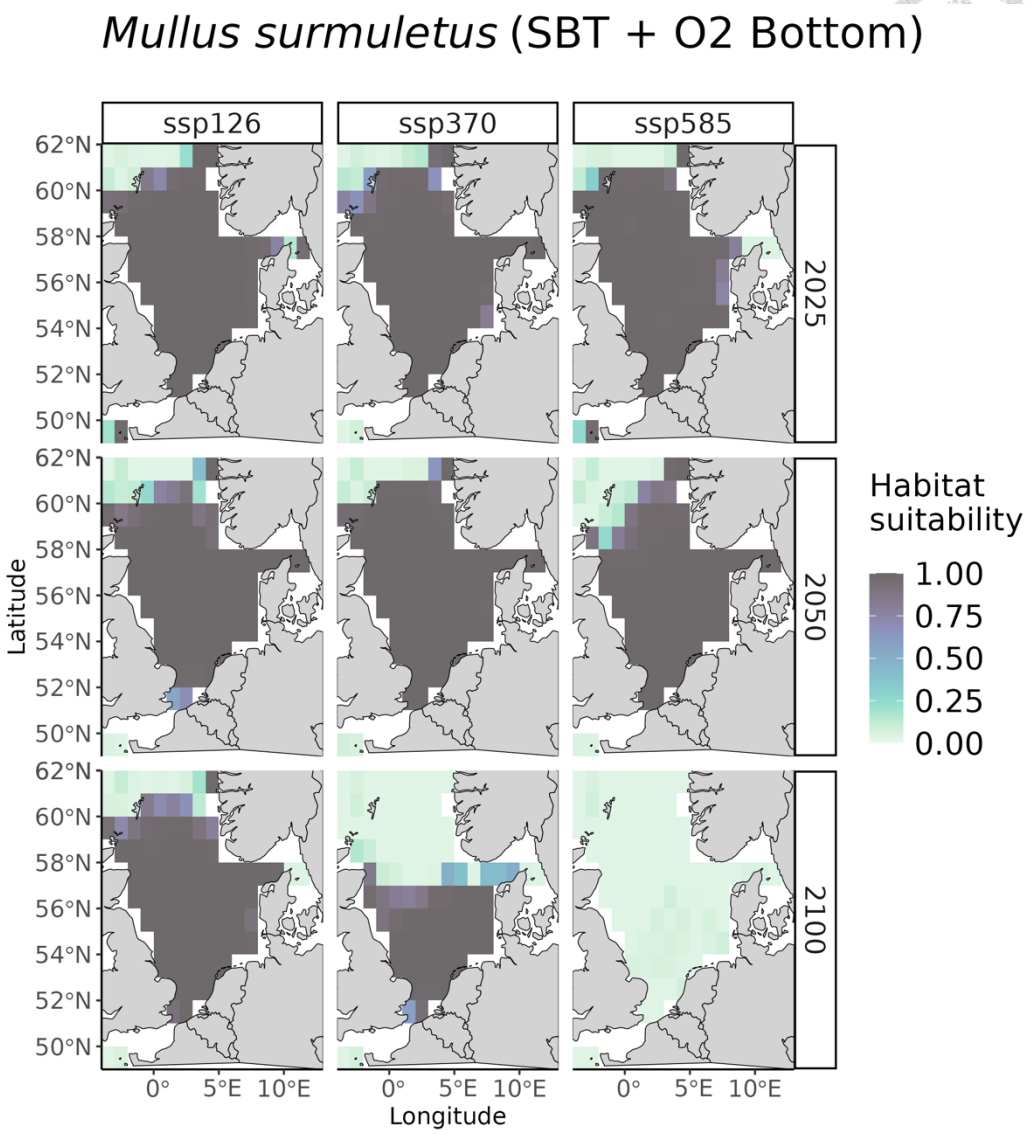

S.33. Projected distributional shifts of *Mullus surmuletus radiata* (based on habitat suitability) in 2025 (top), 2050 (middle) and 2100 (bottom) under 3 climate scenarios (SSP1-2.6, SSP3-7.0, SSP5-8.5). Color shading indicate probability of species occurrence in a grid of habitat suitability (0-1). Color-shading stands for potential habitat suitability, where 1 – suitable, 0 – unsuitable conditions. Each grid refers to resolution 60 arcmin. Applied model is indicated in the heading of each figure.

doi:10.6342/NTU202500202

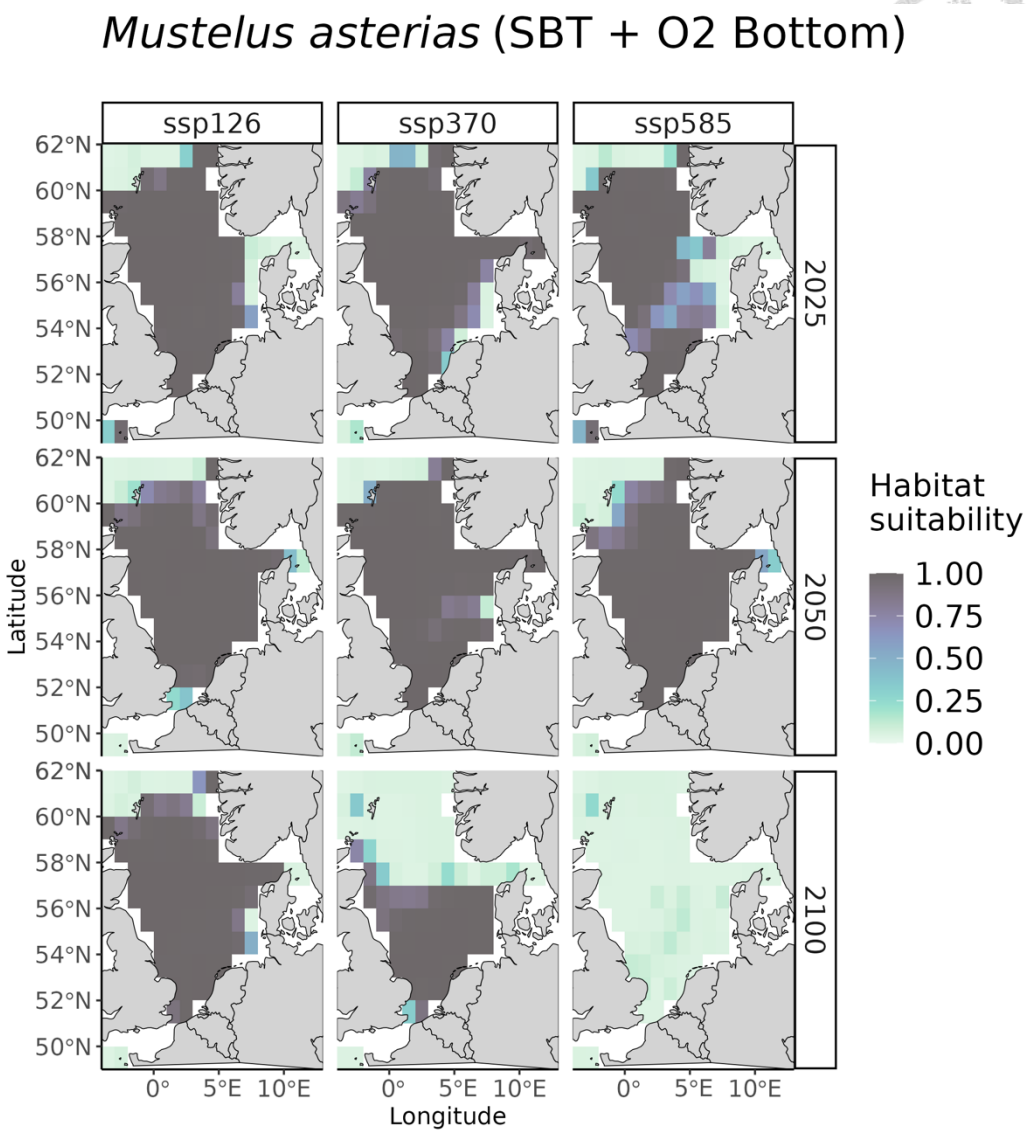

S.34.Projected distributional shifts of *Mustelus asterias radiata* (based on habitat suitability) in 2025 (top), 2050 (middle) and 2100 (bottom) under 3 climate scenarios (SSP1-2.6, SSP3-7.0, SSP5-8.5). Color shading indicate probability of species occurrence in a grid of habitat suitability (0-1). Color-shading stands for potential habitat suitability, where 1 – suitable, 0 – unsuitable conditions. Each grid refers to resolution 60 arcmin. Applied model is indicated in the heading of each figure.

doi:10.6342/NTU202500202

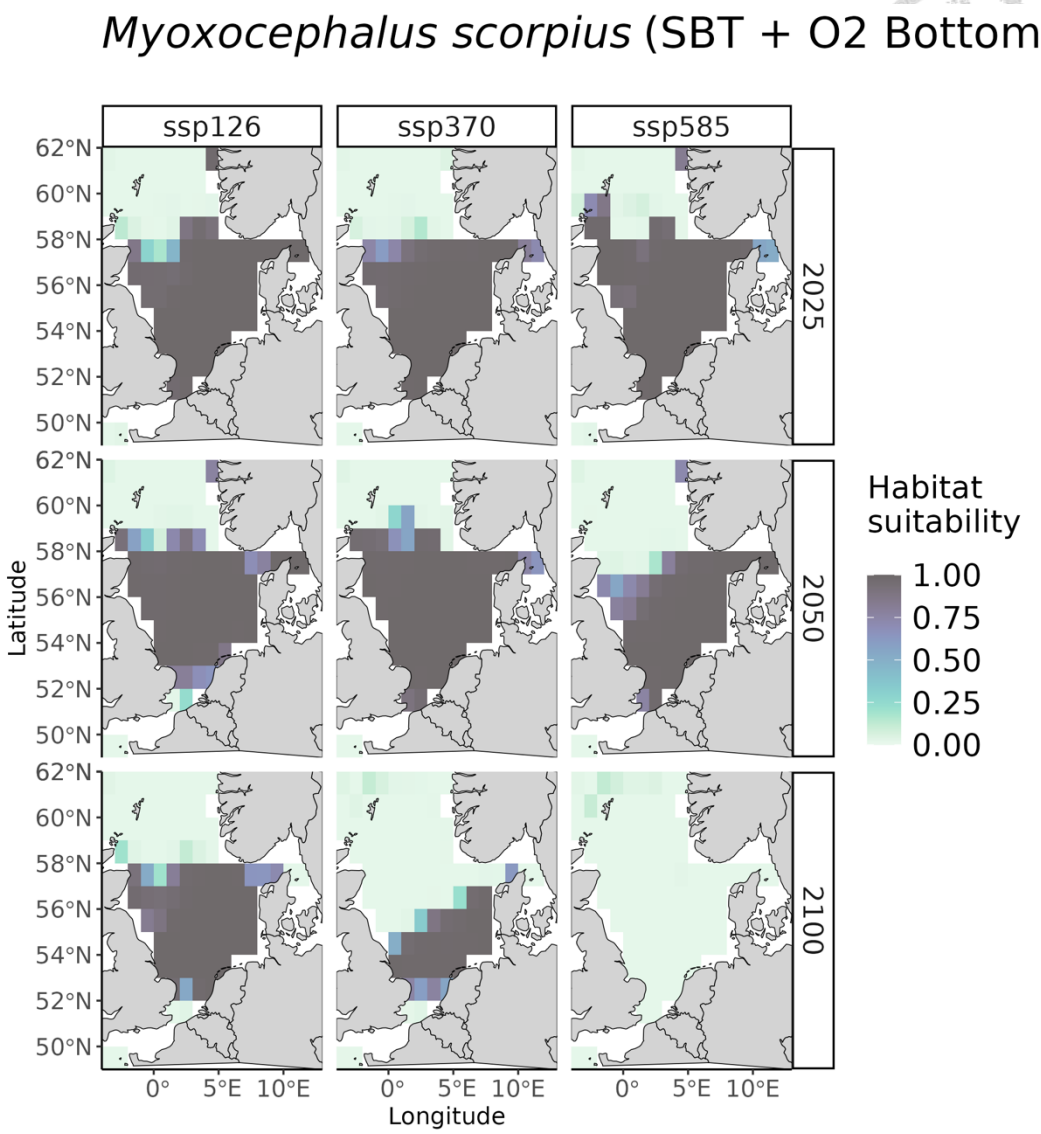

S.35. Projected distributional shifts of *Myoxocephalus scorpius radiata* (based on habitat suitability) in 2025 (top), 2050 (middle) and 2100 (bottom) under 3 climate scenarios (SSP1-2.6, SSP3-7.0, SSP5-8.5). Color shading indicate probability of species occurrence in a grid of habitat suitability (0-1). Color-shading stands for potential habitat suitability, where 1 – suitable, 0 – unsuitable conditions. Each grid refers to resolution 60 arcmin. Applied model is indicated in the heading of each figure.

doi:10.6342/NTU202500202

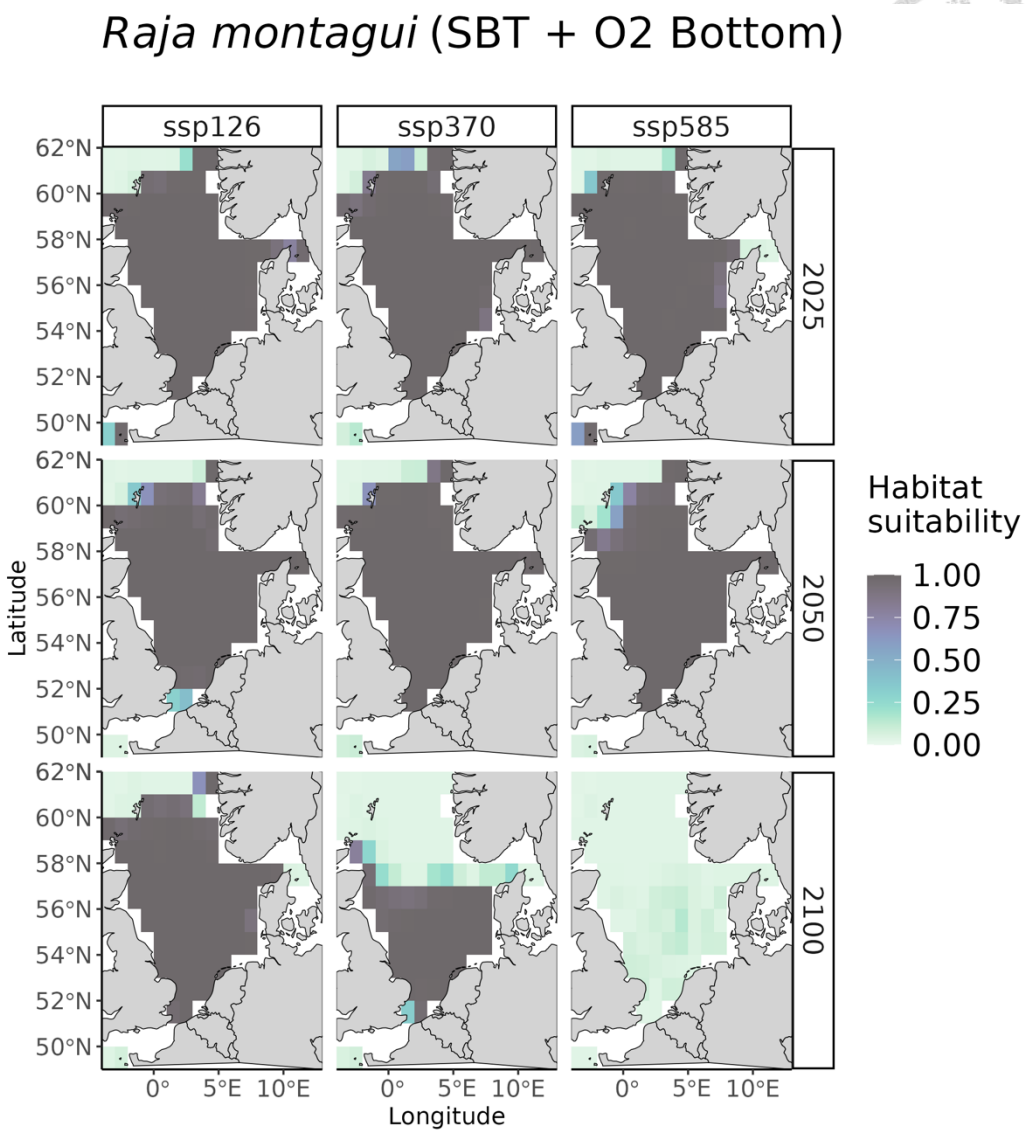

S.36. Projected distributional shifts of *Raja montagui radiata* (based on habitat suitability) in 2025 (top), 2050 (middle) and 2100 (bottom) under 3 climate scenarios (SSP1-2.6, SSP3-7.0, SSP5-8.5). Color shading indicate probability of species occurrence in a grid of habitat suitability (0-1). Color-shading stands for potential habitat suitability, where 1 – suitable, 0 – unsuitable conditions. Each grid refers to resolution 60 arcmin. Applied model is indicated in the heading of each figure.

doi:10.6342/NTU202500202

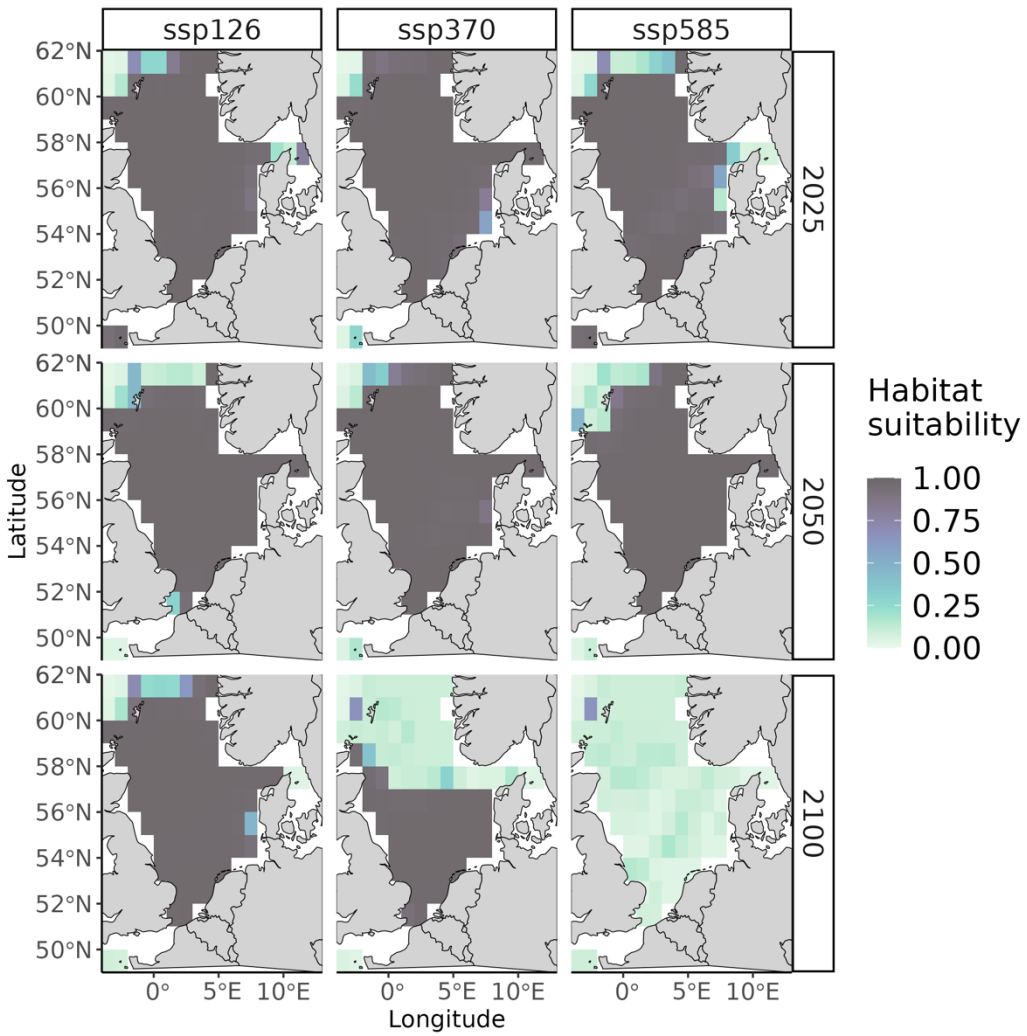

S.37. Projected distributional shifts of *Scyliorhunus canicula radiata* (based on habitat suitability) in 2025 (top), 2050 (middle) and 2100 (bottom) under 3 climate scenarios (SSP1-2.6, SSP3-7.0, SSP5-8.5). Color shading indicate probability of species occurrence in a grid of habitat suitability (0-1). Color-shading stands for potential habitat suitability, where 1 – suitable, 0 – unsuitable conditions. Each grid refers to resolution 60 arcmin. Applied model is indicated in the heading of each figure.

doi:10.6342/NTU202500202

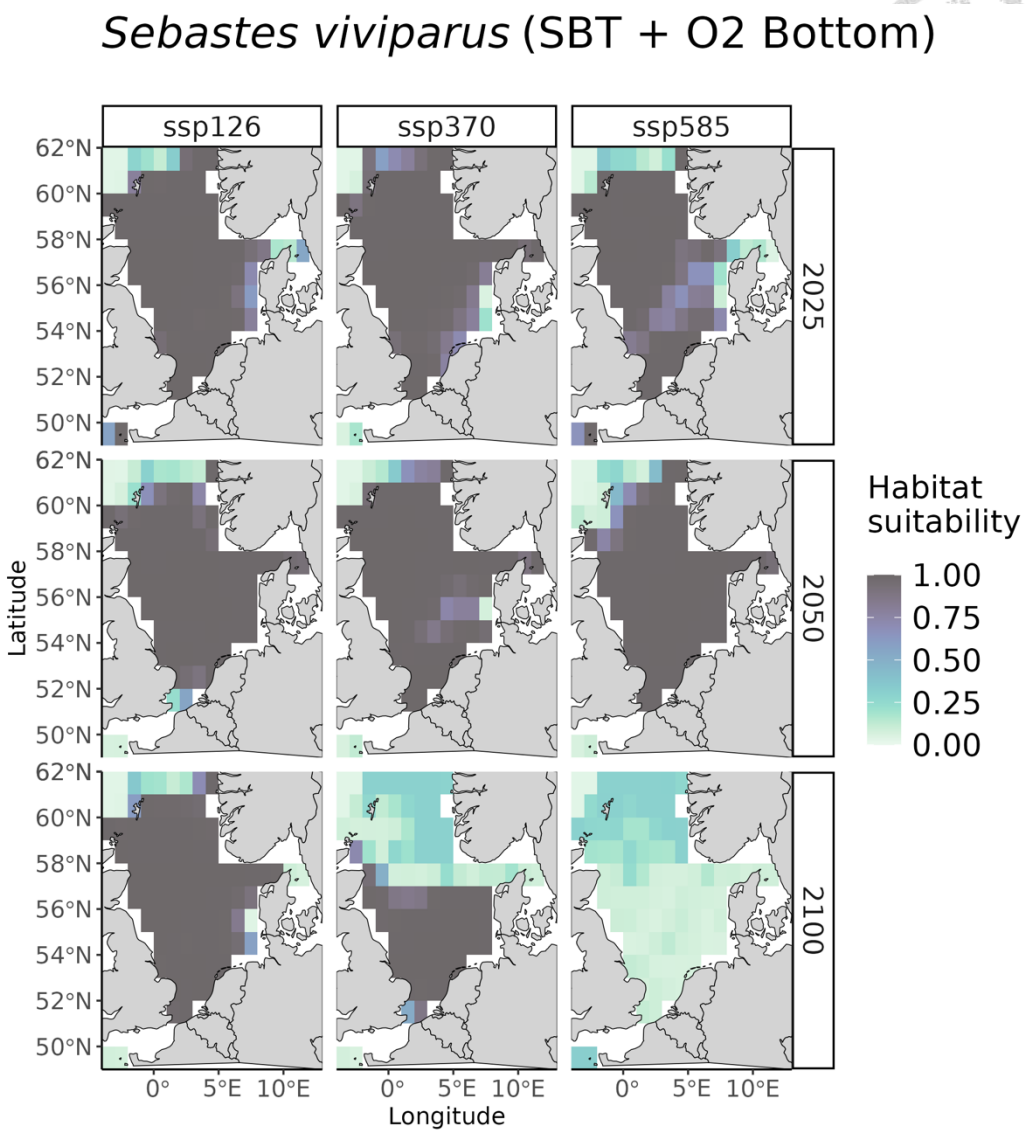

S.38. Projected distributional shifts of *Sebastes viviparus radiata* (based on habitat suitability) in 2025 (top), 2050 (middle) and 2100 (bottom) under 3 climate scenarios (SSP1-2.6, SSP3-7.0, SSP5-8.5). Color shading indicate probability of species occurrence in a grid of habitat suitability (0-1). Color-shading stands for potential habitat suitability, where 1 – suitable, 0 – unsuitable conditions. Each grid refers to resolution 60 arcmin. Applied model is indicated in the heading of each figure.

doi:10.6342/NTU202500202

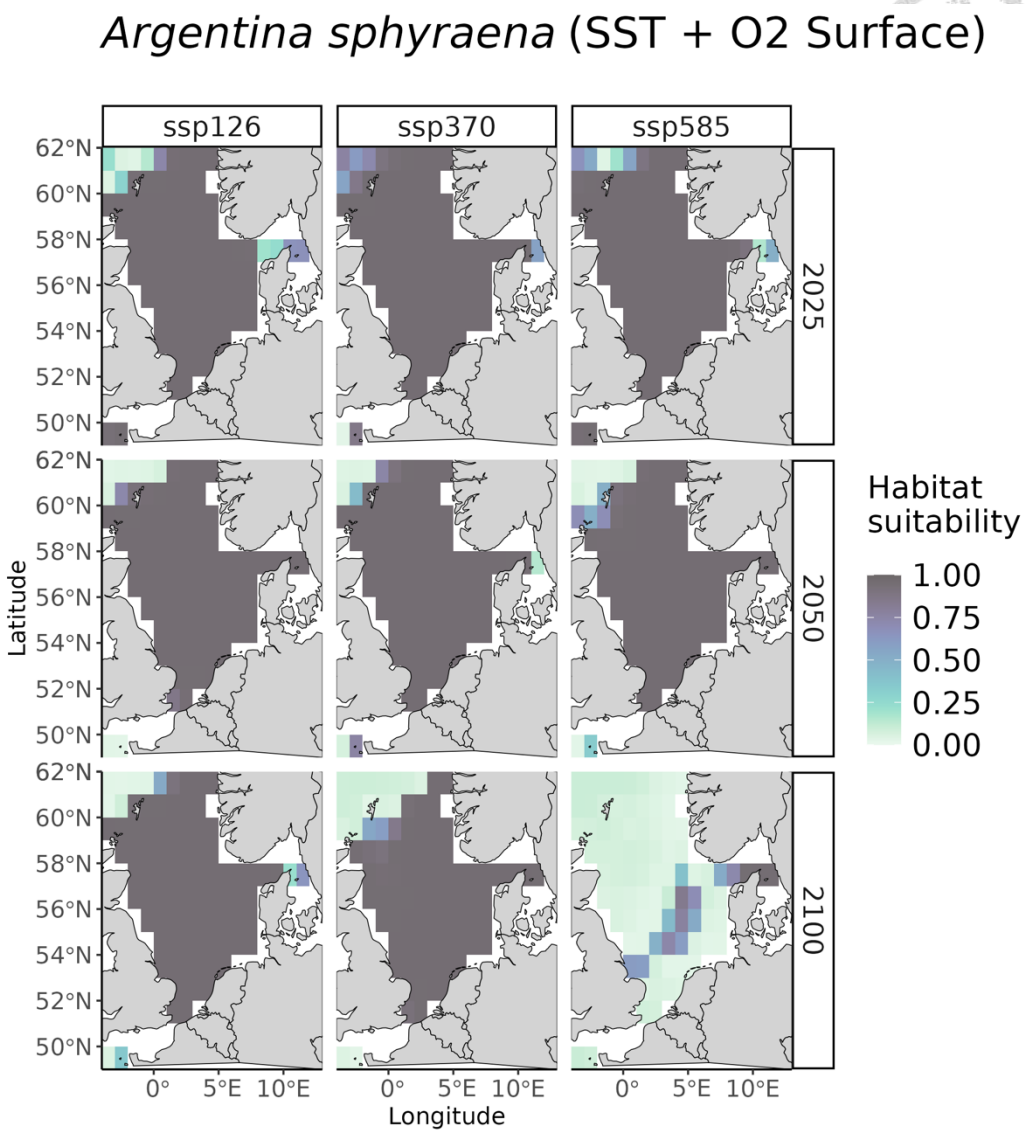

S.39. Projected distributional shifts of *Argentina sphyraena radiata* (based on habitat suitability) in 2025 (top), 2050 (middle) and 2100 (bottom) under 3 climate scenarios (SSP1-2.6, SSP3-7.0, SSP5-8.5). Color shading indicate probability of species occurrence in a grid of habitat suitability (0-1). Color-shading stands for potential habitat suitability, where 1 – suitable, 0 – unsuitable conditions. Each grid refers to resolution 60 arcmin. Applied model is indicated in the heading of each figure.

doi:10.6342/NTU202500202

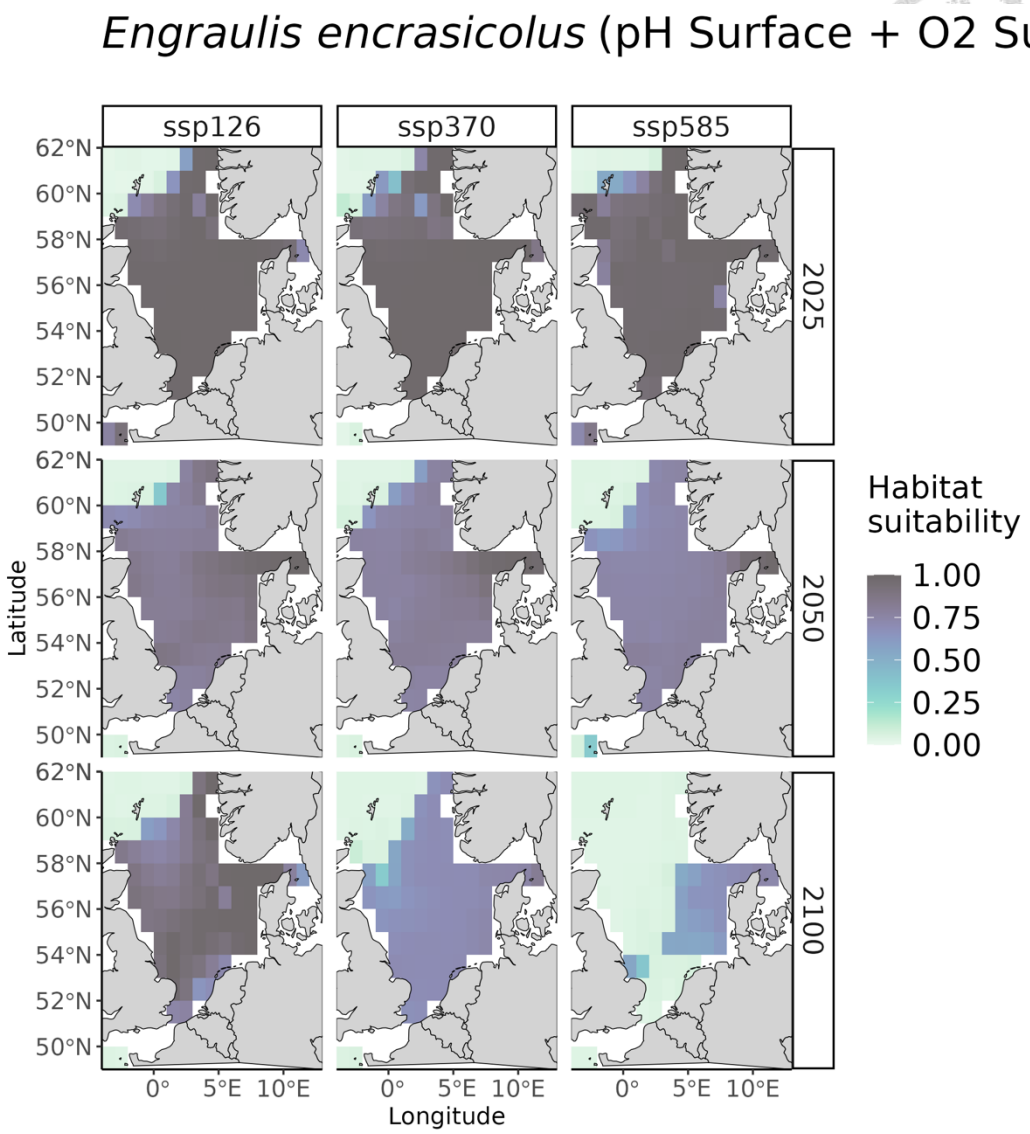

S.40. Projected distributional shifts of *Engraulis encrasicolus radiata* (based on habitat suitability) in 2025 (top), 2050 (middle) and 2100 (bottom) under 3 climate scenarios (SSP1-2.6, SSP3-7.0, SSP5-8.5). Color shading indicate probability of species occurrence in a grid of habitat suitability (0-1). Color-shading stands for potential habitat suitability, where 1 – suitable, 0 – unsuitable conditions. Each grid refers to resolution 60 arcmin. Applied model is indicated in the heading of each figure.

doi:10.6342/NTU202500202

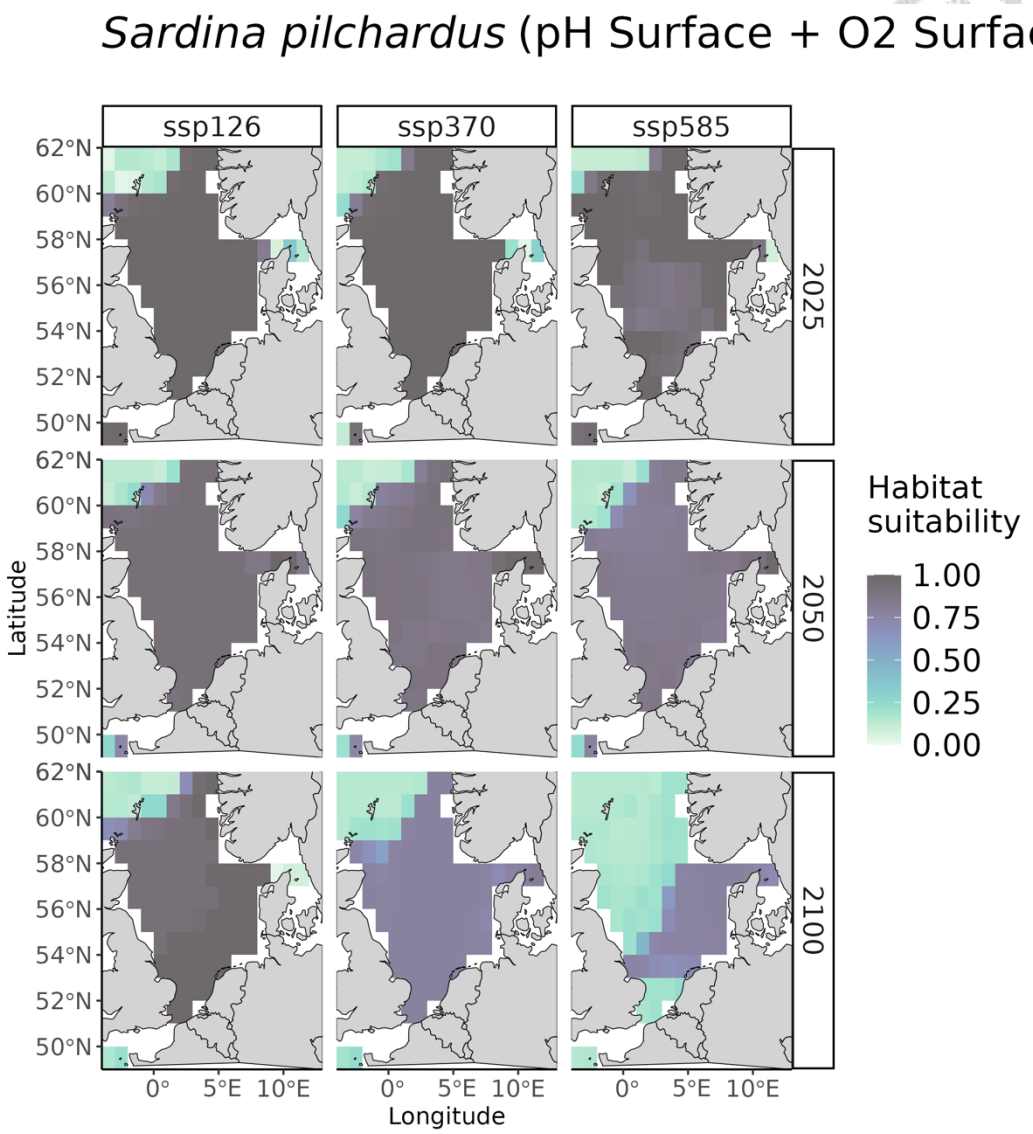

S.41. Projected distributional shifts of *Sardina pilchardus radiata* (based on habitat suitability) in 2025 (top), 2050 (middle) and 2100 (bottom) under 3 climate scenarios (SSP1-2.6, SSP3-7.0, SSP5-8.5). Color shading indicate probability of species occurrence in a grid of habitat suitability (0-1). Color-shading stands for potential habitat suitability, where 1 – suitable, 0 – unsuitable conditions. Each grid refers to resolution 60 arcmin. Applied model is indicated in the heading of each figure.

doi:10.6342/NTU202500202

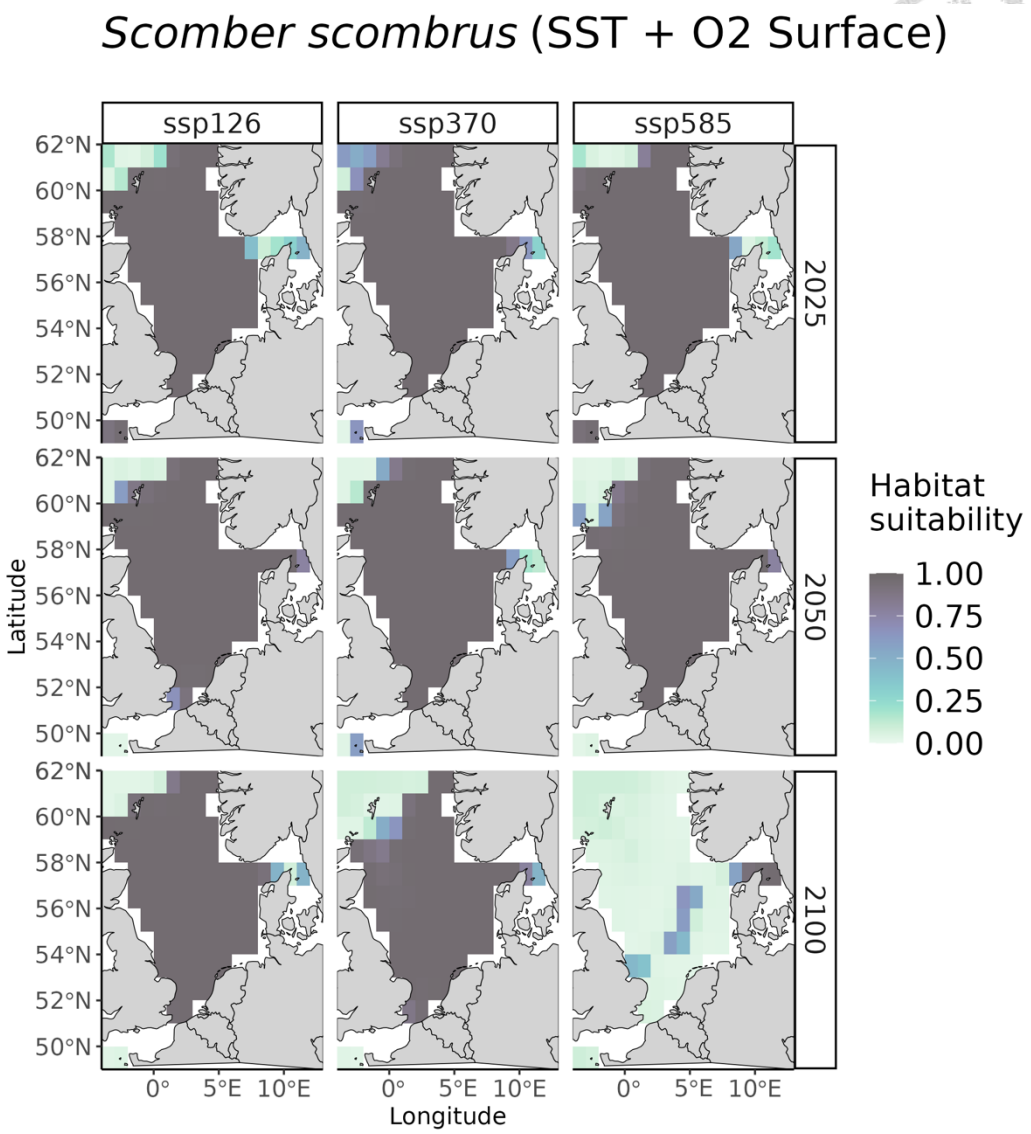

S.42. Projected distributional shifts of *Scomber radiata* (based on habitat suitability) in 2025 (top), 2050 (middle) and 2100 (bottom) under 3 climate scenarios (SSP1-2.6, SSP3-7.0, SSP5-8.5). Color shading indicate probability of species occurrence in a grid of habitat suitability (0-1). Color-shading stands for potential habitat suitability, where 1 – suitable, 0 – unsuitable conditions. Each grid refers to resolution 60 arcmin. Applied model is indicated in the heading of each figure.

doi:10.6342/NTU202500202

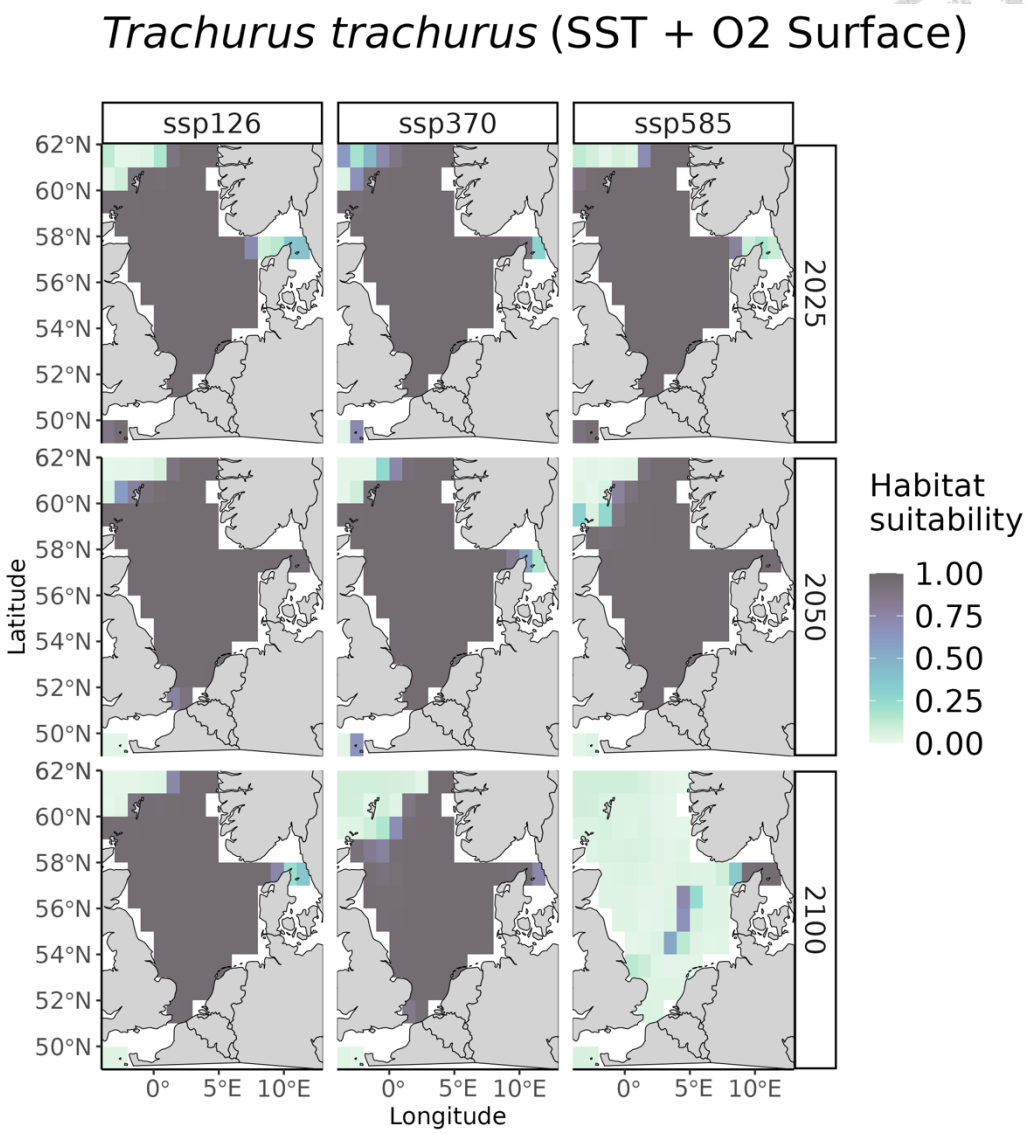

S.43. Projected distributional shifts of *Trachurus trachurus radiata* (based on habitat suitability) in 2025 (top), 2050 (middle) and 2100 (bottom) under 3 climate scenarios (SSP1-2.6, SSP3-7.0, SSP5-8.5). Color shading indicate probability of species occurrence in a grid of habitat suitability (0-1). Color-shading stands for potential habitat suitability, where 1 – suitable, 0 – unsuitable conditions. Each grid refers to resolution 60 arcmin. Applied model is indicated in the heading of each figure.

doi:10.6342/NTU202500202

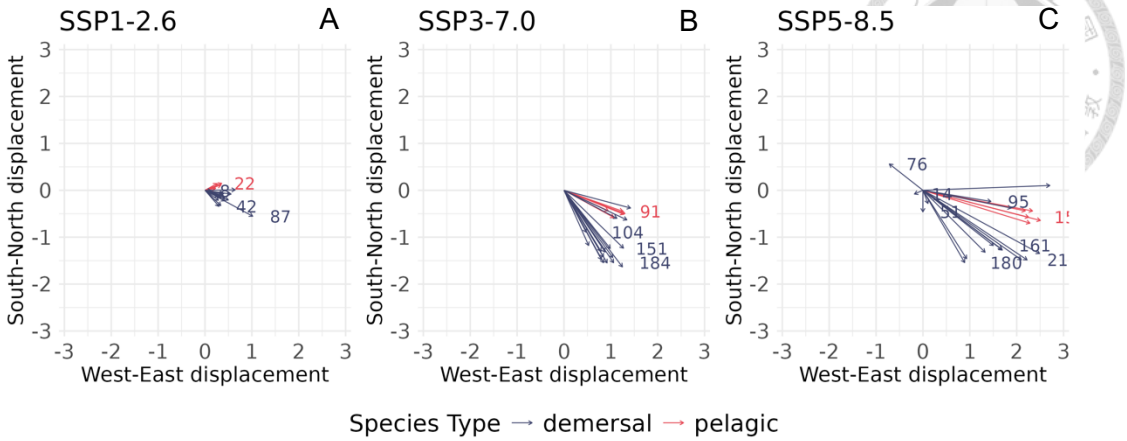

S.44. Distributional centroids vectors for multi-factor models. Shifts from 2024 to 2100 under 3 climate scenarios. The three panels illustrate arrows that are species' movement vectors (direction and magnitude) under SSP1-2.6 (A), SSP3-7.0 (B), and SSP5-8.5 (C). Blue arrows: represent demersal species. Red arrows: indicate pelagic species. The length of the arrows indicates the magnitude of the response. Longer arrows reflect greater shifts in species distributions or probabilities of presence. Numbers represent the distance in kilometers (km). Resolution of 1 grid is 60 arcmin. Each horizontal cell is 1 degree in longitude (West-East displacement) and each vertical cell is 1 degree in latitude (South-North displacement).

doi:10.6342/NTU202500202